Pushover Analysis and Incremental Dynamic Analysis of Steel Braced Reinforced Concrete Frames

Sangar Saud Hamadamin

Submitted to the
Institute of Graduate Studies and Research
in partial fulfillment of the requirements for the Degree of

Master of Science
in
Civil Engineering

Eastern Mediterranean University
October 2014
Gazimağusa, North Cyprus

Approval of the Institute of Graduate Studies and Research

Prof. Dr. Elvan Yilmaz
Director

I certify that this thesis satisfies the requirements as a thesis for the degree of Master of Science in Civil Engineering.

Prof. Dr. Özgür Eren
Chair, Department of Civil Engineering

We certify that we have read this thesis and that in my opinion it is fully adequate in scope and quality as a thesis for the degree of Master of Science in Civil Engineering.

Asst. Prof. Dr. Giray Ozay
Supervisor

Examining Committee

1. Asst. Prof. Dr. Mürüde Çelikağ

2. Asst. Prof. Dr. Giray Ozay

3. Asst. Prof. Dr. Serhan Şensoy

ABSTRACT

The recent earthquakes in some part of the world showed the disastrous effect on civilian areas. Most of the existing RC buildings designed only considering gravity loads without seismic design criteria. Therefore, an accurate knowledge is extremely necessary for those buildings that need seismic retrofitting. Steel bracing system can be considered as the most reasonable solution for seismic performance enhancing of RC buildings. The use of steel braces for retrofitting or strengthening seismically deficient RC frame is a reasonable solution for upgrading seismic resistance. Steel bracing is easy to erect, has the flexibility to design for meeting the required stiffness and strength, occupies less space, and economical. This study discusses the seismic behavior of RC buildings strengthened with various types of concentric steel braces, Diagonal-braced, Inverted V-braced, Zipper-braced, and X-braced. The models that have been studied are 3-storey, 6-storey, 9-storey and 12-storey buildings of which are designed by using Etabs. The static pushover analysis and incremental dynamic analysis have been conducted utilizing Seismostruct software to estimate the lateral capacity and compare the results of all the frames and bracing types. It is observed that adding braces upgrade the global capacity of the buildings in terms of lateral load capacity, displacement and stiffness compared to the cases with no bracing, and the X-braced systems performed much better than the other types of bracing.

Keywords: Earthquake, Seismic design, Retrofitting, Steel bracing, Pushover analysis, Incremental dynamic analysis.

ÖZ

Dünyanın bazıbölgelerinde son depremler sivil alanlarda çokbüyük can kayıplarına sebep olmuştur. Mevcut betonarme binaların çoğu sismik tasarım kriterleri olmadan sadece düşey yükler düşünülerek tasarlanmıştır. Bu nedenle, güçlendirme gerektiren bina stoğunun saptanması son derece önemlidir. Betonarme binalarda çelik çaprazlarla yapılacak bir güçlendirme sismik performansı artırmak için en makul çözüm olarak Kabul edilebilir. Çelik çaprazlarla güçlendirme ekonomik, uygulanması kolay, alan tasarrufu ve istenilen performansa kolayca ulaşılmasını sağlar. Bu çalışma diyagonel, ters V, zipper ve X çaprazlarıyla güçlendirilmiş çerçevelerin deprem davranışını incelemektedir. Seçilen 3, 6, 9 ve 12 katlı yapılar Etabs programı tarafından tasarlanmıştır. Statik itme ve artımsal dinamik analiz (IDA) yöntemleriyle yapılan analizler ve karşılaştırmalar Seismostruct yazılımı kullanılarak yapılmıştır.Sonuç olarak betonarme binalardaki çelik çaprazların bina deprem performansını ve rijitliğini çelik çaprazsız sistemlere oranla büyük ölçüde artırdığıve X-çaprazlı sistemlerin diğerlerine gore daha iyi performans sergilediği gözlenmiştir.

Anahtarkelimeler: Deprem, sismik dizayn, güçlendirme, çelik çaprazlar, static itme analizi, artımsal dinamik analiz.

ACKNOWLEDGMENT

First of all, I thank God for his blessing and the opportunity of attaining this greater height. My vote of thanks also goes to my amiable supervisor, Ass. Prof. Dr. Giray Ozay for his valuable suggestions, thorough criticisms and recommendations.

I would like to use this medium to express my profound gratitude to my father for his endlessly supports and encouragements, may God bless you abundantly.

Finally, I am very grateful for the love, encouragement and support my friends have showed on me, may God keep us together forever.

TABLE OF CONTENTS

ABSTRACT iii

ÖZ iv

AKNOWNLEDGMENT v

LIST OF TABLES xi

LIST OF FIGURES xiii

LIST OF SYMBOLS /ABBREVIATIONS xvii

1 INTRODUCTION 1

1.1 Introduction 1

1.2 Previous Works Done 2

1.3 Objectives and Scope 6

1.4 Organization of the Thesis 6

2 METHODS OF ANALYSIS 8

2.1 General 8

2.2 Static Pushover Analysis 9

2.2.1 General 9

2.2.1.1 Capacity Curve (Pushover Curve) 9

2.2.1.2 Target Displacement 10

2.2.1.3 Base Shear 10

2.2.1.4 Performance Level 10

2.2.1.4.1 Operational Level 10

2.2.1.4.2 Immediate Occupancy Level: 11

2.2.1.4.3 Life Safety Level 11

2.2.1.4.4 Collapse Prevention Level 11

2.2.2 Results of Pushover Analysis 11
2.2.2.1 Drifts and Displacements 12
2.2.2.2 Ductility 12
2.2.2.3 Strength and Stiffness 12
2.2.3 Pushover Analysis Procedure 13
2.2.4 Advantages of Pushover Analysis Method 14
2.2.5 Limitations of Pushover Analysis Method 14
2.3 Incremental Dynamic Analysis (IDA) 15
2.3.1 General 15
2.3.2 IDA's Common Terms 16
2.3.2.1 Scale Factor 16
2.3.2.2 Intensity Measure IM 16
2.3.2.3 Damage Measure DM 16
2.3.2.4 A single Record IDA Study 16
2.3.2.5 A Multi-Record IDA Study 17
2.3.3 IDA Envelope Curve 17
2.3.4 IDA Procedure 17
2.3.5 Advantages of IDA 18
3 METHODOLOGY AND ANALYSIS 19
3.1 Introduction 19
3.2 The Mutual Characteristic and Parameters for Frames 19
3.2.1 Geometrical Properties 20
3.2.2 Steel Bracing 20
3.2.3 Material Properties 21
3.2.4 Applied Loads and Ground Motions 25

3.2.4.1 Gravity Loads....25
3.2.4.2 Seismic Lateral Loads....26
3.2.4.2.1 Earthquake parameters....31
3.2.4.3 Selecting and Scaling of Ground Motion Records....32
3.2.5 Performance Criteria Parameters....35
3.3 Frame Modeling....36
3.3.1 Three Storey Building....36
3.3.1.1 Modeling of the Frame by using Seismostruct Software....38
3.3.2 Six Storey Building....41
3.3.2.1 Modeling of the Frame by using Seismostruct Software....43
3.3.3 Nine Storey Building....46
3.3.3.1 Modeling of the Frame by using Seismostruct Software....48
3.3.4 Twelve Storey Building....52
3.3.4.1 Modeling of the Frame by using Seismostruct Software....54
3.4 Analysis of the Structures....58
3.4.1 Pushover Analysis....58
3.4.1.1 Lateral load calculation....58
3.4.1.1.1 Lateral Load Calculation for the Three Storey Frame....59
3.4.1.1.2 Lateral Load Calculation for the Six Storey Frame....60
3.4.1.1.3 Lateral Load Calculation for the Nine Storey Frame....61
3.4.1.1.4 Lateral Load Calculation for the Twelve Storey Frame....62
3.4.2 Incremental Dynamic Analysis....64
4 RESULTS AND DISCUSSIONS....65
4.1 General....65
4.2 Pushover Analysis....65

4.2.1 Three Storey Frame Results and Discussion 65
4.2.1.1 Capacity Curves 65
4.2.1.2 Performance Criteria Checks for the Three Storey Frame 66
4.2.1.3 Lateral Load Capacity 68
4.2.1.4 Roof Lateral Displacement 69
4.2.1.5 Elastic Stiffness 69
4.2.2 Pushover Results for the Six Storey Frame 70
4.2.2.1 Capacity Curves 70
4.2.2.2 Performance Criteria Checks for the Six Storey Frame 71
4.2.2.3 Lateral Load Capacity 73
4.2.2.4 Roof Lateral Displacement 74
4.2.1.5 Elastic Stiffness 74
4.2.3 Pushover Results for the Nine Storey Frame 75
4.2.3.1 Capacity Curves 75
4.2.3.2 Performance Criteria Checks for the Nine Storey Frame 75
4.2.3.3 Lateral Load Capacity 79
4.2.3.4 Roof Lateral Displacement 79
4.2.3.5 Elastic Stiffness 80
4.2.4 Pushover Results for the Twelve Storey Frame 81
4.2.4.1 Capacity Curves 81
4.2.4.2 Performance Criteria Checks for the Twelve Storey Frame 81
4.2.4.3 Lateral Load Capacity 85
4.2.4.4 Roof Lateral Displacement 85
4.2.4.5 Elastic Stiffness 86
4.3 Incremental Dynamic Analysis 86

4.3.1 IDA Results for the Three Storey Frames 87
4.3.2 IDA Results for the Six Storey Frames..... 92
4.3.2 IDA Results for The nine Storey Frames..... 97
4.3.4 IDA Results for the Twelve Storey Frames 102
4.3.5 General IDA Results and Discussion..... 107
5 CONCLUSION AND RECOMMENDATION 113
5.1 Pushover Analysis Summary 113
5.2 Pushover Analysis Conclusion 113
5.3 Incremental Dynamic Analysis Summary 114
5.4 Incremental Dynamic Analysis Conclusion 115
5.5 Recommendations for Future Studies 115
REFERENCES 116

LIST OF TABLES

Table 2.1: Analysis methods 8

Table 3.1: Material properties of concrete core 21

Table 3.2: Material properties of steel 23

Table 3.3: Live load participation factor 27

Table 3.4 Effective ground acceleration coefficient (A_0) 28

Table 3.5: Building importance factor 29

Table 3.6: Local site classes 30

Table 3.7: Spectrum characteristic periods (T_A, T_B) 31

Table 3.8: Earthquake parameters 31

Table 3.9: Characteristics of earthquake records used for IDA 34

Table 4.1: Number of elements reached the criteria in the 3 storey frames 68

Table 4.2: Lateral load capacity 68

Table 4.3: Lateral roof displacements 69

Table 4.4: Elastic stiffness 70

Table 4.5: Number of elements reached the criteria in the 6 storey frames 73

Table 4.6: Lateral load capacity 73

Table 4.7: Lateral roof displacements 74

Table 4.8: Elastic stiffness 74

Table 4.9: Number of elements reached the criteria in the 9 storey frames 78

Table 4.10: Lateral load capacity 79

Table 4.11: Lateral roof displacements 80

Table 4.12: Elastic stiffness 80

Table 4.13: Number of elements reached the criteria in the 12 storey frames 84

Table 4.14: Lateral load capacity 85

Table 4.15: Lateral roof displacements 85

Table 4.16: Elastic stiffness 86

Table 4.17: Maximum base shear (kN)-TH1 107

Table 4.18: Maximum base shear (kN)-TH2 108

Table 4.19: Maximum base shear (kN)-TH3 108

Table 4.20: Maximum base shear (kN)-TH4 109

Table 4.21: Maximum base shear (kN)-TH5 109

Table 4.22: Maximum base shear (kN)-TH6 110

Table 4.23: Maximum base shear (kN)-TH7 110

Table 4.24: Maximum base shear (kN)-TH8 111

Table 4.25: Maximum base shear (kN)-TH9 111

LIST OF FIGURES

Figure 2.1: Different phases of plastic hinges 10

Figure 3.1: Mander et al. concrete model 22

Figure 3.2: Menegotto Pento steel model 24

Figure 3.3: A typical fiber model of reinforced concrete element by Seismostruct ..25

Figure 3.4: Spectral acceleration coefficient versus time period 33

Figure 3.5: Geometric views of the three storey building 37

Figure 3.6: Section details for the three storey frame 38

Figure 3.7: Discretization of the three storey frame's section..... 39

Figure 3.8: The three storey frame with and without bracings 41

Figure 3.9: Geometric views of the six storey building..... 42

Figure 3.10: Section details for the six storey frame 43

Figure 3.11: Discretization of the six storey frame's section 44

Figure 3.12: The six storey frame with and without bracings 45

Figure 3.13: Geometric views of the nine storey building 47

Figure 3.14: Section details for the nine storey frame 49

Figure 3.15: Discretization of the nine storey frame's section..... 50

Figure 3.16: The nine storey frame with and without bracings..... 51

Figure 3.17: Geometric views of the twelve storey building 53

Figure 3.18: Section details for the twelve storey frame 55

Figure 3.19: Discretization of the twelve storey frame's section..... 56

Figure 3.20: The twelve storey frame with and without bracings..... 58

Figure 3.21: Fundamental period and first mode shape created by Etabs 59

Figure 3.22: Fundamental period and first mode shape created by Etabs 60

Figure 3.23: Fundamental period and first mode shape created by Etabs 61
Figure 3.24: Fundamental period and first mode shape created by Etabs 63
Figure 4.1: Capacity curve for the three storey frames 66
Figure 4.2: The performance criteria checks for the three storey frames, the concrete crack is identified by the green color, concrete cover crush by yellow, concrete core crush by red, steel yielding by black and steel fracture by blue color 67
Figure 4.3: Capacity curve for the six storey frames 70
Figure 4.4: The performance criteria checks for the six storey frames, the concrete crack is identified by the green color, concrete cover crush by yellow, concrete core crush by red, steel yielding by black and steel fracture by blue color. 72
Figure 4.5: Capacity curve for the nine storey frames 75
Figure 4.6: The performance criteria checks for the nine storey frames, the concrete crack is identified by the green color, concrete cover crush by yellow, concrete core crush by red, steel yielding by black and steel fracture by blue color. 78
Figure 4.7: Capacity curve for the twelve storey frames 81
Figure 4.8: The performance criteria checks for the nine storey frames, the concrete crack is identified by the green color, concrete cover crush by yellow, concrete core crush by red, steel yielding by black and steel fracture by blue color 84
Figure 4.9: IDA curve for the three storey frames, TH1 87
Figure 4.10: IDA curve for the three storey frames, TH2 88
Figure 4.11: IDA curve for the three storey frames, TH3 88
Figure 4.12: IDA curve for the three storey frames, TH4 89
Figure 4.13: IDA curve for the three storey frames, TH5 89
Figure 4.14: IDA curve for the three storey frames, TH6 90
Figure 4.15: IDA curve for the three storey frames, TH7 90

Figure 4.16: IDA curve for the three storey frames, TH8 91
Figure 4.17: IDA curve for the three storey frames, TH9 91
Figure 4.18: IDA curve for the six storey frames, TH1 92
Figure 4.19: IDA curve for the six storey frames, TH2 93
Figure 4.20: IDA curve for the six storey frames, TH3 93
Figure 4.21: IDA curve for the six storey frames, TH4 94
Figure 4.22: IDA curve for the six storey frames, TH5 94
Figure 4.23: IDA curve for the six storey frames, TH6 95
Figure 4.24: IDA curve for the six storey frames, TH7 95
Figure 4.25: IDA curve for the six storey frames, TH8 96
Figure 4.26: IDA curve for the six storey frames, TH9 96
Figure 4.27: IDA curve for the nine storey frames, TH1 97
Figure 4.28: IDA curve for the nine storey frames, TH2 98
Figure 4.29: IDA curve for the nine storey frames, TH3 98
Figure 4.30: IDA curve for the nine storey frames, TH4 99
Figure 4.31: IDA curve for the nine storey frames, TH5 99
Figure 4.32: IDA curve for the nine storey frames, TH6 100
Figure 4.33: IDA curve for the nine storey frames, TH7 100
Figure 4.34: IDA curve for the nine storey frames, TH8 101
Figure 4.35: IDA curve for the nine storey frames, TH9 101
Figure 4.36: IDA curve for the twelve storey frames, TH1 102
Figure 4.37: IDA curve for the twelve storey frames, TH2 103
Figure 4.38: IDA curve for the twelve storey frames, TH3 103
Figure 4.39: IDA curve for the twelve storey frames, TH4 104
Figure 4.40: IDA curve for the twelve storey frames, TH5 104

Figure 4.41: IDA curve for the twelve storey frames, TH6 105

Figure 4.42: IDA curve for the twelve storey frames, TH7 105

Figure 4.43: IDA curve for the twelve storey frames, TH8 106

Figure 4.44: IDA curve for the twelve storey frames, TH9 106

LIST OF SYMBOLS AND ABBREVIATIONS

ATC	Applied technology council
ACI	American concrete institute
$A(T_1)$	Spectral acceleration coefficient relative to first natural period of building
A_0	Effective ground acceleration coefficient
DM	Damage measure
DPO	Dynamic pushover
D.L	Dead load
FEMA	Federal emergency management agency
f_c	Compressive strength
f_t	Tensile strength
F	Loads due to weight and pressures of fluids
F_i	Design seismic load acting at i'th Storey
g_i	Total dead load at i'th storey of building
H	Loads due to weight and pressures of soil, water in soil or other materials
H_i	The height of i'th storey of building measured from the top foundation level
h_1	Topmost layer thickness
IM	Intensity measure
IDA	Incremental dynamic analysis
I	Building importance factor

k_c	Confinement factor
L.L	Live load
L_r	Roof live load
N	Total number of stories of building from the foundation level
n	Live load participation factor
NSP	Nonlinear static procedure
NTH	Nonlinear time history
PGA	Peak ground acceleration
PEER	Pacific earthquake engineering research
q_i	Total live load at i'th storey of building
R	Structural behavior factor
$R_a(T)$	Seismic load reduction factor
RC	Reinforced concrete
S	Snow load
SF	Scale factor
$S(T)$	Spectrum coefficient
T	Building natural period
Te	Cumulative effect of temperature, creep and shrinkage
T_1	First natural vibration period of building
T_A, T_B	Spectrum characteristic periods
TEC2007	Turkish earthquake code (2007)
UPN200	European standard channels with taper flanges
V_t	Total base shear
W	Total weight of building calculated by considering live load participation factor.

w_i	The weight of i'th storey of building by considering live load participation factor.
Z	Local site classes
ε_c	Strain at peak stress
γ	Specific weight
ΔH_N	Additional equivalent seismic load acting on the top of the building.

Chapter 1

INTRODUCTION

1.1 Introduction

Prevention of catastrophic caused by an earthquake has become progressively important in recent years. Catastrophic prevention includes the reduction of seismic risk through rehabilitating and strengthening of the existing buildings in order to meet seismic safety requirements. Retrofitting of the deficient existing building to improve its seismic performance will be a pathway to assure the safety of the building in the event of future earthquakes. There are different retrofitting techniques and to select suitable one, an accurate evaluation of the condition and seismic performance of an existing structure is necessary.

Steel bracing is one of the most effective methods that have been utilized for retrofitting of the existing reinforced concrete buildings against lateral loads, especially earthquake activities. Moment-resisting reinforced concrete buildings are exhibited to several damages during moderate to high ground motions. Many existing buildings do not meet the seismic strength requirement. The need for seismic retrofitting in existing building can arise due to building not designed to code, subsequent updating of code and design practice, subsequent upgrading of seismic zone, deterioration of strength and aging, modification of existing structure, lack of efficiency of execution in the construction process, and change in the use of the building. A steel bracing system can be inserted into a frame to provide lateral

stiffness, strength, ductility, hysteretic energy dissipation, or any combination of these.

Steel bracing systems have some economical and practical advantages. The main advantage of this method is that it is not necessary to retrofit the foundation system. Since the bracing system does not introduce great additional gravity loads to the existing building and steel bracings are usually inserted between existing vertical members.

In the present study, steel bracing as a retrofitting technique is investigated. Initially, four reinforced concrete frames different in height are designed for gravity loads by Etabs software, subsequently, many types of bracing is incorporated. Seismostruct which is finite element software has been utilized to perform the pushover and incremental dynamic analysis. Buildings with and without bracings is compared in terms of static pushover capacity and dynamic pushover capacity curves.

1.2 Previous Works Done

A summarized audit of previous studies on the use of steel bracing systems to rehabilitate of the RC frames is discussed below. This literature audit concentrates on works that have been done a decade ago and more relevant to the present study.

Ghoborah, A. and H. A. Elfath, investigated the seismic performance of a three storey RC building retrofitted with steel bracing. An analysis was performed using different ground motions. The efficiency of steel bracing on the seismic performance of the retrofitted frame was investigated. Also, the effect of distributing the steel bracing over the height of the building was examined. Story drifts and damage indicators were used as performance expressions [1].

Safarizki, H. A., et al, used steel bracing to evaluate the possible improvement of seismic performance of an existing RC building. Three types of analysis were used for this study, which are nonlinear static pushover displacement coefficient method according to FEMA 356, improved nonlinear static pushover displacement coefficient method according to FEMA 440 and dynamic time history analysis by the Indonesian Code of Seismic Resistance Building Criteria. By using static pushover analysis it was discovered that target displacement in both (Y and X) directions is decreased by 16%-55% after installing proper X-bracing arrangement. Furthermore, it is found that the story drift in Y direction exceeds the serviceability limit criterion when the recorded ground motion was applied for dynamic time history analysis, but after retrofitting the building, the story drift was within the limit criteria [2].

Massumi, A. and A. A. Tasnimi, examined a series of experimental test on eight (one bay, one story) reinforced concrete model frames scaled to 1:2.5, under lateral and cyclic loading. Two of them un-braced and other frames were X-braced, frames, but five different detailed connections was used between bracing members and column-beam joints in order to investigate the effectiveness of steel bracing and the type of connection on in-plane shear capacity of concrete frames. The test results demonstrated the impressive increase in the lateral strength and displacement ductility of braced frames [3].

Dubina, D., et al, most of the RC buildings before 1960 were designed only to carry gravity loads only, even they were in risk seismic zones. Therefore, when subjected to earthquakes, they are at risk in the view of the fact that poor detail and lack capacity. Steel bracing as one of the rehabilitating methods was used to examine its strength, stiffness and ductility both numerically and experimentally. The portal

frames separated from a genuine structure. Monotonic and cyclic loads were applied to un-braced and braced frames. Conventional concentric V-braces and buckling restrained V-braces have been installed. Behavior factor has been obtained to compare the capacity between the portal and braced frames. Structure strengthened with buckling restrained V-braces had a good behavior, more capacity and ductility compared to the un-braced structure. Conventional brace system increases stiffness and strength but less than buckling restrained brace system [4].

Kevadkar, M. D. and P.B. Kodag, presented an investigation to utilize shear wall and steel brace to reinforced concrete buildings that built in risk seismic zones. A (Ground+12) story building was analyzed to find out the effect of the lateral load systems during a strong earthquake following Indian Standards. Three analyses were performed, first is building without bracing and shear wall, second is building with shear wall and third is building with different steel brace systems. The performance of the building was evaluated in terms of story shear and story drifts, lateral displacement, demand capacity and base shear. It was discovered that X-bracing system is contributing to the structural stiffness and reduces the maximum inter story drift, demand capacity and lateral displacement more than the shear wall system [5].

Mohammad, E.K, investigated the effectiveness of knee braced frames and concentric braced frames after inserting to existing reinforced concrete building in order to increase lateral strength against earthquake. These investigations were focused on ductility and stiffness. One bay RC frames in two levels used, one story and ten storeys in three modes which are RC frame without braces, RC with knee brace system and RC frame with concentric brace system. Displacement based method was used for investigating stiffness and pushover analysis was performed to

evaluate ductility of the system. Additionally, cyclic loading was applied for obtaining more accurate results. It was found both systems are capable for retrofit and strengthen reinforced concrete buildings. The Knee-braced system is more effective for the purpose of designing or retrofitting for collapse-level earthquake [6].

Mehmet, A., studied the use of steel bracing as a method of retrofitting and strengthening of existing buildings which are lacking in lateral capacity. Reinforced concrete frames, which were different in height classified as low, intermediate and comparatively high rise were utilized. Diagonal steel bracing in several patterns was installed. The peak lateral load capacity was determined by load-controlled pushover analysis. The post-tensioned effect of preloading was additionally examined [7].

Amini, M. and M. Alirezaei, utilized chevron bracing system and zipper bracing system to take out adequate lateral capacity against earthquake loads. Chevron bracing system and zipper bracing system were compared in terms of drift ratio and ductility. The three steel building, which were different in height 4-storey, 8-storey and 12-story were considered. Incremental dynamic analysis was performed to evaluate over-strength, inelastic strength and deformation capacity for the whole structure. Six recorded ground motions were exercised. Zipper bracing systems were capable to achieve more acceptable distribution of uniform damage over the height of the buildings [8].

Kadid, A. and D. Yahiaoui, studied using various types of steel bracing to upgrade performance of existing reinforced concrete frames. The seismic behavior of reinforced concrete building was investigated using various types of steel braces, X-braced, ZX-braced, Inverted V-braced, and Zipper braced. Different size and type of

bracing also were considered. Two buildings were modeled as 3-story and 6-story. Static nonlinear pushover analysis method has been applied to measure capacity for all various cases. The study achieved that adding bracing improves the global capacity in terms of ductility, deformation and strength check against building without bracing, also Zipper bracing and X- bracing systems performed better regarding on the size and type of cross section [9].

1.3 Objectives and Scope

The purpose of this study is to investigate the effect of the various types of concentric steel bracing systems on existing RC buildings. The comparison between the different types of bracings has been studied in terms of capacity curves, lateral displacement, performance criteria checks and elastic stiffness.

Both static pushover analysis and IDA performed using the seismic specialist software which is Seismostruct software.

1.4 Organization of the thesis

This study is comprised of five chapters:

Chapter one aims to give a general introduction, previous works done and objectives of the present study.

Chapter two is specialized to define and summarize methods of analysis, which is consists of two main sections. In the first section, static pushover analysis method is briefly explained, procedure, related terms, advantages and disadvantages also described. Second, an IDA method has been introduced, which includes related terms, procerdure to perform IDA and anvantages.

Chapter three is a methodology and analysis; it includes a brief definition about types of bracing, the mutual characteristics and parameters of the frames, the methodology of design of the frames by Etabs software, calculating base shear for all frames, selecting and scaling of suitable ground motions records, performing analysis by Seismostruct software.

Chapter four includes results and discussion. In this chapter, results and discussions are divided into two main parts, first is static pushover results and discussion in terms of static capacity curves, lateral load capacity, lateral displacement and stiffness for the different frames and bracing types. In addition to these, the performance criterion was checked for different types of strains. The second part is incremental dynamic analysis results and discussion in terms of dynamic capacity curves for all cases.

Chapter five includes conclusion and recommendations. The conclusion of the thesis is summarized differently for both pushover analysis method and incremental dynamic analysis method. The recommendations for future studies are suggested.

Chapter 2

METHODS OF ANALYSIS

2.1 General

The utilization of seismic analysis, both in practice and research has risen significantly because of the increase of verified and easy to use software and the accessibility of quick and simple electronic devices. The most important methods of structural analysis utilized within seismic engineering are outlined through Table 2.1. The methods surveyed are classified into static analysis methods or dynamic analysis methods.

Table 2.1: Analysis methods

Static Analysis Methods	**Dynamic Analysis Methods**
1. Static analysis (non-variable loading)	1. Dynamic time-history analysis
2. Static pushover	2. Incremental dynamic analysis-IDA
3. Static adaptive pushover	

In the present study, both static pushover analysis and IDA are carried out using Seismostruct software.

2.2 Static Pushover Analysis

2.2.1 General

The pushover analysis is a form of nonlinear static analysis method, which was established in to practice in 1970's, but the potential of the pushover analysis has been familiar for past twenty years.

Pushover analysis procedure is a static nonlinear analysis, under permanent gravity loads and progressively increasing lateral loads. Capacity curve, which is base shear against roof displacement can obtained through the pushover analysis. The structural pushover analysis assesses performance by estimating force and deformation capacity and seismic demand using a nonlinear static analysis algorithm. The seismic demand parameters are story drifts, global displacements, story forces, component deformations and component forces.

Pushover analysis procedure is illustrated in some guidelines like FEMA356 [10] and ATC-40 [11]. The terms related to pushover analysis as described in FEMA356 and ATC-40 are:

2.2.1.1 Capacity Curve (Pushover Curve)

Capacity curve is evaluated the capability of a building against earthquakes. It is the plot of the total lateral force on a structure, against the lateral deflection of the roof of the structure. Performance point and location of hinges in different stages can be determined in capacity curves as illustrated in Figure 2.1. A to B is the elastic range, B to IO represents the immediate occupancy range, IO to LS represents the life safety range, and LS to CP represents the collapse prevention range.

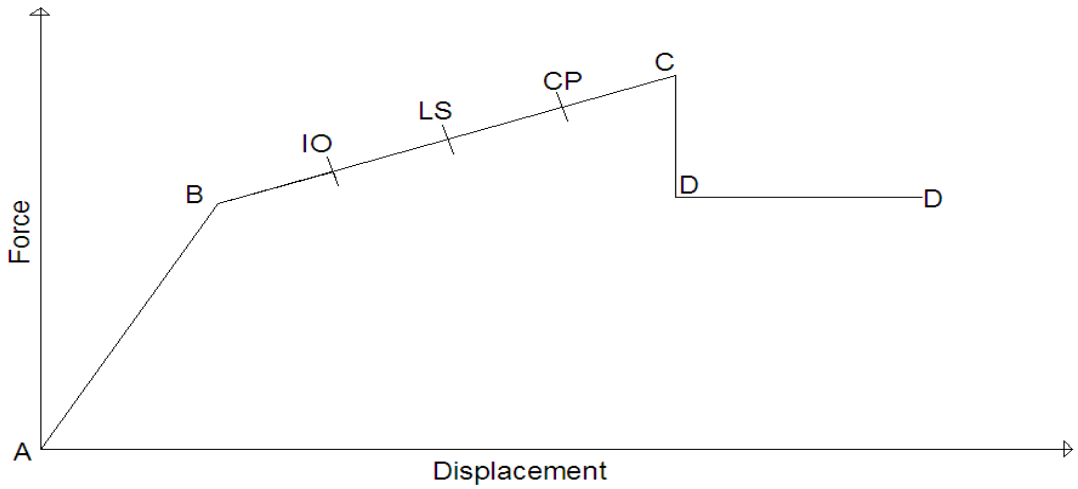

Figure 2.1: Different phases of plastic hinges.

2.2.1.2 Target Displacement

The target displacement is intended to represent the maximum displacement likely to be experienced during design earthquake.

2.2.1.3 Base Shear

Base shear is an estimate of the maximum expected lateral force that will occur due to seismic ground motion at the base of a structure.

2.2.1.4 Performance Level

A limiting damage state or condition described by the physical damage within the building, the threat to life safety of the building's occupants due to the damage, and the post-earthquake serviceability of the building. A building performance level is the combination of a structural performance level and a non structural performance level.

2.2.1.4.1 Operational Level

This is the performance level related to functionality and any required repairs are small and unimportant.

2.2.1.4.2 Immediate Occupancy Level (IO)

This corresponds to the most widely used criteria for essential facilities. The building's spaces and systems are expected to be rationally applicable.

2.2.1.4.3 Life Safety Level (LS)

This level is intended to achieve a damage state that presents an extremely low probability of threat to life safety, either from structural damage or from falling or tipping of nonstructural building component.

2.2.1.4.4 Collapse Prevention Level (CP)

This damage state addresses only the main building frame or vertical load carrying system and requires only stability under vertical loads. At this stage, the structure continues to support gravity loads, but retains no margin against collapse.

2.2.2 Results of Pushover Analysis

The expectation from pushover analysis is to estimate critical response parameters imposed on structural system and its components as close as possible to those predicted by nonlinear dynamic analysis. Pushover analysis provides information on many response characteristics that cannot be obtained from an elastic static or elastic dynamic analysis. These are [12]:

- Inter-story drift and its distribution along the height of the building.
- Determination of force demands of brittle members, such as axial force demands on columns, the moment demands on beam-column joints.
- Determination of deformation demands for ductile members.
- Identification of location of weak points in the structure.
- Consequences of strength deterioration of individual members on the behavior in the structural system.

- Identification of strength discontinuities in plan or elevation that will lead to changes in dynamic characteristics in the elastic range.
- Investigation of the perfection and sufficiency of load path.

2.2.2.1 Drifts and Displacements

Many terms are used to define displacement with different meaning as described below:

- Global displacements, indicates the displacement relative to the base of an equivalent SDOF system representing the structure.

- Roof displacement, describes to the lateral displacement of the roof of the building with respect to the base.

- Inter-story drift, refers to the relative displacement between two adjacent floors bounding the story.

- Drift, ratio corresponds to the inter-story drift dividing by the story height.

- Roof drift, represents the roof displacement over the total height of the building.

It is found that the use of displacement parameters instead force parameters as demand parameters are more effective way to control the damage of the buildings during earthquake resistance design procedure. Therefore, the drift parameters should be considered in earthquake engineering.

2.2.2.2 Ductility

It is the ability of a structural component, element, or system to undergo both large deformations and/or several cycles of deformations beyond its yield point or elastic limit, and maintain its strength without significant degradation or abrupt failure.

2.2.2.3 Strength and Stiffness

The ability of a member or a structure to withstand against loading is called strength**.** The extra reserve of strength of the structure before reaching its maximum strength

named as over-strength. The over-strength factor is the global behavior of a structure as a ratio of the structural yield level of the code prescribed strength demand arising from the application of prescribed loads and forces.

Stiffness is an important characteristic of buildings that resist lateral loads, so it is desired to measure stiffness if deformations under the lateral forces are to be reliably quantified and subsequent controlled.

2.2.3 Pushover Analysis Procedure

There are two main ways to perform pushover analysis, which are displacement controlled and force controlled method depending on the properties of the load and expected reaction of the structure. Force controlled option is preferred when complete knowledge about applied loads is available and the structure is expected to hold the entire load. When the structure expected to be unstable or lose strength and the magnitude of the load is not known in advance, displacement controlled method is applied.

In the present study, Seismostruct software is used to perform pushover analysis following the load controlled method. The main steps of pushover analysis regarding Seismostruct software are:

1. Building a computational model of the structure.
2. Defining member behavior :
    - Beams: moment-rotation relations.
    - Columns: moment-rotation and interaction diagrams.
    - Beam-column joints: assume rigid and special links to extra members.
    - Walls.

3. Gravity load as the predefined lateral load pattern is applied, which is consists of dead load plus a portion of live load.
4. Lateral loads are increased until numerical collapse occurs.
5. High target loads are used to obtain numerical collapse.
6. Roof displacement against base shear is plotted (capacity curve) at the stage when numerical collapse occurred.

2.2.4 Advantages of Pushover Analysis Method

Pushover analysis is preferred because:

1. Earthquake load leads to nonlinear behavior to the structure.
2. Pushover analysis would help to understanding building behavior, such that recognizing weak elements and realistic prediction of element demands.
3. Less conservative acceptance criteria and parameters can be used with consequences understood.

2.2.5 Limitations of Pushover Analysis Method

Although pushover analysis has pros over elastic analysis procedures, underlying assumptions, the accuracy of pushover predictions and limitations of current pushover procedures must be identified. The estimate of target displacement, selection of lateral load patterns and identification of failure mechanisms due to higher modes of vibrations are important issues that affect the accuracy of pushover analysis result. The pushover analysis is a useful, but not impeccable, tools for assessing inelastic strength and deformation demands and for exposing design weaknesses. It must be emphasized that the pushover analysis is approximate in nature and is basic on static loading. As such, it cannot represent dynamic phenomena with a large degree of accuracy [13]. Thus, in the present study IDA also is performed.

2.3 Incremental dynamic analysis (IDA)

2.3.1 General

It has been long recognized that the current nonlinear static procedures (NSP) based on invariant loading vectors such as those recommended in FEMA 356 process inherent drawbacks in adequately representing the effects of varying dynamic characteristics during the inelastic response of structures [14]. Although some improved NSPs have been developed over the past few years, their validity for a variety of structural systems and a range of ground motion characteristics have yet to be demonstrated. The results of nonlinear time history (NTH) analysis based on actual earthquake recordings serve as the only reliable benchmark solutions against which the NSP results can be compared. In that respect, IDA has emerged as a potential tool for seismic evaluation since it involves a series of time history analysis. IDA was developed by Vamvatsikos (2002), an IDA involves increasing the severity of the record till a collapse limit state is reached.

The IDA, also known as dynamic pushover, is a parametric analysis method that has recently emerged to evaluate more thoroughly structural performance under seismic loads [15]. It is more reliable, because it is gives a continuous description of the system reaction, starting from elasticity to yielding and in the end to collapse. IDA involves subjecting a structural model to one or more ground motion records, each scaled to multiple levels of intensity, thus producing one or more curves of response parameterized versus intensity level. The peak values of base shear are then plotted against their top displacement counterparts, for each of the dynamic runs, giving rise to the so-called dynamic pushover or IDA envelope curves [20].

2.3.2 IDA's Common Terms

The common terms related to IDA are [15]:

2.3.2.1 Scale Factor

The scale factor (SF) of a scaled accelerogram, is the nonnegative scalar $[0,+\infty]$ that produces a scaled accelerogram when multiplicatively applies to the un-scaled acceleration time-history.

2.3.2.2 Intensity Measure IM

Intensity measure IM or a monotonic scalable ground motion intensity measure of a scaled accelerogram, is a non negative scalar $[0,+\infty]$ that constitutes a function that relies upon the un-scaled accelerogram, and is monotonically raises with the scale factor.

2.3.2.3 Damage Measure DM

Damage measure of the structural state variable, is a nonnegative scalar $[0,+\infty]$ that characterizes the additional response of the structural model due to a prescribed seismic loading. Possible choices could be maximum base shear, node rotations, peak storey ductility, various proposed damage indices or the stability index, peak roof drift, the floor peak inter-storey drift angles of n-storey structure, their maximum, and the maximum peak inter-storey drift.

2.3.2.4 A Single Record IDA Study

A single record IDA study is a dynamic analysis study of a given structural model parameterize by the scale factor of the given ground motion time history. Also known simply as dynamic pushover, it involves a series of dynamic nonlinear runs performed under scaled images of an accelerogram, whose IMs are, ideally, selected to cover the whole range from elastic to nonlinear and finally to collapse of the structure.

2.3.2.5 A Multi-Record IDA Study

A multi-record IDA study is a collection of single-record IDA studies of the same structural model, under different accelerograms.

2.3.3 IDA Envelope Curve

It is the plot of the peak values of base shear versus maximum values of relative displacement (drift) at the node chosen by the user, as obtained in each of the dynamic runs. It is possible to plot:

i. The maximum relative displacement versus the peak base shear value that found around the maximum drift (corresponding base shear),

ii. The maximum relative displacement versus the maximum base shear value recorded throughout the entire time-history (maximum base shear), or

iii. The maximum base shear versus the peak relative displacement that found around the maximum shear (corresponding drift).

2.3.4 IDA Procedure

The main steps for performing incremental dynamic analysis are illustrated below [16]:

1) Define and select an appropriate ground motion record consistent.
2) Define a monotonic scalable ground-motion IM, e.g. the PGA, PVA, PVD or combination of them.
3) Define a DM.
4) Define a group of multiple scale factors to apply to the selected IM in (2).
5) Scale the selected ground motion record in (1) to create a set of ground motion records that will examine the structure during its response range, from elastic response to collapse.

6) Perform response history analysis of the structural model subjected to the scaled accelerogram at the lowest IM.
7) Estimate the DM in (3) corresponding to the scaled IM in (2).
8) Repeat steps (6) to (7) for all the scaled IMs.

2.3.5 Advantages of IDA

The IDA advantages are as follows [15]:

- Thorough understanding of the range of response or demands versus the range of potential levels of a ground motion record,
- Better understanding of the structural implication of rarer/more severs ground motion levels,
- Better understanding of the changes in the nature of the structural response as the intensity of ground motion increases (e.g. changes in peak deformation patterns with height, onset of stiffness and strength degradation and their patterns and magnitudes),
- Producing estimates of the dynamic capacity of the global structural system,
- And finally, given a multi-record IDA study, understanding how stable (or variable) all these items are from one ground motion record to another.

Chapter 3

METHODOLOGY AND ANALYSIS

3.1 Introduction

In order to evaluate the effectiveness of different types of steel bracings of reinforced concrete frames, four models with different floor heights have been adopted. Pushover analysis and IDA are carried out.

Initially, ETABS software is utilized to design all frames, subsequently, Seismostruct which is the finite element analysis software is used to make models and run entire analysis.

The Seosmostruct software is a finite element package capable of predicting the large displacement behavior of frames under static or dynamic loading, taking into account both geometric nonlinearities and material inelasticity [17]. The Seismosignal software is also used to arrange and modify ground motion records. The Microsoft Excel was used to extract data and record values in graphs.

3.2 The Mutual Characteristic and Parameters for Frames

The models which have been utilized for this study, are symmetric three-storey, six-storey, nine-storey and twelve-storey reinforced concrete frames. The mutual properties of models are illustrated below:

3.2.1 Geometrical Properties

The main common geometrical properties between frames are as follow:

- Number of bays are 5 in both Y and X direction
- Width of bays is 6 m
- The height of each storey is 3.4 m
- 3-storey, 6-storey, 9-storey and 12-storey building considered

3.2.2 Steel Bracing

A steel bracing system can be inserted in a frame to provide lateral stiffness, strength, ductility, hysteretic energy dissipation, or any combination of these. The braces are effective for relatively more flexible frames, those such as without infill walls. The braces can be added at the exterior frames with less disruption of the building use, as used in this study. Passive energy dissipation devices may be incorporated in the braces to enhance the seismic absorption. The connection between the braces and the existing frames is an important consideration in this strategy. There are two main techniques in installation of braces to reinforced concrete designed frames. One technique of installing braces is to provide a steel frame within the designated RC frame. Else, the braces can be connected directly to the RC frame [18]. Since the braces are connected to the frames at the beam-column joints, the forces resisted by the braces are transferred to the joints in the form of axial forces, both in compression and tension. While the addition of compressive forces may be tolerated, the resulting tensile forces are in concern.

Steel braced frames are mainly categorized as concentrically braced frames and eccentrically braced frames. In this study, different types of concentrically braced frames are investigated.

Concentrically braced frames are more economical and high stiffness, but also they are less ductile than eccentric systems.

3.2.3 Material properties

- ACI 318-02 design code is selected.
- Three types of materials are defined:

1. Concrete for core: Mander et al. nonlinear concrete model is utilize [19]. Properties are shown in Table3.1 and Figure 3.1:

Table 3.1: Material properties of concrete core

Material properties	**Values**
Compressive strength-f_c	21000 kPa
Tensile strength-f_t	0 kPa
Strain at peak stress-ε_c	0.002 m/m
Confinement factor-k_c	(1.2 for core) and (1 for cover)
Specific weight-γ	24 kN/m³

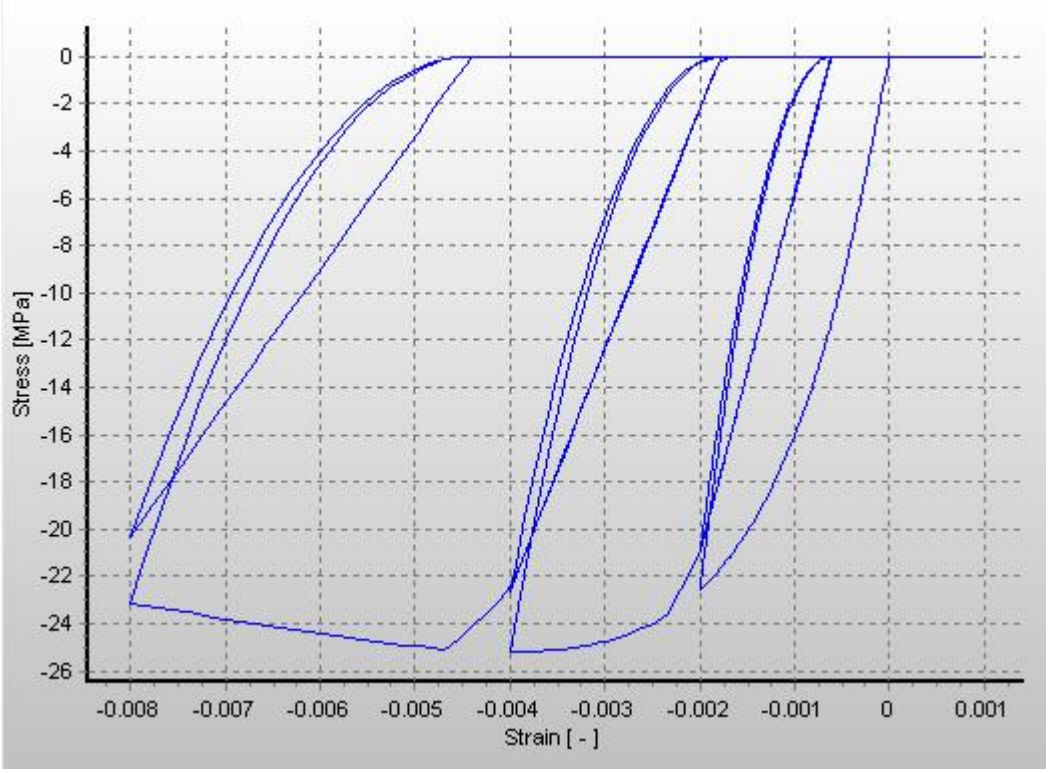

Figure 3.1: Mander et al. concrete model [19]

2. Concrete for cover: same material as the concrete core used.

3. Steel material: Menegotto-Pinto steel model is used [19]. Ten parameters should be defined to fully describe the mechanical properties of the Menegotto-Pinto steel model material, as shown in Table 3.2 and Figure 3.2:

Table 3.2: Material properties of steel

Material Properties	**Values**
Modulus of elasticity	200,000,000 kPa
Yield strength	250,000 kPa
Strain hardening parameter	0.005
Transition curve initial shape parameter	20
Transition curve shape calibrating coefficient A1	18.5
Transition curve shape calibrating coefficient A2	0.15
Isotropic hardening calibrating coefficient A3	0
Isotropic hardening calibrating coefficient A4	1
Fracture/buckling strain	0.1
Specific weight (kN/m^3)	78

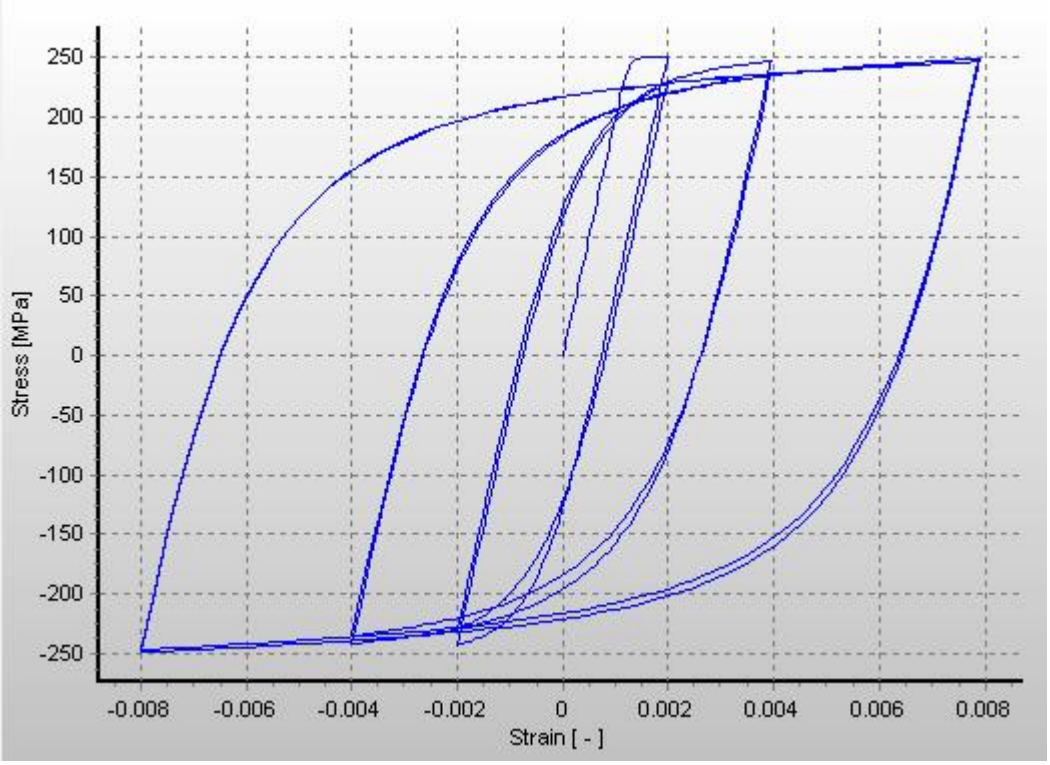

Figure 3.2: Menegotto Pento steel model [19]

Consequently, in the modeling by Seismodtruct, the structural element is divided in three types of fibers [17]:

- Some fibers are used for modeling of longitudinal steel reinforcing bars,
- Some of fibers are used to define nonlinear behavior of confined concrete which consists of core concrete,
- And other fibers are defined in unconfined concrete, which includes cover concrete.

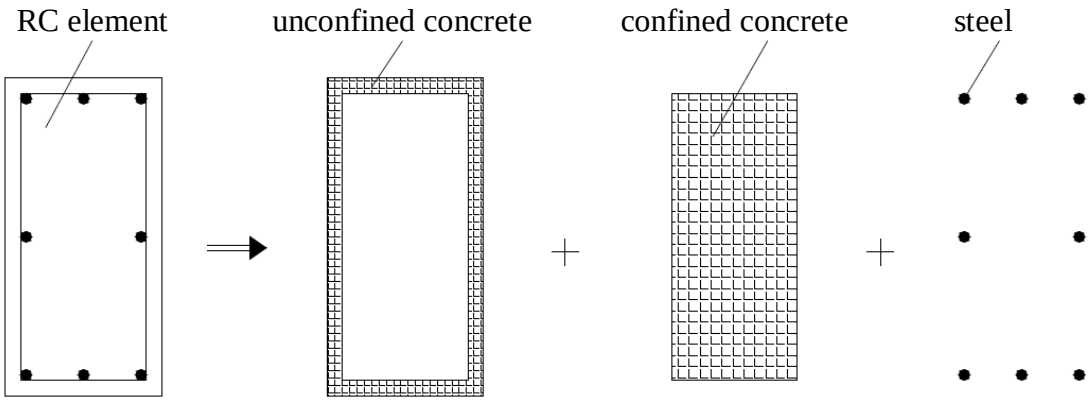

Figure 3.3: A typical fiber model of the reinforced concrete element of Seismostruct [17].

3.2.4 Applied Loads and Ground Motions

In order to perform design and analysis, all possible load cases are assigned. These are as follows:

3.2.4.1 Gravity Loads

Gravity loads on the structure include the self weight of beam, column, slabs, walls and the other permanent members. The self weight of beams, columns, and slabs is automatically considered by the program itself. The wall loads have been calculated and assigned as uniformly distributed loads on the beams. Only gravity loads have been used for design on all models.

- Wall load as a uniform distributed load 10 kN/m is applied to all beams.
- 2 kN/m² live load (L.L.) has been assigned for residential building.
- 0.7 kN/m² dead load (D.L.) as a weight of gypsum plaster and tile has been assigned for residential building [19].
- 1.2 (D.L. +F+T_e) +1.6 (L.L. +H) +0.5 ($L_r$or S or R) is a load combination according to ACI318-02 [24]. In this study, just D.L. and L.L are considered.

3.2.4.2 Seismic Lateral Loads

The lateral loads in different floor levels have been calculated corresponding to fundamental period and are applied to models in order to run the static pushover analysis.

The triangular lateral load pattern is applied to the structures according to the Turkish Earthquake Code 2007 [20]. The lateral load pattern is calculated according following formulas:

$$F_i = (V_t - \Delta F_N)\frac{w_i H_i}{\sum_{j=1}^{N} w_j H_j} \quad \text{(Eq.3.1)}$$

Where F_i= Design seismic load acting at i'th storey

V_t= Total base shear, shall be determined by the following formula:

$$V_t = \frac{W A(T_1)}{R_a(T_1)} \quad \text{(Eq.3.2)}$$

$$\Delta F_N = 0.0075\, N\, V_t \quad \text{(Eq.3.3)}$$

ΔH_N= Additional equivalent seismic load acting on the N'th storey (top) of the building.

N= Total number of stories of building from the foundation level (in buildings with rigid peripheral basement walls, total number of stories from the ground floor level).

H_i= The height of i'th storey of building measured from the top foundation level (in buildings with rigid peripheral basement walls, the height of i'th storey of building measured from the top of ground floor level).

$$w_i = g_i + n\, q_i \quad \text{(Eq.3.4)}$$

w_i= The weight of i'th storey of building by considering live load participation factor

g_i= A total dead load at i'th storey of building

n= Live load participation factor, it is given in Table 3.3 [20].

Table 3.3: Live load participation factor

Purpose of occupancy of building	$\boldsymbol{n}$
Depot, warehouse, etc.	0.8
School, dormitory, sport facility, cinema, theatre, concert hall, car park, restaurant, shop, etc.	0.6
Residence, office, hotel, hospital, etc.	0.3

q_i= Total live load at i'th storey of building

W = Total weight of a building calculated by considering live load participation factor.

$$W = \sum_{i=1}^{N} w_i \quad \text{(Eq.3.5)}$$

$A(T_1)$= Spectral acceleration coefficient relative to first natural period of building

$$A(T_1) = A_0\, I\ \ S(T_1) \quad \text{(Eq.3.6)}$$

T_1= First natural vibration period of building

A_0 = Effective ground acceleration coefficient, this factor which is shown in Table 3.4 [20]. It is dependent on seismic zone, for the present study, Famagusta city from north Cyprus has been chosen and all local and seismic characteristics are selected according to the Turkish Earthquake Code 2007 [20].

Table 3.4: Effective ground acceleration coefficient (A_0)

Seismic zone	$\boldsymbol{A_0}$
1	0.4
2	0.3
3	0.2
4	0.2

$I =$ Building importance factor, it has been selected in Table 3.5 [20].

Table 3.5: Building importance factor

Purpose of Occupancy or Type of Building	**Importance Factor**
1. Buildings required to be utilized after the earthquake and buildings containing hazardous material: a) Buildings required to be utilized immediately after the earthquake (Hospitals, dispensaries, etc). b) Buildings containing or storing Toxic, explosive and flammable materials, etc.	1.5
2. Intensively and long-term occupied buildings: a) Schools, other educational buildings and facilities, dormitories and hotels, military barracks, prisons, etc. b) Museums	1.4
3. Intensively but short-term occupied buildings: Sport facilities, cinema, and concert halls, etc.	1.2
4. Other buildings:	1

$S(T) =$ Spectrum coefficient shall be determined by the following formula, depending on the local site conditions and the building natural period (T):

$$S(T) = 1 + 1.5\frac{T}{T_A} \qquad (0 \le T \le T_A) \qquad \text{(Eq.3.7a)}$$

$$S(T) = 2.5 \qquad (T_A < T \le T_B) \qquad \text{(Eq.3.7b)}$$

$$S(T) = 2.5\left[\frac{T_B}{T}\right]^{0.8} \qquad (T_B < T) \qquad \text{(Eq.3.7c)}$$

It is important to describe spectrum characteristic periods (T_A ,T_B) which is depend on local site classes (Z) as shown in the Table 3.6 [20] and Table 3.7 [20]. In order to find a local class site, initially, soil group shall be specified. Soil class site in Famagusta has been defined as class D [21].

Table 3.6: Local site classes

Local site class	**Soil group, according to topmost layer thickness (h_1)**
Z1	Group (A) soils Group (B) soils with h_1 ≤15m
Z2	Group (B) soils with h_1 ≥15m Group (C) soils with h_1 ≤15m
Z3	Group (C) soils with 15m < h_1 ≤ 50m Group (D) soils with h_1 ≤ 10m
Z4	Group (C) soils with h_1 >50m Group (D) soils with h_1 > 10m

Table 3.7: Spectrum characteristic periods (T_A, T_B)

Local site class	T_A **(seconds)**	T_B **(seconds)**
Z1	0.10	0.30
Z2	0.15	0.40
Z3	0.15	0.60
Z4	0.20	0.90

3.2.4.2.1 Earthquake Parameters

The earthquake parameters, regarding previous tables are tabulated in table 3.8.

Table 3.8: Earthquake parameters

Earthquake load parameters	**Value**
Seismic zone	2
Effective ground acceleration coefficient (A_0)	0.3
Building importance factor (I)	1
Soil class (Z)	Z4 (T_A=0.2, T_B=0.9)
Live load participation factor (n)	0.3

$R_a(T)$= Seismic load reduction factor shall be determined according following formula:

$R_a(T)$=1.5+$(R-1.5)\frac{T}{T_A}$ $(0 \leq T \leq T_A)$ (Eq.3.8a)

$R_a(T) = R$ ($T_A < T$) (Eq.3.8b)

R= Structural behavior factor

According to TEC 2007 [20], for the cast in-site reinforced concrete buildings in which seismic loads are fully resisted by frames and systems of high ductility level, structural behavior factor (R) = 8 .

3.2.4.3 Selecting and Scaling of Ground Motion Records

Application of IDA involves a series of non-linear dynamic time-history analysis, thus it is essential to have a suitable ground motion record series [22]. Ground motion selection for time-history analysis is a very complicated task since they will have different effects on structural response due to differences in their characteristics. In addition to this, since the accuracy of IDA results is affected by the number of selected ground motions, this issue becomes more complicated. The ground motions have been downloaded from the PEER website [23]. The user-defined spectrum is selected as a model to generate a target spectrum, the spectrum acceleration coefficient ($A(T)$) versus time period (T) coordinates have been uploaded to the website in the form of excel file.

$A(T) = A_0\, I\; S(T)$ (Eq.3.9)

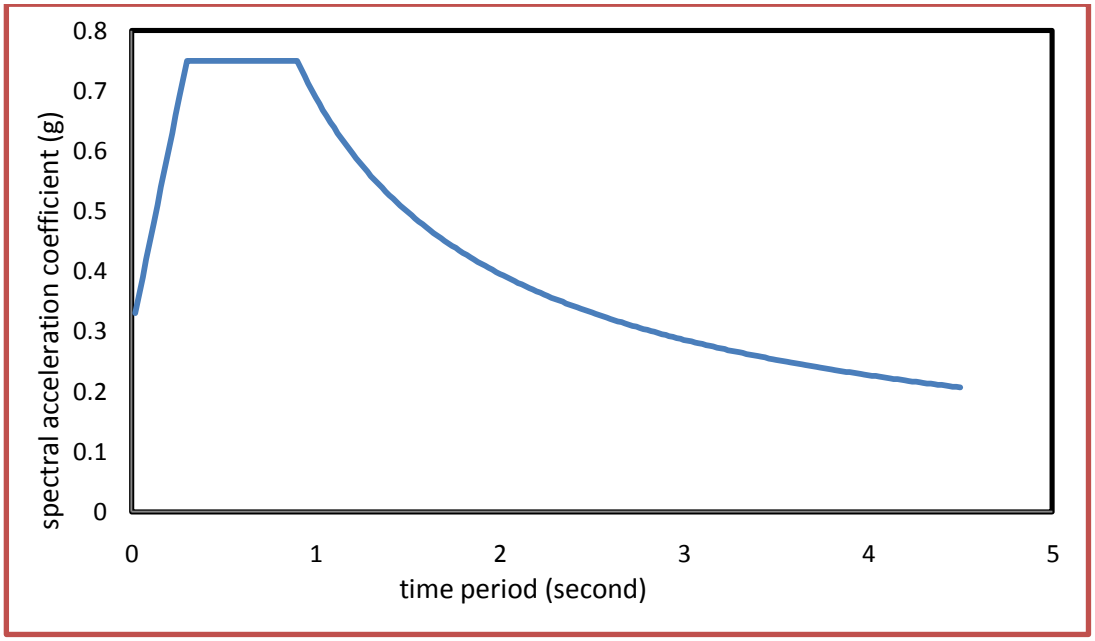

Figure 3.4: Spectral acceleration coefficient versus time period

The limitations were chosen to balance selection of large motions, summary of PEER ground motion database search criteria:

- Duration: 10-15 second
- Soil shear wave velocity (Vs): <220 m/second, (soil type D is considered)
- Closest distance to rupture plane (Rrup): (0-40km) assumed
- Joyner-Boor distance to rupture plane (Rjb): (0-40km) assumed

Table 3.9: Characteristics of earthquake records used for IDA [23]

Record	Station	Earthquake Date	Magnitude	Vs (m/sec)	Fault Type	Rjp (km)	Rrup (km)
1.Imperical Valley (TH1)	Brawley Airport	10/15/1979	6.53	208.7	Strike Slip	8.5	10.4
2.Imperical Valley (TH2)	EC CO Centre FF	10/15/1979	6.53	192.1	Strike Slip	7.3	7.3
3.Imperial Valley (TH3)	EC Meloland Overoass FF	10/15/1979	6.53	186.2	Strike Slip	0.1	0.1
4.Imperial Valley (TH4)	El Centro array#10	10/15/1979	6.53	202.8	Strike Slip	6.2	6.2
5.Imperial Valley (TH5)	El Centro array#3	10/15/1979	6.53	162.9	Strike Slip	10.8	12.8
6.Imperial Valley (TH6)	El Cennto array#4	10/15/1979	6.53	208.9	Strike Slip	4.9	7
7.Imperial Valley (TH7)	El Centro arra#6	10/15/1979	6.53	203.2	Strike Slip	0	1.4
8.Imperial Valley (TH8)	Holtville Post Office	10/15/1979	6.53	202.9	Strike Slip	5.5	7.7
9.Superstition Hills (TH9)	Wildlife liquefy array	11/24/1987	6.22	207.5	Strike Slip	17.6	17.6

TH= Time history, it is used instead name of ground motions.

Next issue after selecting scaled ground motions from the PEER database website is to apply them to the models in the Seismostruct software. Seismostruct software has a scale factor module when incremental dynamic analysis is to be performed, in the present study, scale factors (0.1, 0.2, 0.3, 0.4, 0.5, 0.6 …) are applied until first collapse criteria will appear.

3.2.5 Performance Criteria Parameters

It is paramount that analysis and engineers are capable of identifying the instants at which different performance limit states (e.g. non-structural damage, structural damage, and collapse) are reached. This can be efficiently carried out in Seismostruct through the definition of performance criteria module, whereby the attainment a given threshold value of material strain, sectional curvature, element-chord rotation and/or element shear during the analysis of a structure is automatically monitored by the program.

The type of criteria to be used does clearly depend on the objectives of the user. However, within the context of a fiber-based modeling approach, such as its implemented in Seismostruct, material strains do usually constitute the best parameter for identification of the performance state of a given structure. The available on material strains are [19]:

- **Cracking of structural elements:** It can be identified by checking for concrete strains. [Typical value: +0.0001],
- **Spalling of cover concrete:** It can be identified by checking for cover concrete strains. [Typical value: -0.002],
- **Crushing of core concrete:** It can be identified by checking for core concrete strains. [Typical value: -0.006],

- **Yielding of steel:** It can be identified by checking for steel strains. [Typical value: +0.0025],
- **Fracture of steel:** It can be identified by checking for steel strains. [Typical value: +0.060].

3.3 Frame Modeling

The 3D reinforced concrete buildings have been designed by Etabs software and the exterior frame in the designed model is exported to remodel it by Seismostruct software, in order to run both static pushover and incremental dynamic analysis.

3.3.1 Three Storey Building

The three storey building is considered as a low rise building. Its detail is shown in Figure 3.5:

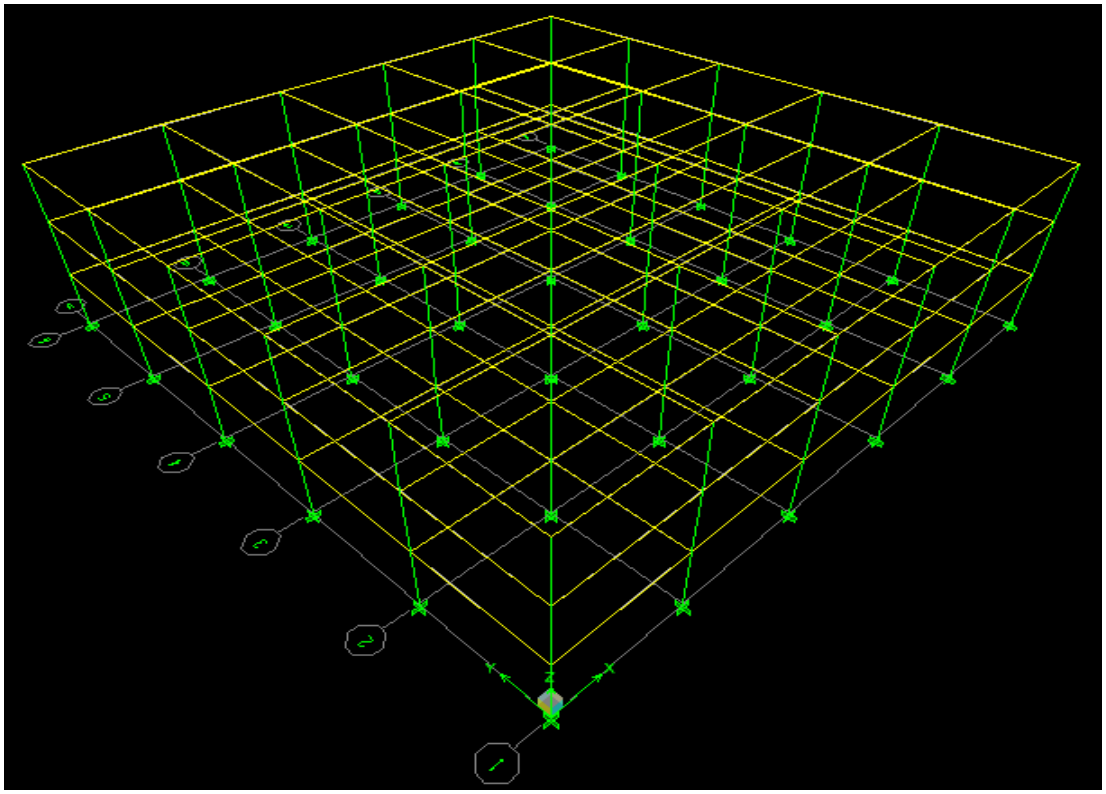

a- 3-D view of the three storey building created by Etabs

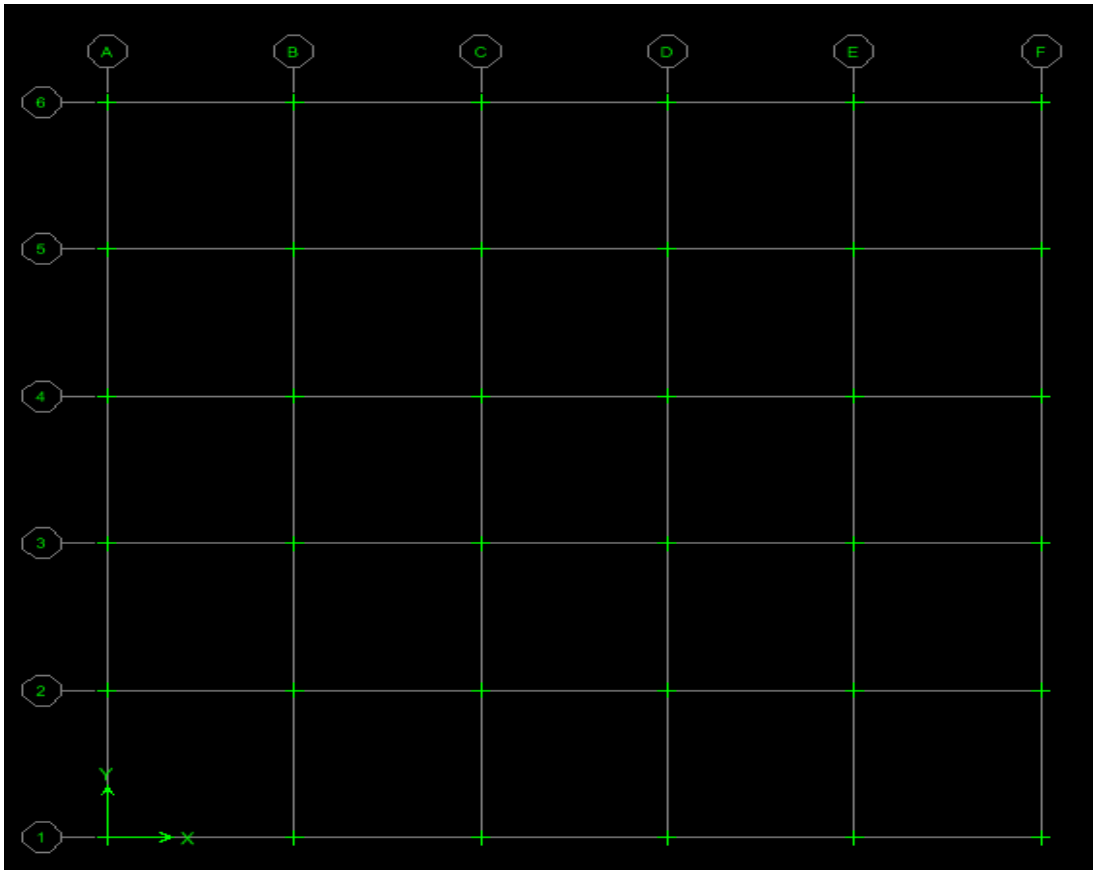

b- Plan view of the three storey of building created by Etabs

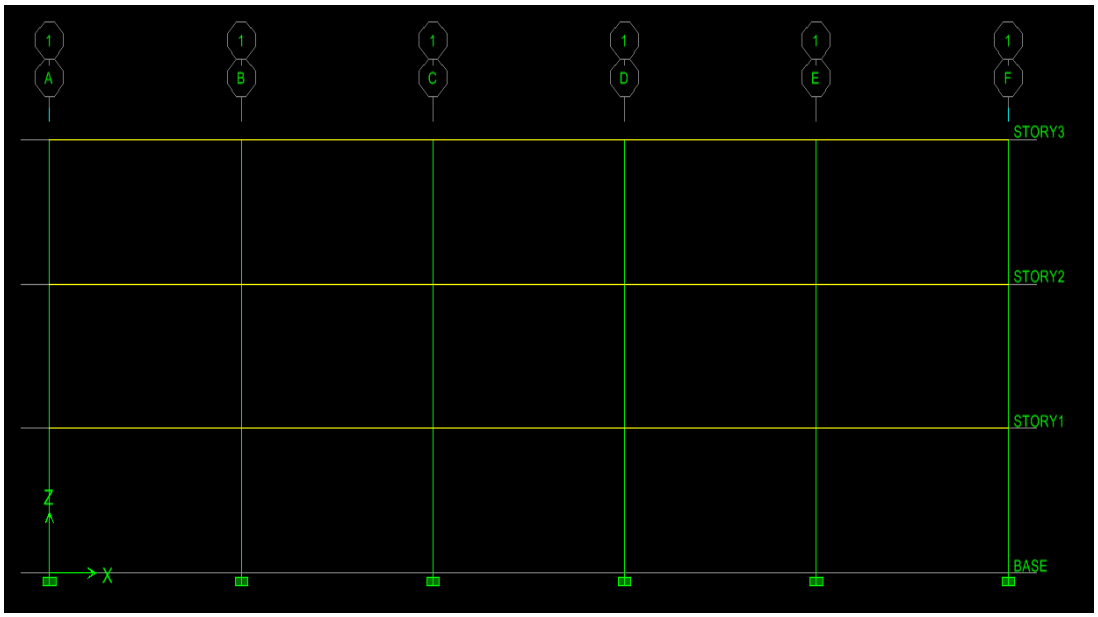

c- Elevation view of the three storey building created by Etabs

Figure 3.5: Geometric views of the three storey building

3.3.1.1 Modeling of the Frame by Using Seismostruct Software

Details of the sections and discretization views are described and shown below:

- Columns: 0.35m×0.35m rectangular section, 8 No.16 mm reinforcement
- Beams: 0.40m×0.35m rectangular section, 6 No .18 mm reinforcement
- Braces: UPN200 European standard channels with tapered flanges

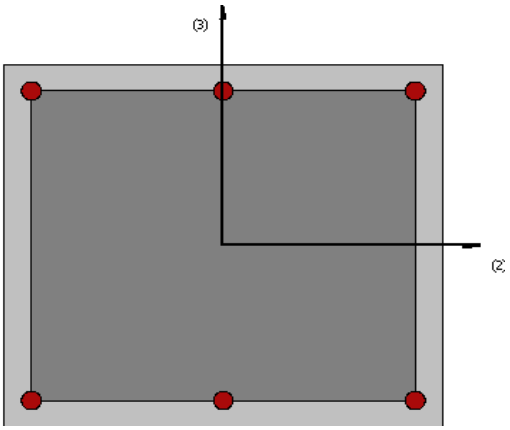

a- Beam section (0.40m×0.35m)

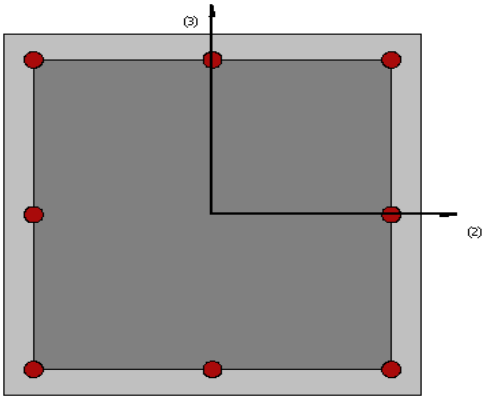

b- Column section (0.35m×0.35m)

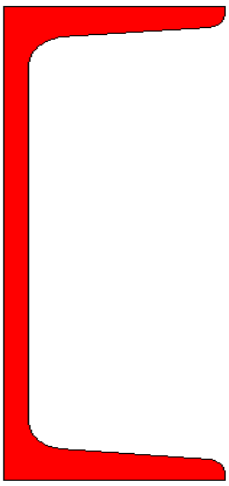

c- UPN200 brace section

Figure 3.6: Sectional members for the three storey frame

For all element types, the number of section fibres used in equilibrium computations carried out at each of the element's integration section need to be defined, it is named as discretization.

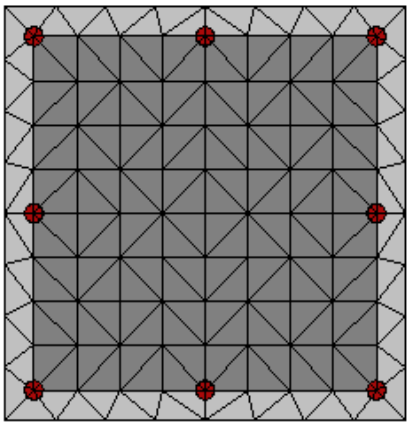

a- Beam (0.40m×0.35m)

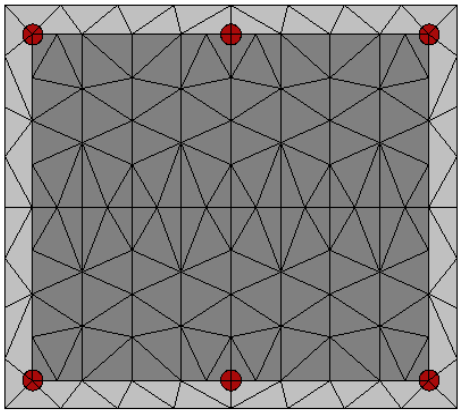

b- Column (0.35m×0.35m)

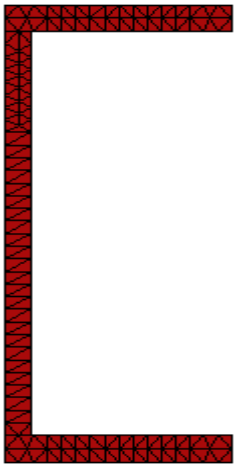

c- UPN200

Figure 3.7: Discretization of sections of the three storey frame's sections

Models with and without braces are shown in Figure 3.8:

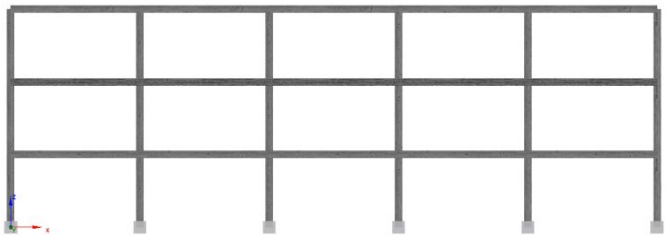

a- Frame without bracing

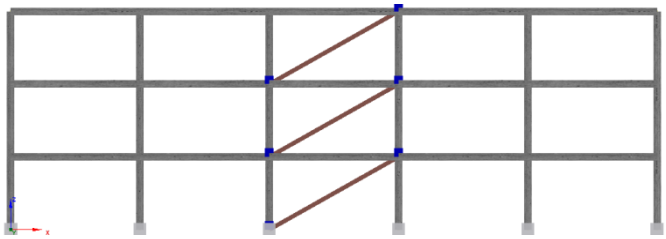

b- Frame with Diagonal bracing

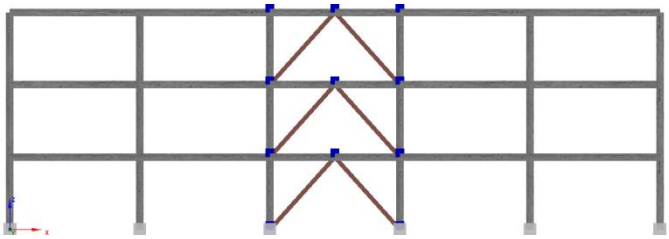

c- Frame with Inverted-V bracing

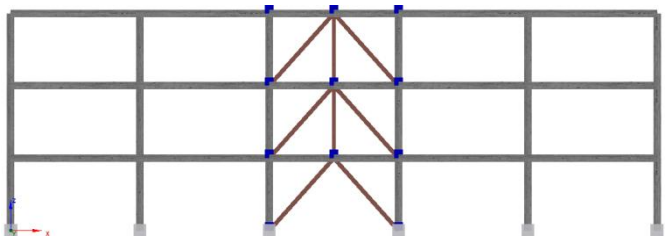

d- Frame with Zipper bracing

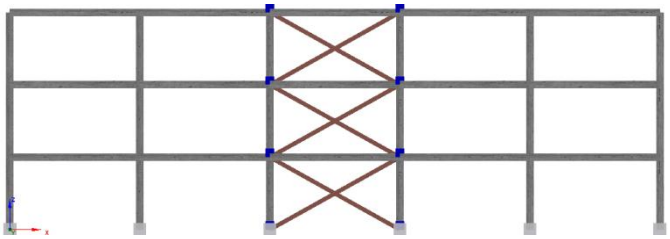

e- Frame with X- bracing

Figure 3.8: The three storey frame with and without bracings

3.3.2 Six Storey Building

The six storey building is considered as a mid-rise building. Its detail is shown in Figure 3.9:

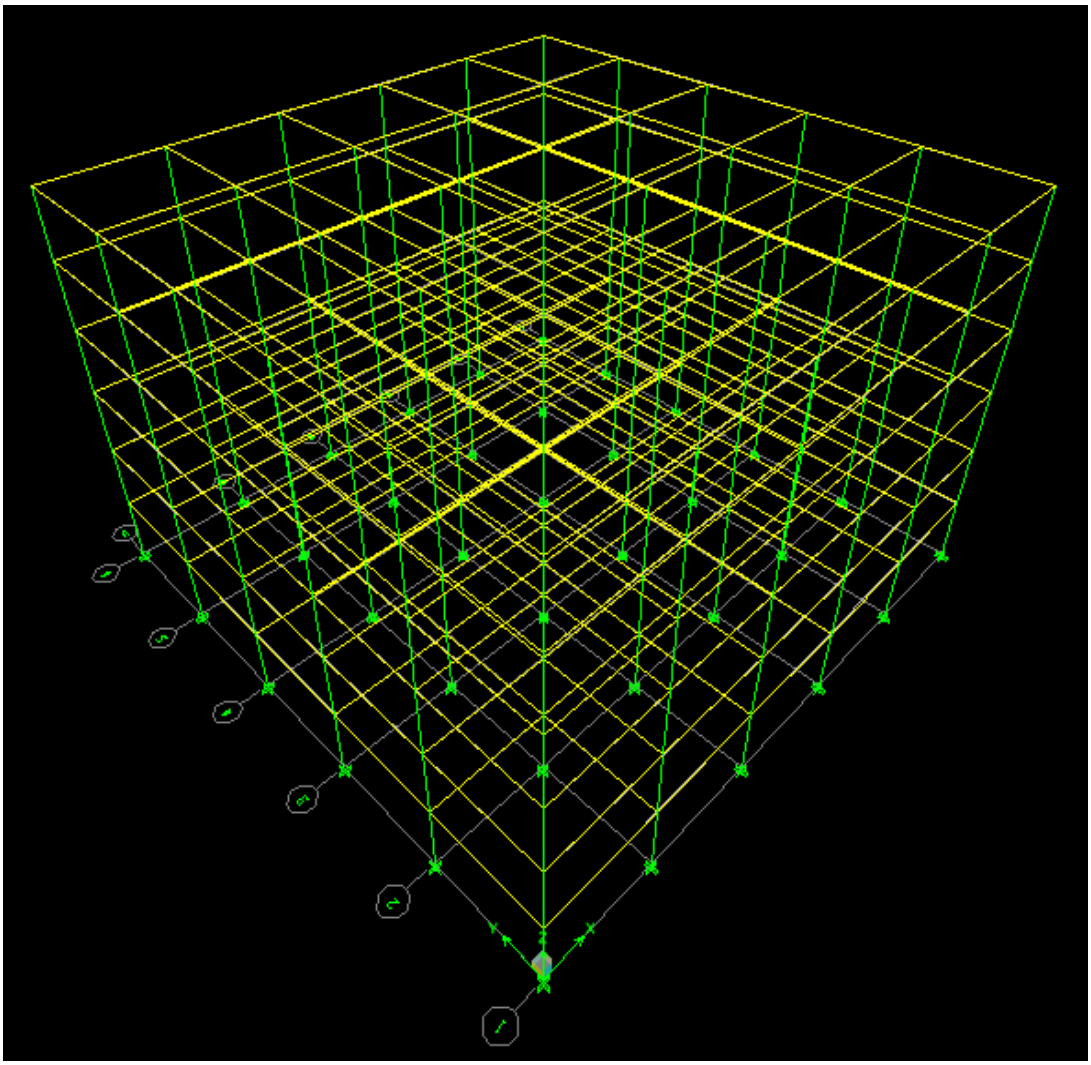

a- 3-D view of the six storey building created by Etabs

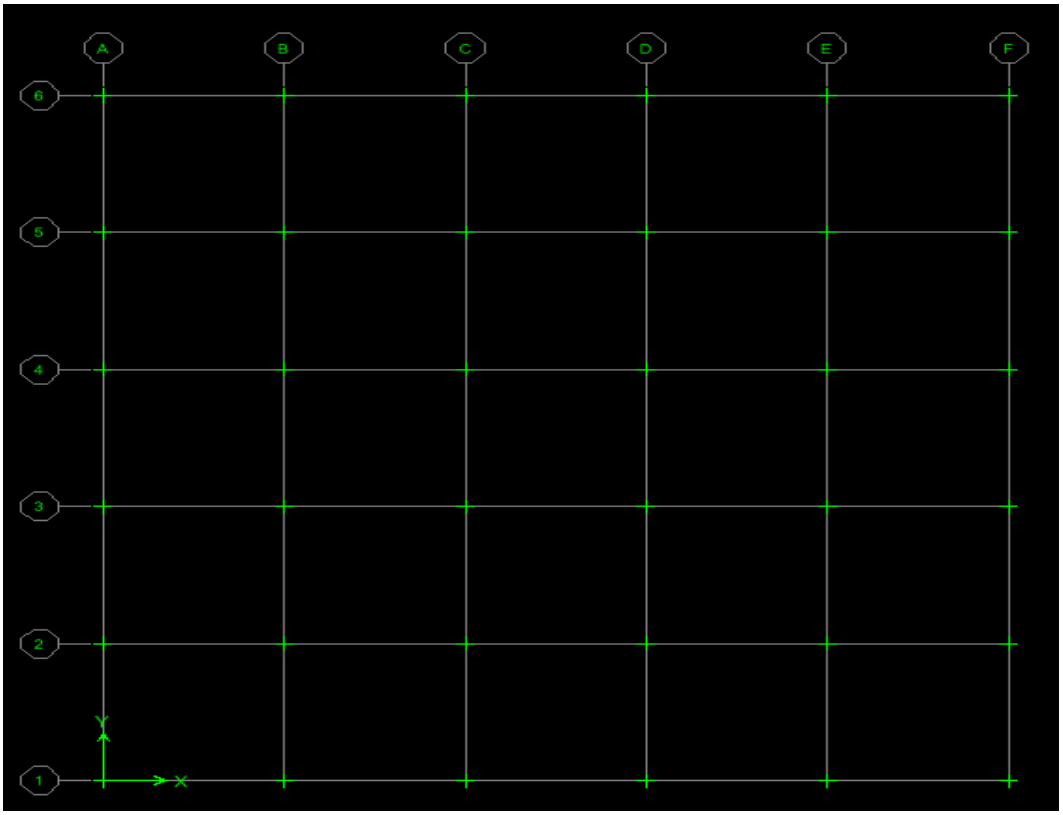

b- Plan view of the six storey of the building created by Etabs

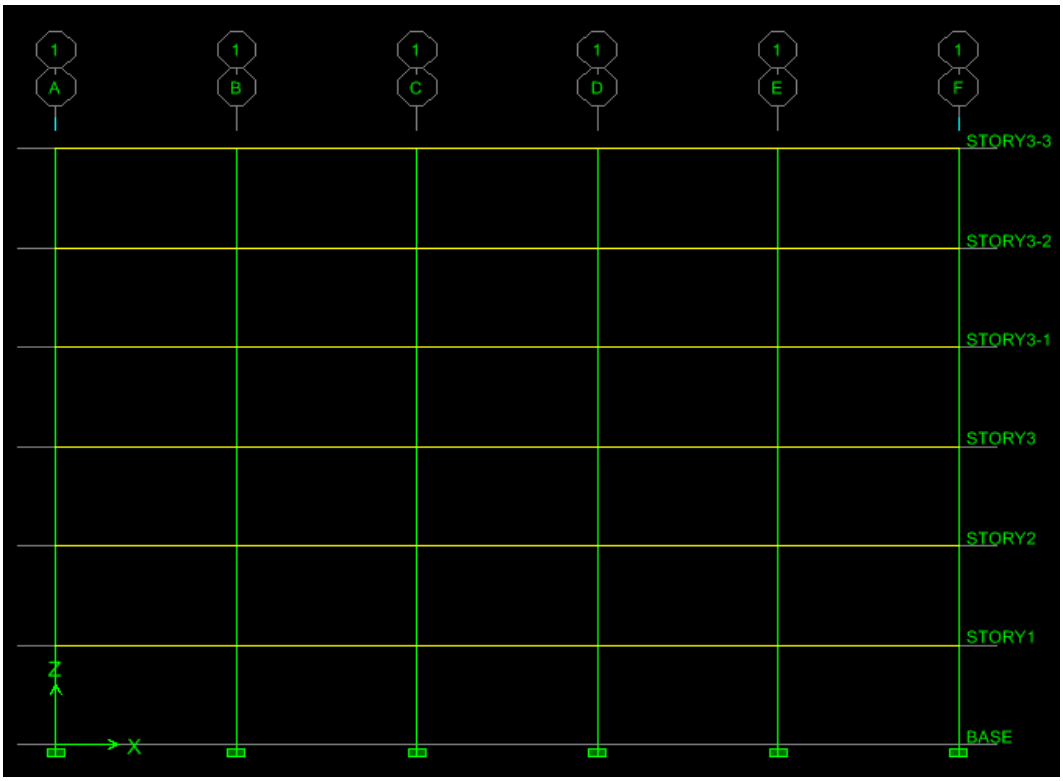

c- Elevation view of the six storey building created by Etabs

Figure 3.9: Geometric views of the six storey building

3.3.2.1 Modeling of the Frame by Using Seismostruct Software

Details of the sections and discretization views are described and shown in Figures 3.10 and 3.11:

- Columns: 0.45m×0.45m rectangular section, 8 No.20 mm reinforcement (1^{st},2^{nd}, and 3^{rd} storey)
- Columns: 0.35m×0.35m rectangular section, 8 No.16 mm reinforcement (4^{th}, 5^{th}, and 6^{th} storey)
- Beams: 0.40m×0.35m rectangular section, 6 No.18 mm reinforcement
- Braces: UPN200 European standard channels with tapered flanges

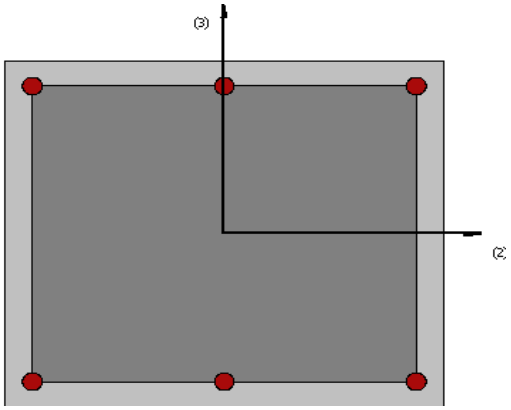

a- Beam section (0.40m×0.35m)

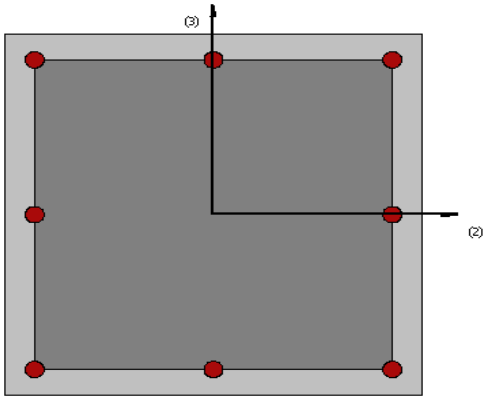

b- Column section (0.35m×0.35m)

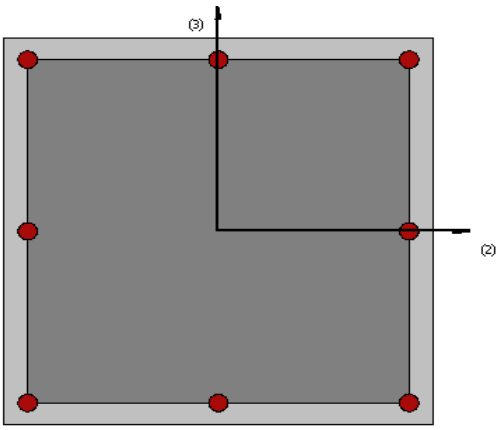

c- Column section (0.45m×0.45m)

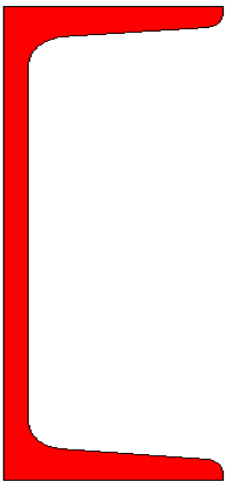

d- UPN200 brace section

Figure 3.10: Sectional member details of the six storey frame

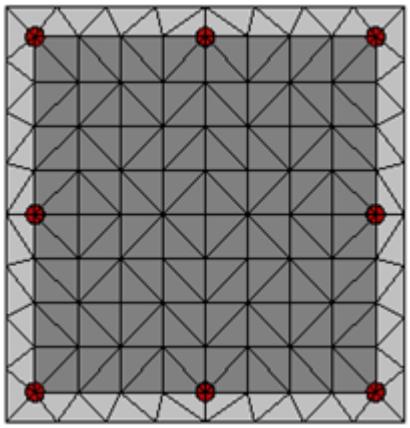

a- Beam (0.40m×0.35m)

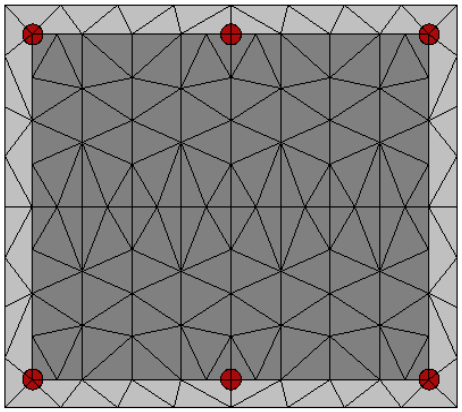

b- Column (0.35m×0.35m)

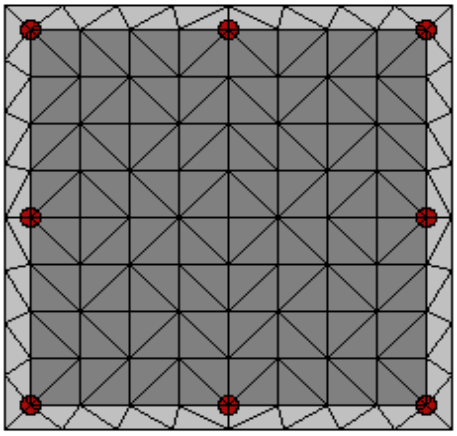

c- Column (0.45m×0.45m)

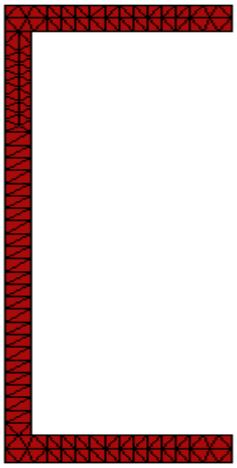

d- UPN200

Figure 3.11: Discretization of sections of the six storey frames

Models with and without braces are shown in the Figures 3.12 and 3.13:

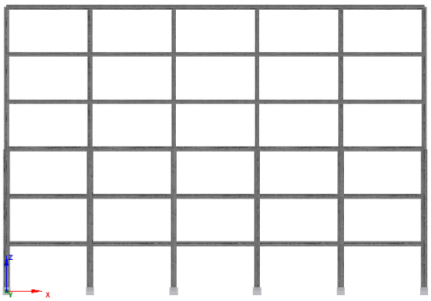

a- Frame without bracing

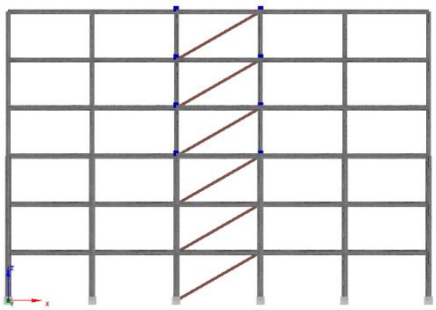

b- Frame with Diagonal bracing

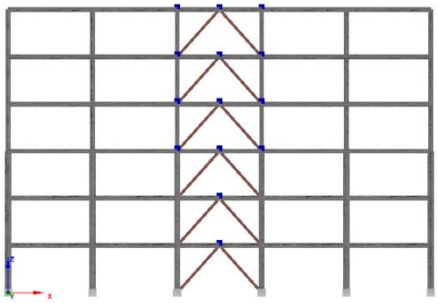

c- Frame with Inverted-V bracing

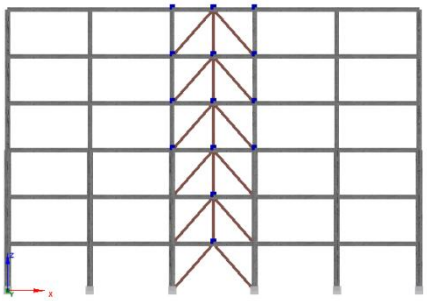

d- Frame with Zipper bracing

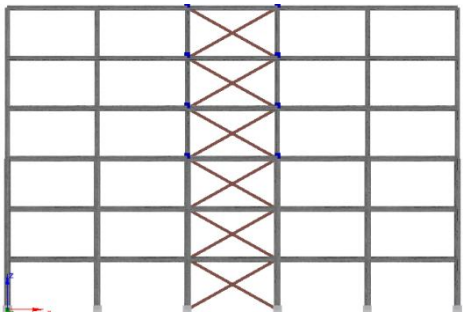

e- Frame with X- bracing

Figure 3.12: The six storey frame with and without bracings

3.3.3 Nine Storey Building

The nine storey building is considered as a mid-rise building. Its details are shown in Figure 3.13:

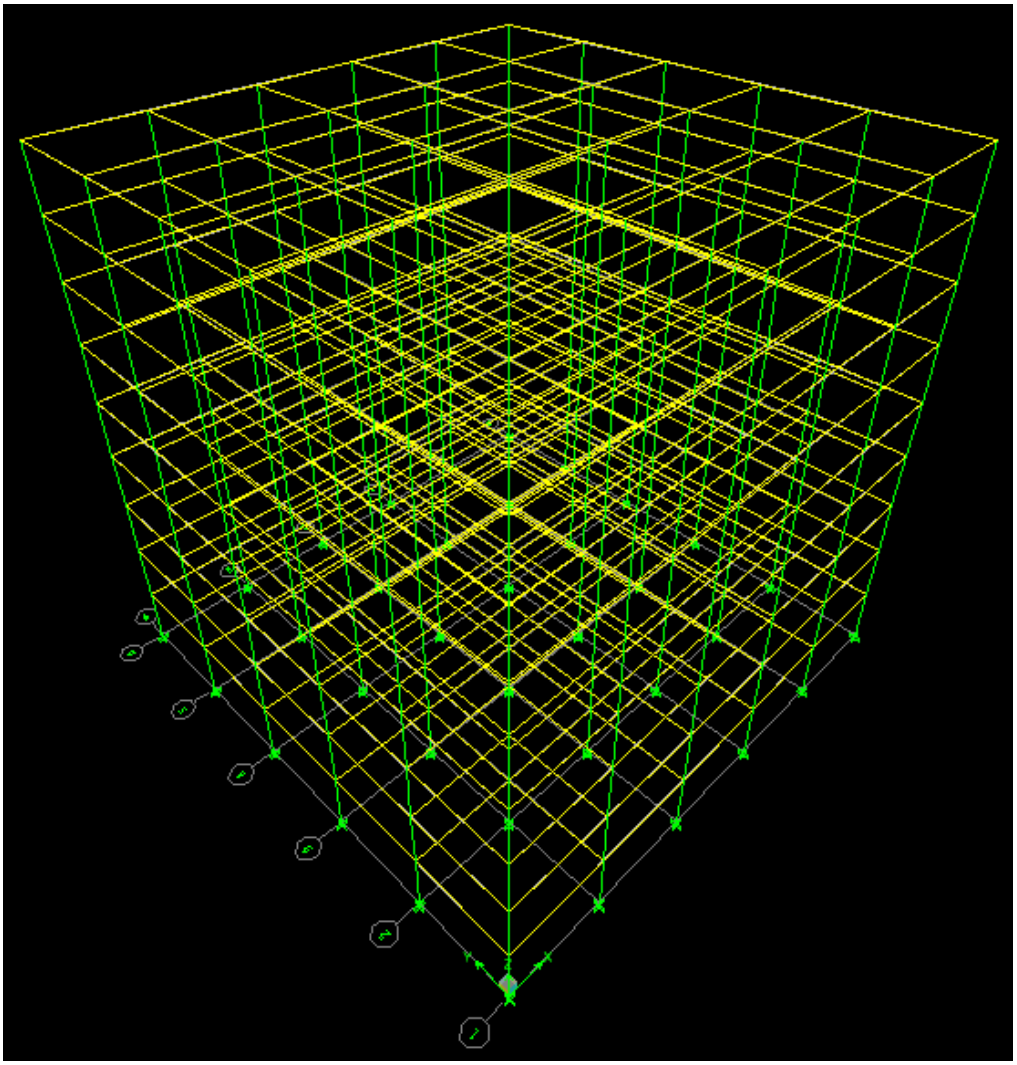

a- 3-D view of the nine storey building created by Etabs

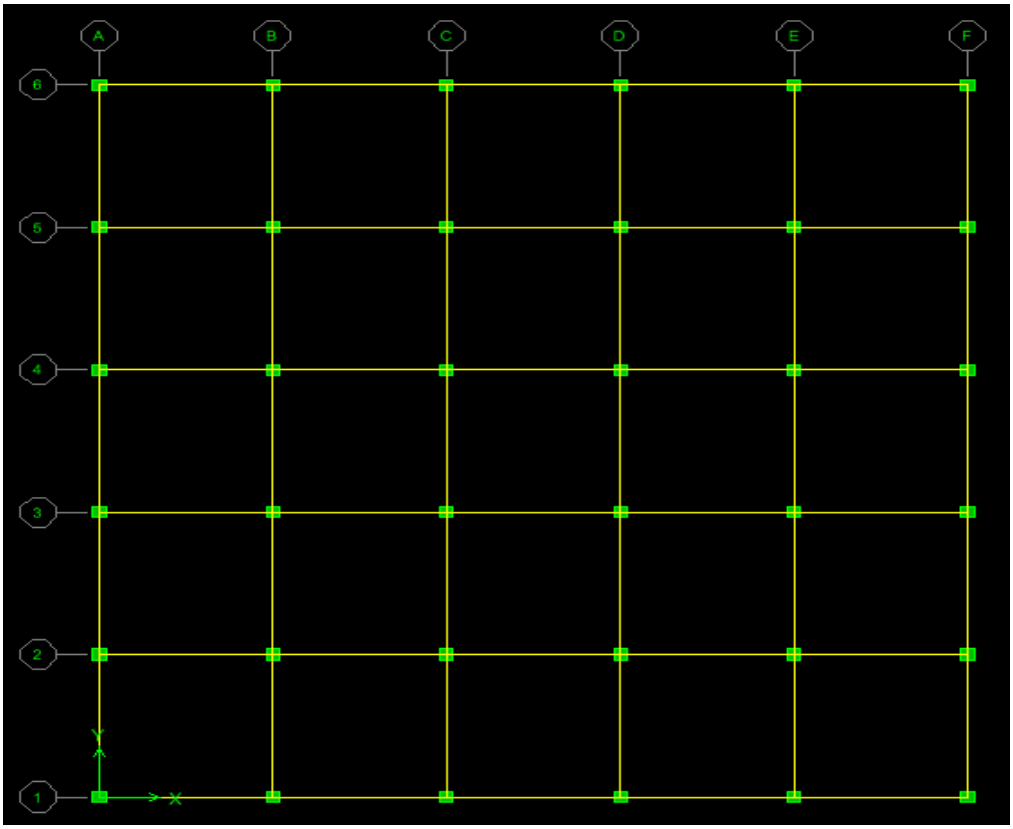

b- Plan view of the nine storey of the building created by Etabs

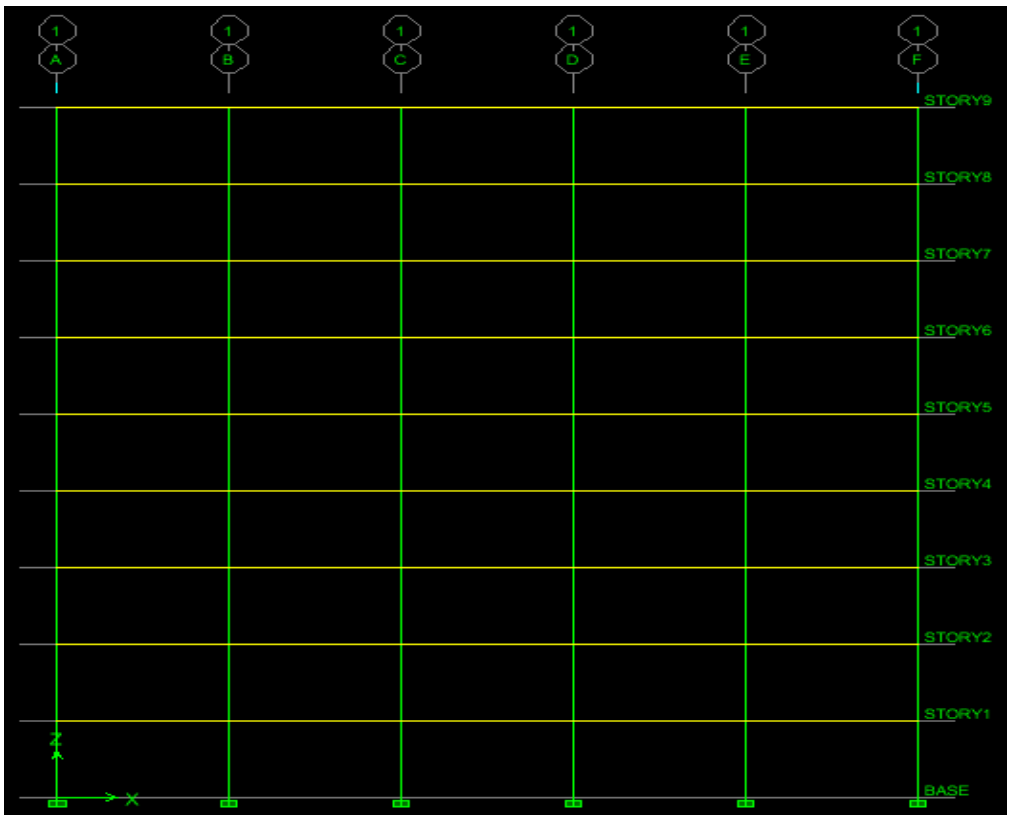

c- Elevation view of the nine storey building created by Etabs

Figure 3.13: Geometric views of the six storey building

3.3.3.1 Modeling of the Frame by Using Seismostruct Software

Details of the sections and discretization views are described and shown below:

- Columns: 0.55m×0.55m rectangular section, 12 No.20 mm reinforcement (1^{st},2^{nd}, and 3^{rd} storey)
- Columns: 0.45m×0.45m rectangular section, 8 No.20 mm reinforcement (4^{th}, 5^{th}, and 6^{th} storey)
- Columns: 0.35m×0.35m rectangular section, 8 No.16 mm reinforcement (7^{th}, 8^{th}, and 9^{th} storey)
- Beams: 0.40m×0.35m rectangular section, 6 No.18 mm reinforcement
- Braces: UPN200 European standard channels with tapered flanges

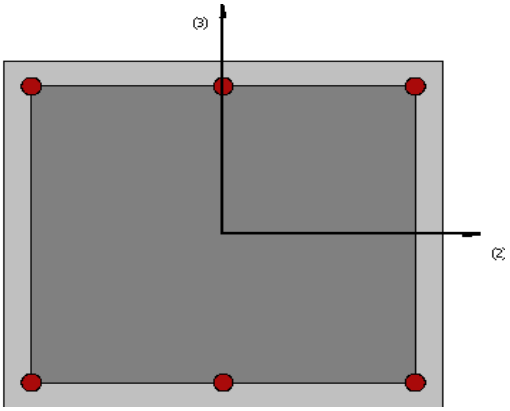

a- Beam section (0.40m×0.35m)

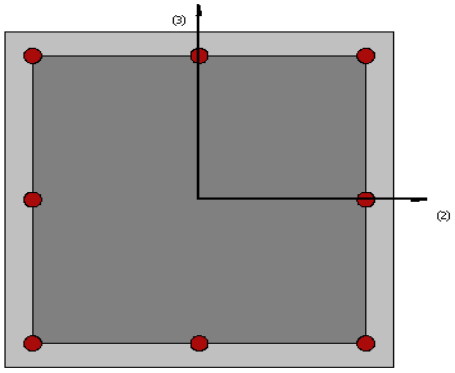

b- Column section (0.35m×0.35m)

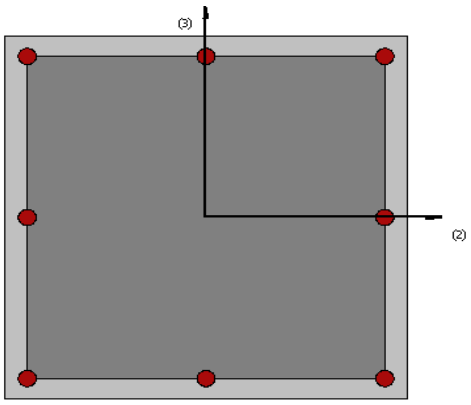

c- Column section (0.45m×0.45m)

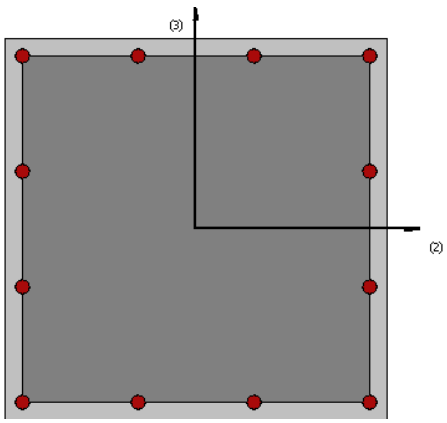

d- Column section (0.55m×0.55m)

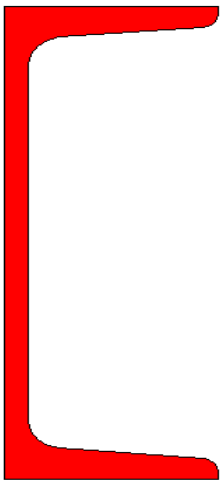

e- UPN200 brace section

Figure 3.14: Sectional members of the nine storey frame

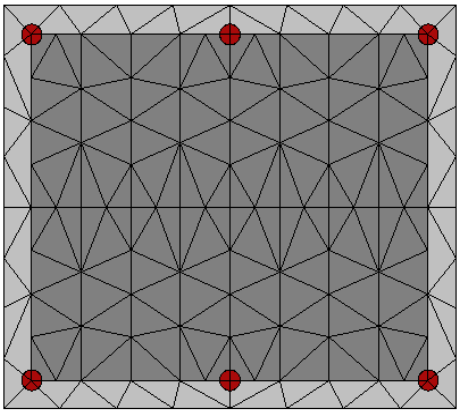

a- Beam (0.40m×0.35m)

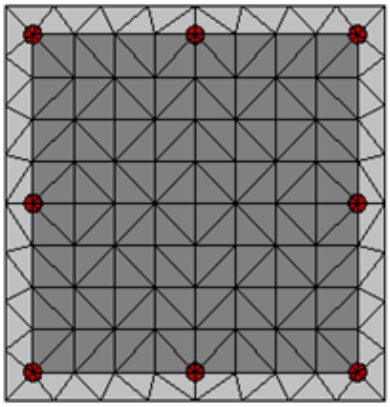

b- Column (0.35m×0.35m)

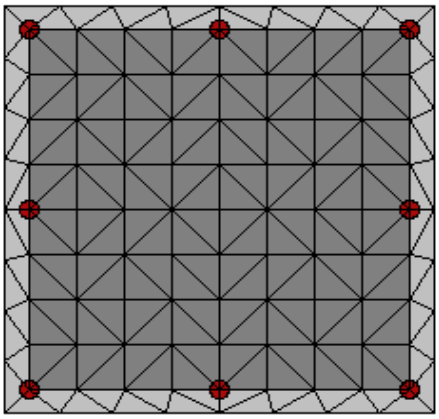

c- Column (0.45m×0.45m)

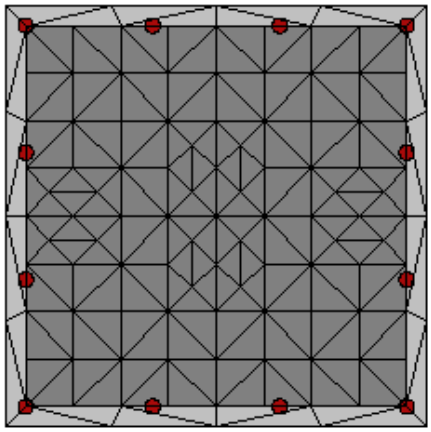

d- Column (0.55m*×0.55m)

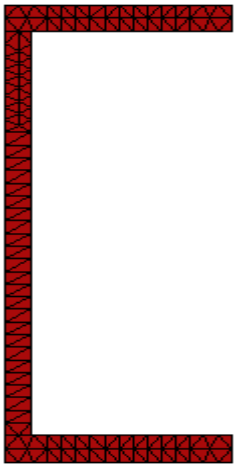

e- UPN200

Figure 3.15: Discretization of the sections of nine storey frame

Models with and without braces are shown in the figures below:

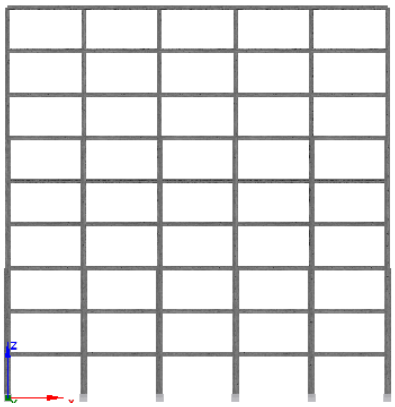

a- Frame without bracing

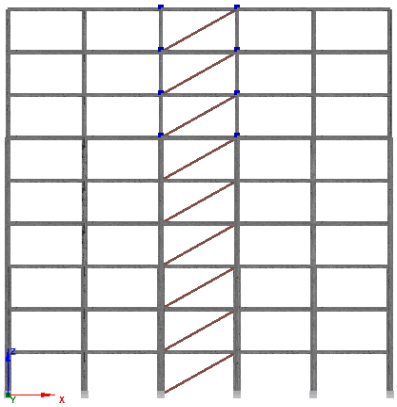

b- Frame with Diagonal bracing

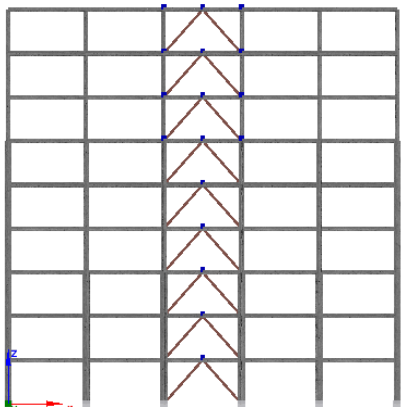

c- Frame with Inverted-V bracing

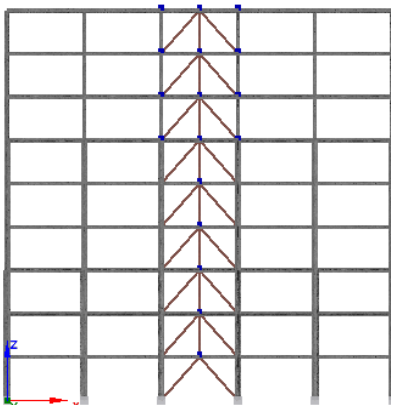

d- Frame with Zipper bracing

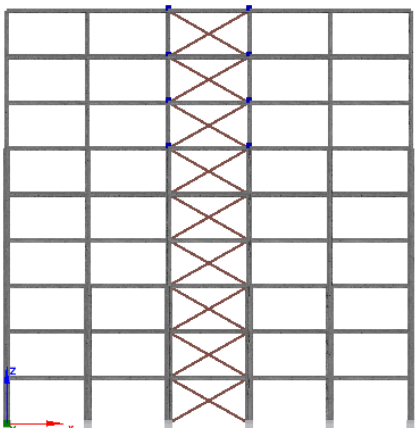

e- Frame with X- bracing

Figure 3.16: The nine storey frame with and without bracings

3.3.4 Twelve Storey Building

The twelve storey building is considered as high rise building. Its details are shown in Figure 3.17:

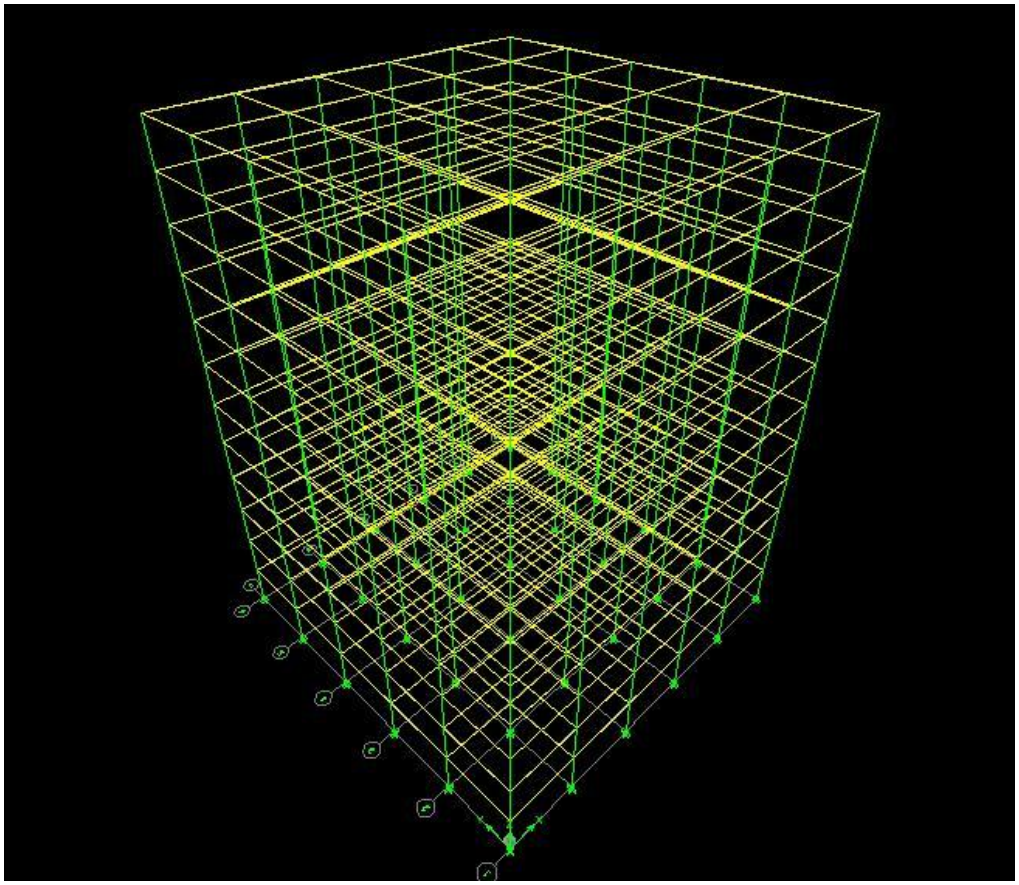

a- 3-D view of the twelve storey building created by Etabs

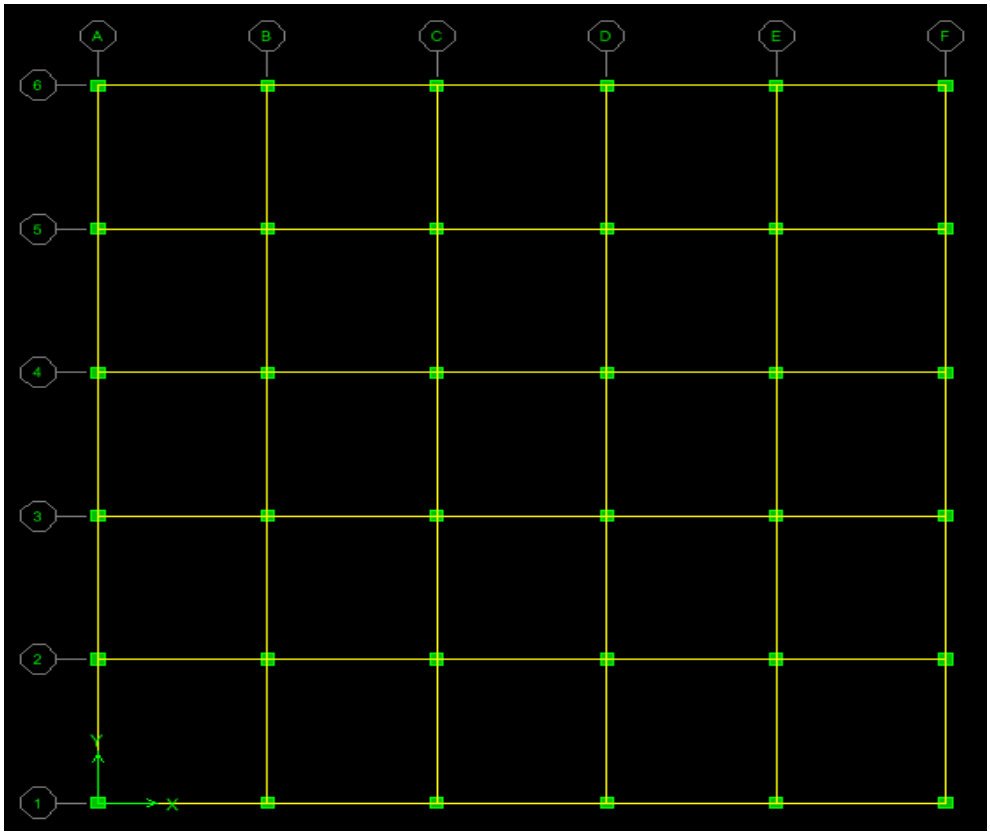

b- Plan view of the twelve storey of the building created by Etabs

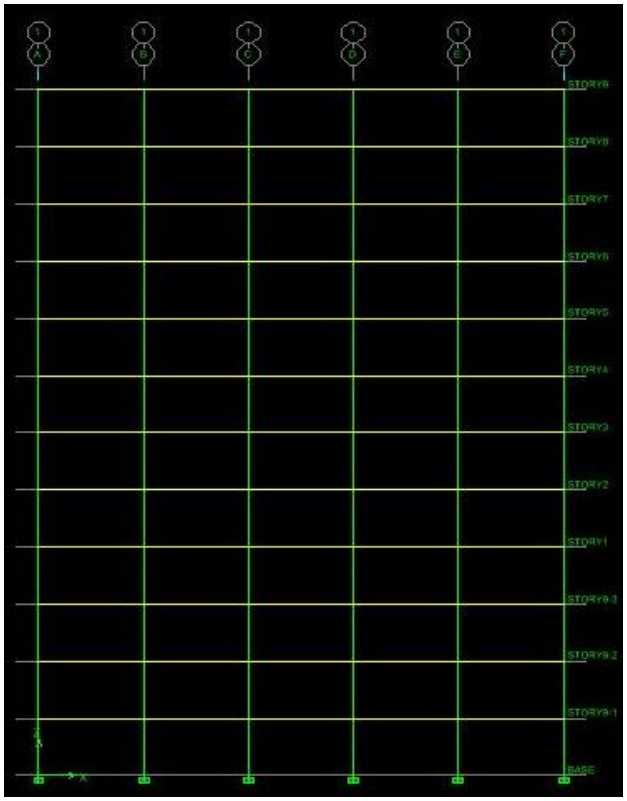

c- Elevation view of the twelve storey building created by Etabs

Figure 3.17: Geometric views of the twelve storey building

3.3.4.1 Modeling of the Frame by Seismostruct Software

Details of the sections and discretization views are described and shown in Figures 3.18 and 3.19:

- Columns: 0.65m×0.65m rectangular section, 12 No.20 mm reinforcement (1^{st},2^{nd}, and 3^{rd} storey)
- Columns: 0.55m×0.55m rectangular section, 12 No.20 mm reinforcement (4^{th}, 5^{th}, and 6^{th} storey)
- Columns: 0.45m×0.45m rectangular section, 8 No.20 mm reinforcement (7^{th}, 8^{th}, and 9^{th} storey)
- Columns: 0.35m×0.35m rectangular section, 8 No.16 mm reinforcement (10^{th}, 11^{th}, and 12^{th} storey)
- Beams: 0.40m×0.35m rectangular section, 6 No.18 mm reinforcement
- Braces: UPN200 European standard channels with taper flanges

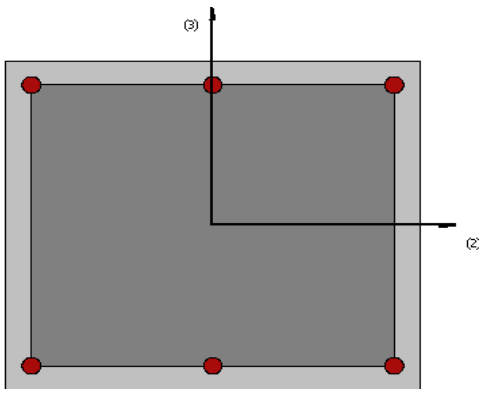

a- Beam section (0.40m×0.35m)

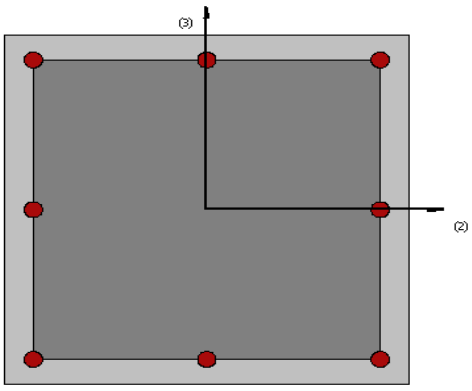

b- column section (0.35m×0.35m)

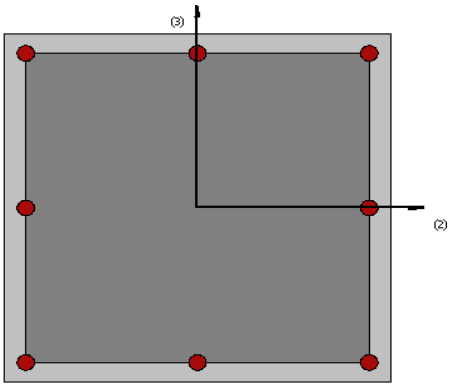

c- Column section (0.45m×0.45m)

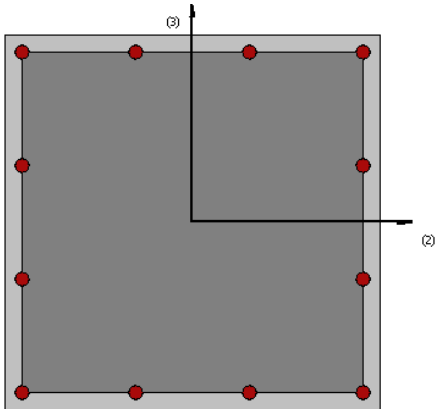

d- Column section (0.55m×0.55m)

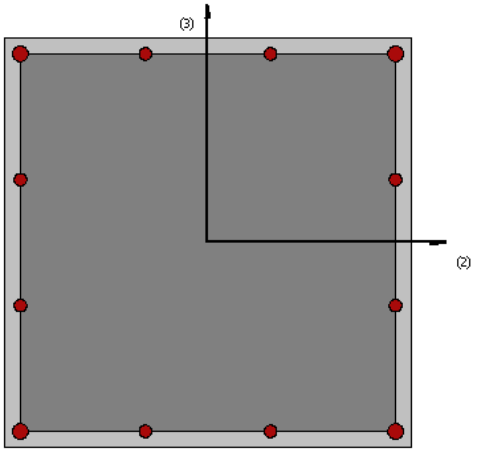

e- Column section (0.65m×0.65m)

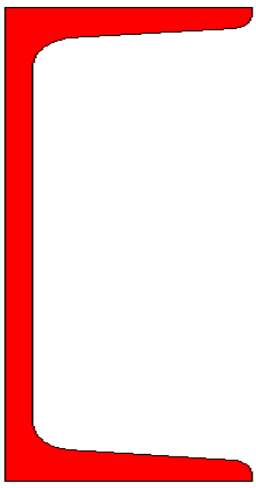

f- UPN200-brace section

Figure 3.18: Section members of the twelve storey frame

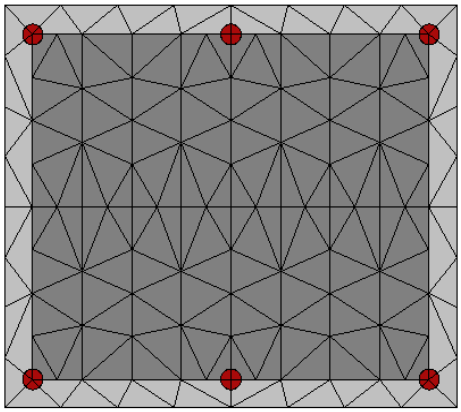

a- Beam (0.40m×0.35m)

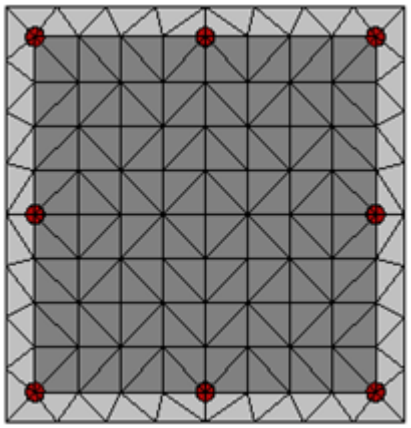

b- Column (0.35m×0.35m)

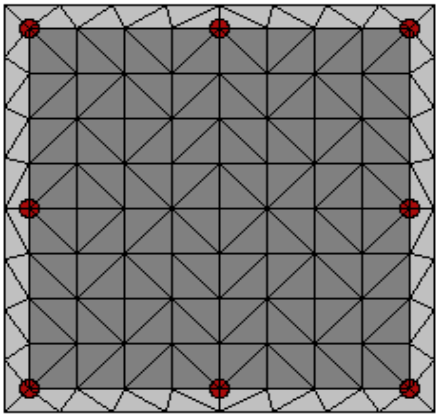

c- Column (0.45m×0.45m)

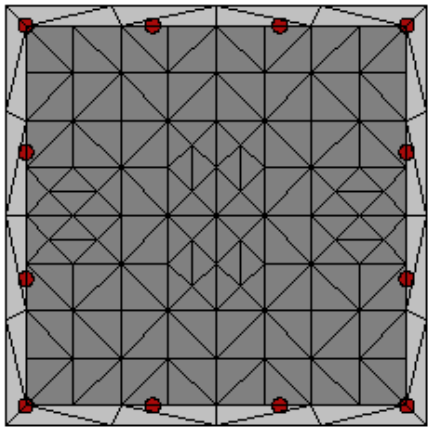

d- Column (0.55m×0.55m)

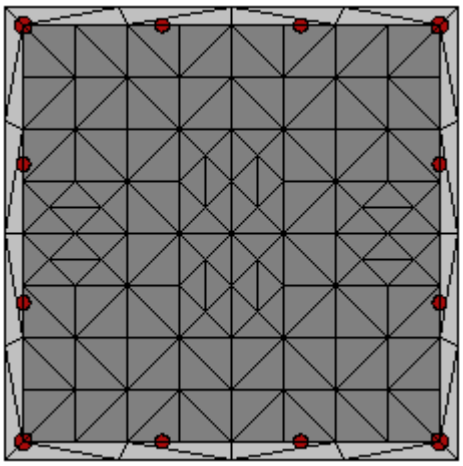

e- Column (0.65m×0.65m)

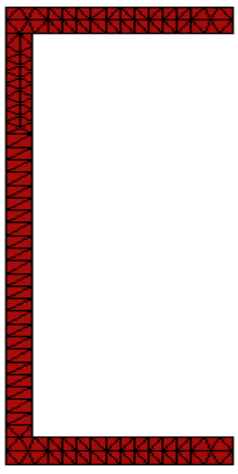

f- UPN200

Figure 3.19: Discretization of the sections of twelve storey frame

Models with and without braces are shown in the Figure 3.20:

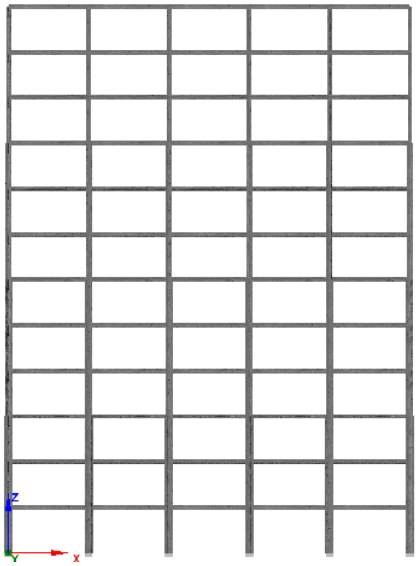

a- Frame without bracing

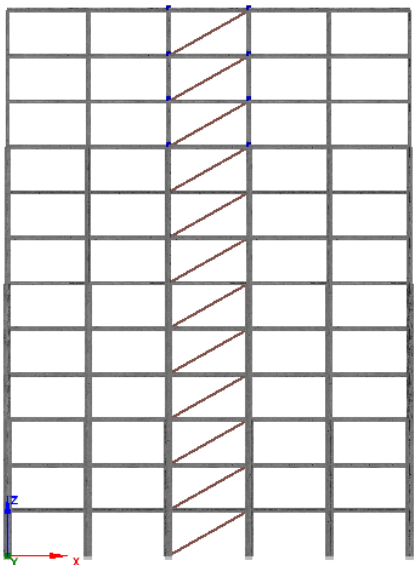

b- Frame with Diagonal bracing

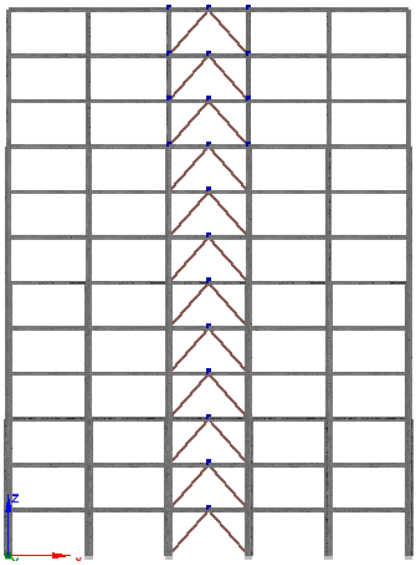

c- Frame with Inverted-V bracing

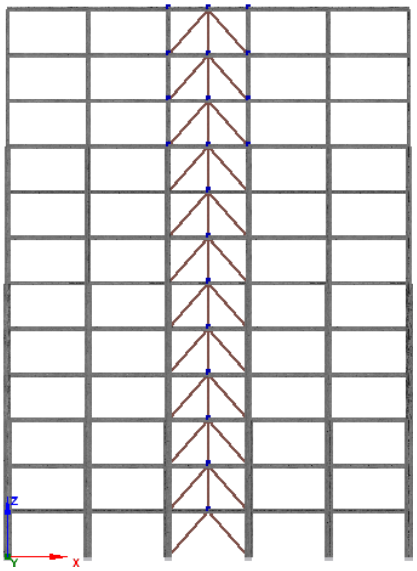

d- Frame with Zipper bracing

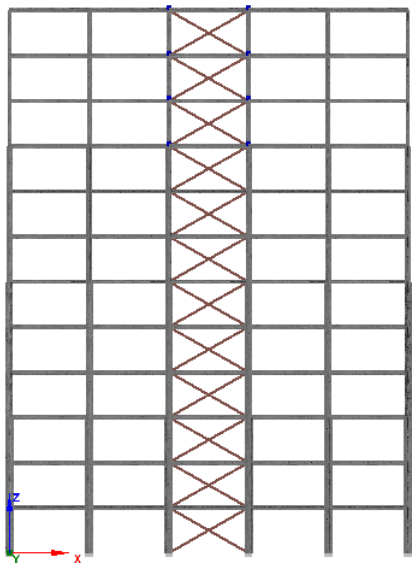

e- Frame with X- bracing

Figure 3.20: The twelve storey frame with and without bracings

3.4 Analysis of the Structures

In the present study, two types of analysis procedure have been performed, which are:

- Pushover analysis
- Incremental dynamic analysis

3.4.1 Pushover analysis

3.4.1.1 Lateral Load Calculation

The triangular lateral load pattern is applied to the structures according to Turkish Earthquake Code 2007, also it corresponds to the first mode shape of the structure which is found by Etabs software.

The total lateral load (total base shear) and its distributing along the building height have been calculated using the procedure given in (3.2.4.2):

3.4.1.1.1 Lateral Load Calculation for the Three Storey Frame

$W = w_1 + w_2 + w_3$ (Eq.3.5)

$W = 1207 + 1207 + 1207 = 3621\ kN$

$T_1 = 1.21\ \ sec$ as (shown in Figure 3.21.)

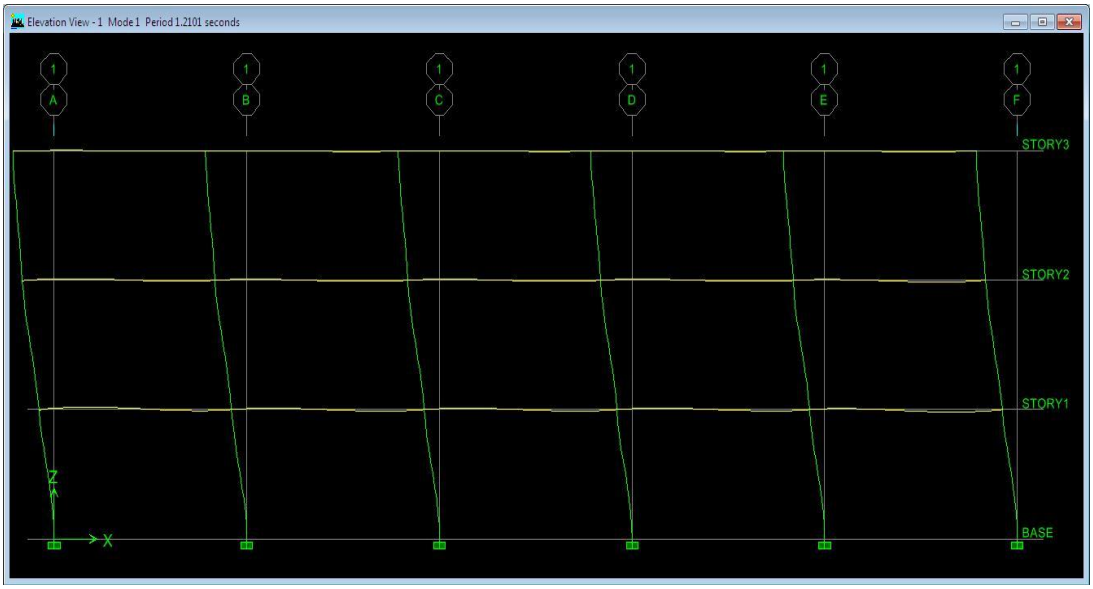

Figure 3.21: Fundamental period and first mode shape created by Etabs

$A_0 = 0.3$ Table 3.4

$I = 1.0$ Table 3.5

$S(T_1) = 1.97$ (Eq.3.7c)

$A(T_1) = 0.59$ (Eq.3.6)

$R_a(T_1) = R = 8$ (Eq.3.8b)

$V_t = 267\ kN$ (Eq.3.2)

$N = 3$

$\Delta F_3 = 6$ kN (Eq.3.3)

Design seismic load acting at each storey: (Eq.3.1)

$F_1 = 44.5$ kN

$F_2 = 89$ kN

F_3 =133.5+6=139.5 kN

3.4.1.1.2 Lateral Load Calculation for the Six Storey Frame

$W = w_1 + w_2 + w_3 + w_4 + w_5 + w_6$ (Eq.3.5)

$W = 1227 + 1227 + 1227 + 1227 + 1227 + 1227 = 7362\ kN$

$T_1 = 1.85\ sec$ as (shown in Figure 3.22.)

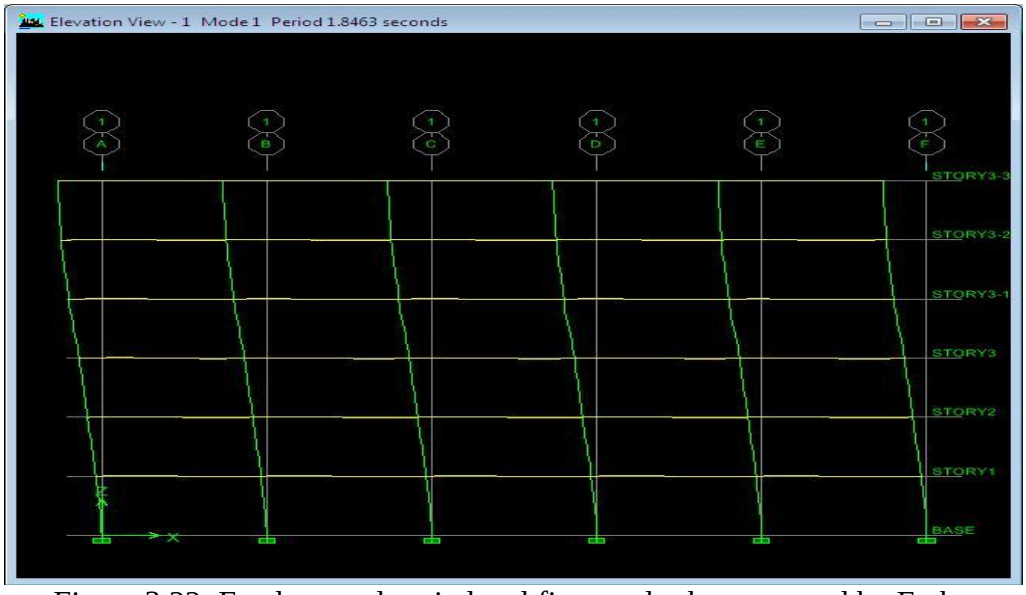

Figure 3.22: Fundamental period and first mode shape created by Etabs

$A_0 = 0.3$ Table 3.4

$I = 1.0$ Table 3.5

$S(T_1) = 1.4$ (Eq.3.7c)

$A(T_1)$ =0.42 (Eq.3.6)

$R_a(T_1) = R = 8$ (Eq.3.8b)

$V_t = 386.5\ kN$ (Eq.3.2)

$N = 6$

ΔF_6 =17.4 kN (Eq.3.3)

Design seismic load acting at each storey: (Eq.3.1)

F_1 =18.4 kN

F_2 =36.8 kN

F_3 =55.2 kN

F_4 =73.6 kN

F_5 =92 kN

F_6 =110.4+17.4=127.8 kN

3.4.1.1.3 Lateral Load Calculation for the Nine Storey Frame

$$W = w_1 + w_2 + w_3 + w_4 + w_5 + w_6 + w_7 + w_8 + w_9 \quad \text{(Eq.3.5)}$$

$$W = 1256 + 1256 + 1256 + 1256 + 1256 + 1256 + 1256 + 1256 + 1256$$

$$W = 11304\ kN$$

$T_1 = 2.56\ sec$ as (shown in Figure 3.23.)

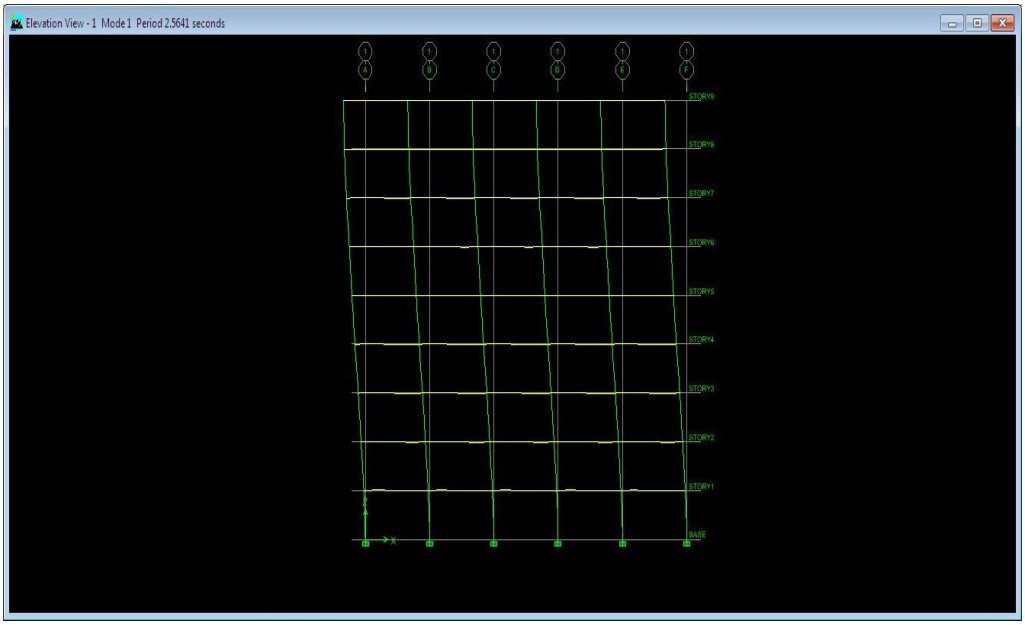

Figure 3.23: Fundamental period and first mode shape created by Etabs

$A_0 = 0.3$ Table 3.4

$I = 1.0$ Table 3.5

$S(T_1) = 1.08$ (Eq.3.7c)

$A(T_1)$ =0.33 (Eq.3.6)

$R_a(T_1) = R = 8$ (Eq.3.8b)

$V_t = 466.3\ kN$ (Eq.3.2)

$N = 9$

ΔF_9 =31.5 kN (Eq.3.3)

Design seismic load acting at each storey: (Eq.3.1)

F_1 =10.4 kN

F_2 =20.7 kN

F_3 =31.1 kN

F_4 =41.4 kN F_5 =51.8 kN

F_6 =62.2 kN

F_7 =72.5 kN

F_8 =82.9 kN

F_9 =93.2+31.5=124.7 kN

3.4.1.1.4 Lateral Load Calculation for the Twelve Storey Frame

$W = w_1 + w_2 + w_3 + w_4 + w_5 + w_6 + w_7 + w_8 + w_9 + w_{10} + w_{11} + w_{12}$

(Eq.3.5)

$W = 1293 + 1293 + 1293 + 1293 + 1293 + 1293 + 1293 + 1293 + 1293 +$

$1293 + 1293 + 1293$

$W = 15516\ kN$

$T_1 = 3.24\ \ sec$ as (shown in Figure 3.24.)

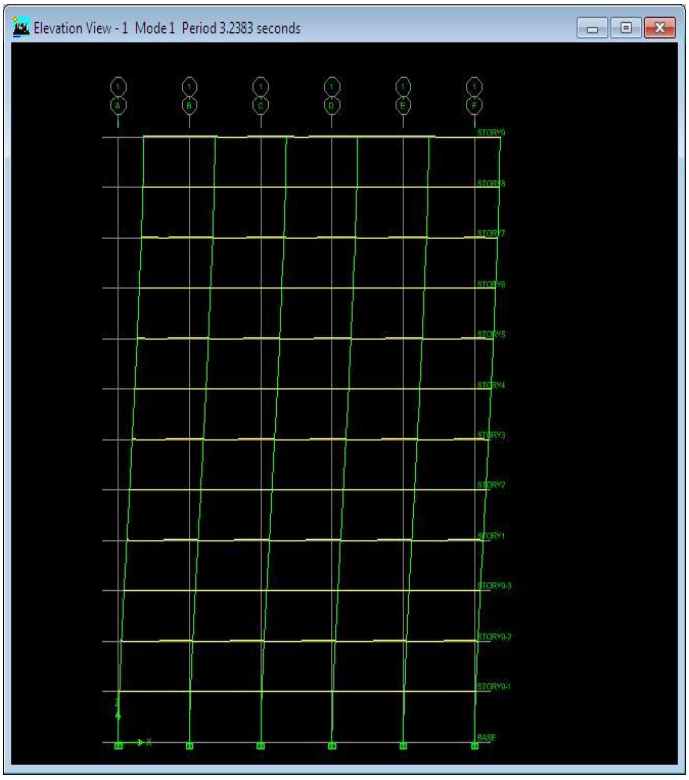

Figure 3.24: Fundamental period and first mode shape created by Etabs

$A_0 = 0.3$ Table 3.4

$I = 1.0$ Table 3.5

$S(T_1) = 0.9$ (Eq.3.7c)

$A(T_1)$ =0.3 (Eq.3.6)

$R_a(T_1) = R = 8$ (Eq.3.8b)

$V_t = 522\ kN$ (Eq.3.2)

$N = 12$

ΔF_{12} =47 kN (Eq.3.3)

Design seismic load acting at each storey: (Eq.3.1)

F_1 =6.7 kN

F_2 =13.4 kN

F_3 =20.1 kN

F_4 =26.8 kN

F_5 =33.5 kN

F_6 =40.2 kN

F_7 =46.9 kN

F_8 =53.6 kN

F_9 =60.3 kN

F_{10} =67 kN

F_{11} =73.7 kN

F_{12} =80.4+47=127.4 kN

3.4.2 Incremental Dynamic Analysis

As it was discussed in section (3.2.4.3) there are 9 earthquake records that should be applied one by one to the all reinforced concrete frames and each of them should be incrementally increased till collapse occurs. All of the steps in order to do incremental dynamic analysis are conducted automatically by the Seismostruct as it is explained in section (2.3.4).

Chapter 4

RESULTS AND DISCUSSIONS

4.1 General

Seismostruct has been used to compute the response of a three, six, nine, and twelve stories reinforced concrete frames to evaluate the effect of different types of steel bracing in terms of capacity curves, lateral displacement and stiffness.

Pushover analysis and incremental dynamic analysis have been performed, the results of pushover analysis were utilized to determine capacity curve and check performance criteria. IDA envelope curves have been implemented from the incremental dynamic analysis results.

4.2 Pushover Analysis

Pushover analysis has been conducted to all frames that are mentioned in previous chapters, using triangular lateral load pattern. The results were used to compare the capacity curves and notify the strain performance criteria. In addition, comparisons in terms of lateral load capacity, lateral displacement and elastic stiffness have been applied.

4.2.1 Three Storey Frame Results and Discussion

4.2.1.1 Capacity Curves

The pushover curves for all cases of the three storey frames based on load control method are shown in Figure 4.1. It is observed that the effect of X-braced system is more than the other types of bracing. X-braced, Zipper-braced, Inverted V-braced

and Diagonal-braced systems affected the capacity curve from higher to less effect respectively.

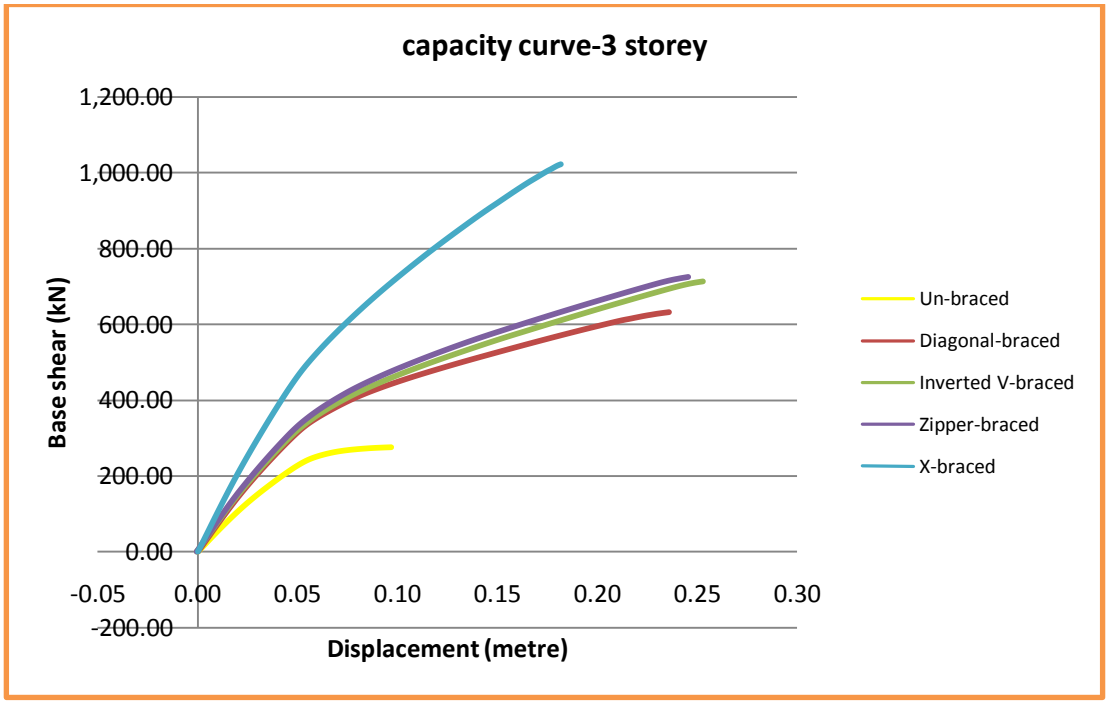

Figure 4.1: Capacity curve for the three storey frames

4.2.1.2 Performance Criteria Checks for the Three Storey Frame

Performance criteria checks are illustrated through the Table 4.1 and Figure 4.2. It affirms the difference of capacity curves between types of bracing.

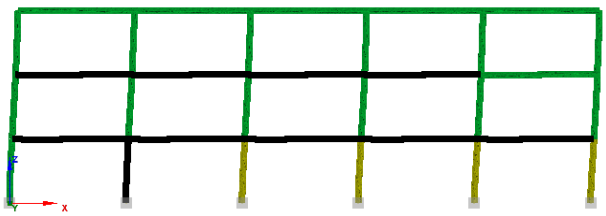

a-Performance criteria checks for the Un-braced frame, 3 storey

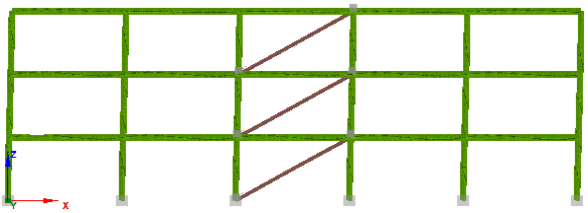

b- Performance criteria checks for the Diagonal-braced frame, 3 storey

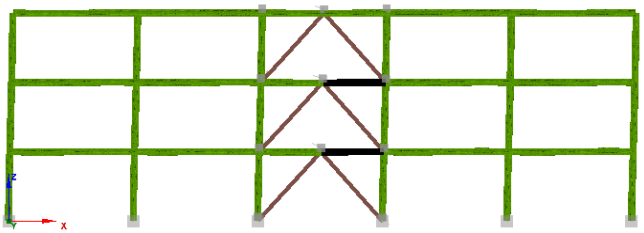

c- Performance criteria checks for the Inverted V-braced frame, 3 storey

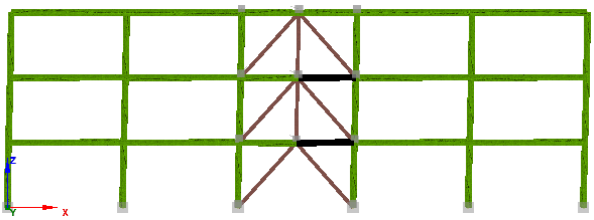

d- Performance criteria checks for the Zipper-braced frame, 3 storey

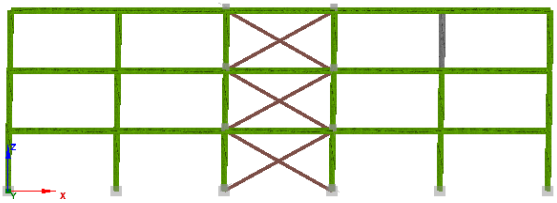

e- Performance criteria checks for the X-braced frame, 3 storey

Figure 4.2: The performance criteria checks for the three storey frames, the concrete crack is identified by the green color, concrete cover crush by yellow, concrete core crush by red, steel yielding by black and steel fracture by blue color.

Table 4.1: Number of elements reached the criteria in the 3 storey frames

Type of criteria	Un-braced	Diagonal-braced	Inverted V-braced	Zipper-braced	X-braced
Concrete crack	33	33	33	33	32
Concrete cover crush	5	0	0	0	0
Concrete core crush	0	0	0	0	0
Steel yielding	15	0	0	0	0
Steel fracture	0	0	0	0	0

As shown in the Table 4.1 and Figure 4.2, the number of elements reached criteria is decreased in braced frames compared to un-braced frame. The compression has been taken for the lateral load when collapse occurs in un-braced frame.

4.2.1.3 Lateral Load Capacity

The strength defines the capacity of a member or an assembly of members to resist actions. In this study, the capacity is related to the lateral loads that resisted by frames till collapse occurred. The lateral load capacity for different brace types is presented in Table 4.2.

Table 4.2: Lateral load capacity

Case	Un-braced	Diagonal-braced	Inverted V-braced	Zipper-braced	X-braced
Lateral load (kN)	275	632	714	726	1024

As shown in the Table 4.2, compared to the brace type, for the three storey frames, the lateral load of X-braced, Zipper-braced, Inverted V-braced and Diagonal-braced systems are increased by a factor of 3.72, 2.64, 2.6, and 2.3 respectively. This indicates that the lateral load capacity of RC frames can be greatly enhanced through the addition of steel braces especially with the X-braced systems.

4.2.1.4 Roof Lateral Displacement

The lateral displacement of un-braced frame is compared with that of braced frames in the same amount of lateral load which that collapse occurs in the un-braced frame (275 KN). Results presented in Table 4.3.

Table 4.3: Lateral roof displacements

Case	Un-braced	Diagonal-braced	Inverted V-braced	Zipper-braced	X-braced
Displacement (mm)	97	42	41	40	27

The lateral displacement of X-braced, Zipper-braced, Inverted V-braced and Diagonal-braced systems are decreased by a ratio of 72%, 59%, 58%, and 57% respectively compared to un-braced frame. It is observed that the lateral displacements are reduced to the largest extend for X-braced system.

4.2.1.5 Elastic Stiffness

Elastic stiffness is the slope of the elastic part of the pushover curve, results which are extracted in pushover curves are presented in Table 4.4.

Table 4.4: Elastic stiffness

Case	Un-braced	Diagonal-braced	Inverted V-braced	Zipper-braced	X-braced
Stiffness (kN/m)	4445	5980	6135	6241	8289

The elastic stiffness of X-braced, Zipper-braced, Inverted V-braced and Diagonal-braced systems are increased by a ratio of 87%, 40%, 38%, and 35% respectively compared to un-braced frame. It is observed that the elastic stiffness are increased to the largest extend for X-braced system

4.2.2 Pushover Results for the Six Storey Frame

4.2.2.1 Capacity Curves

The pushover curves for all cases of the six storey frames based on load control method are shown in Figure 4.3. It is observed that the effect of X-braced system is more than the other types of bracing. X-braced, Zipper-braced, Inverted V-braced and Diagonal-braced systems are affected the capacity curve from higher to less effect respectively.

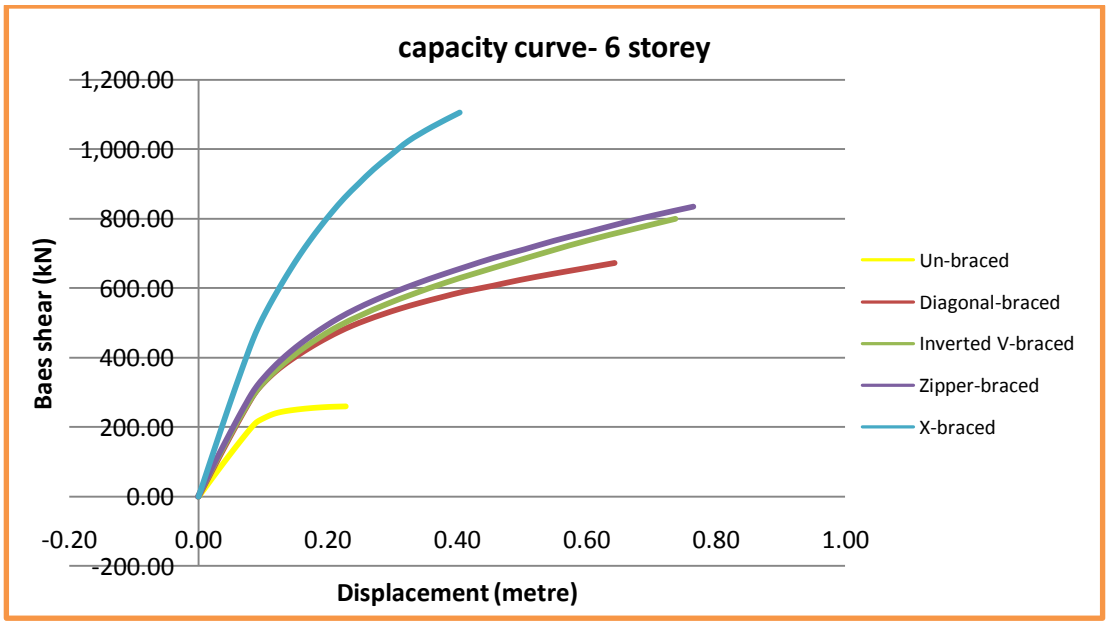

Figure 4.3: Capacity curve for the six storey frames

4.2.2.2 Performance Criteria Checks for the Six Storey Frame

Performance criteria checks are illustrated through the Table 4.5 and Figure 4.4. It affirms the difference of capacity curves between types of bracing.

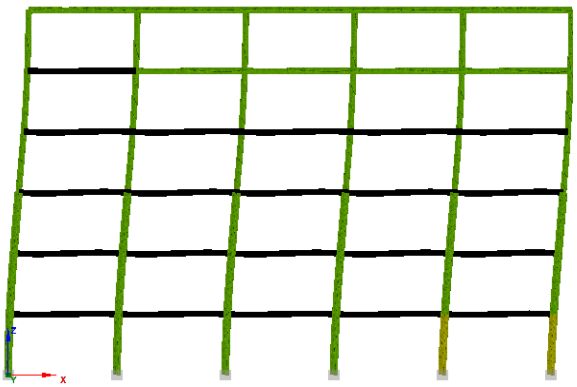

a- Performance criteria checks for the Un-braced frame, 6 storey

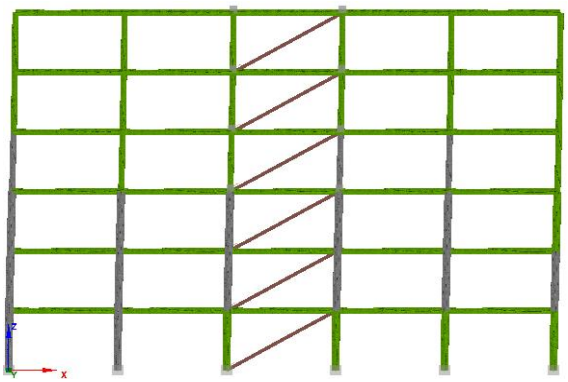

b- Performance criteria checks for the Diagonal-braced frame, 6 storey

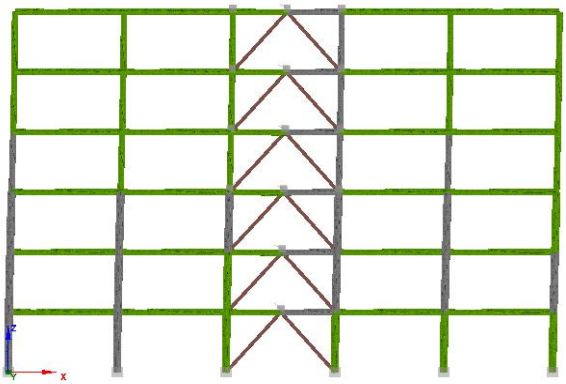

c- Performance criteria checks for the Inverted V-braced frame, 6 storey

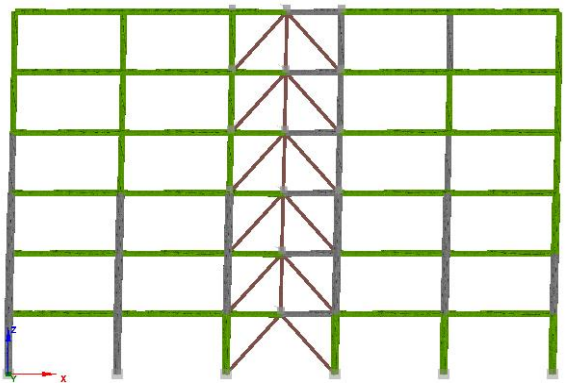

d- Performance criteria checks for the Zipper-braced frame, 6 storey

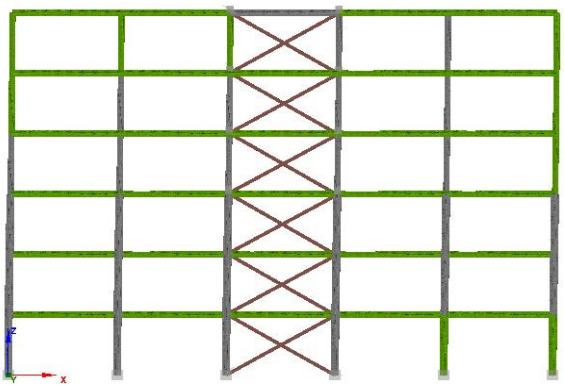

e- Performance criteria checks for the X-braced frame, 6 storey

Figure 4.4: The performance criteria checks for the six storey frames, the concrete crack is identified by the green color, concrete cover crush by yellow, concrete core crush by red, steel yielding by black and steel fracture by blue color.

Table 4-5: Number of elements reached the criteria in the 6 storey frames

Type of criteria	Un-braced	Diagonal-braced	Inverted V-braced	Zipper-braced	X-braced
Concrete crack	66	50	49	47	38
Concrete cover crush	2	0	0	0	0
Concrete core crush	0	0	0	0	0
Steel yielding	22	0	0	0	0
Steel fracture	0	0	0	0	0

As shown in the Table 4.5 and Figure 4.4, the number of elements reached criteria is decreased in braced frames compared to un-braced frame. The compression has been taken for the lateral load when collapse occurs in un-braced frame.

4.2.2.3 Lateral Load Capacity

The lateral load capacity for different brace types is putted in Table 4.6.

Table 4-6: Lateral load capacity

Case	Un-braced	Diagonal-braced	Inverted V-braced	Zipper-braced	X-braced
Lateral load (kN)	260	673	800	835	1105

As shown in the Table 4.6, compared to the brace type, for the six storey frames, the lateral load of X-braced, Zipper-braced, Inverted V-braced and Diagonal-braced

systems are increased by a factor of 4.25, 3.21, 3.1, and 2.59 respectively. This indicates that the lateral load capacity of RC frames can be greatly enhanced through the addition of steel braces especially with the X-braced systems.

4.2.2.4 Roof Lateral Displacement

The lateral displacement of un-braced frame is compared with that of braced frames in the same amount of lateral load which that collapse load occurs in the un-braced frame (260 KN). Results presented in Table 4.7.

Table 4.7: Lateral roof displacements

Case	Un-braced	Diagonal-braced	Inverted V-braced	Zipper-braced	X-braced
Displacement (mm)	228	76	75	64	48

The lateral displacement of X-braced, Zipper-braced, Inverted V-braced and Diagonal-braced systems are decreased by a ratio of 79%, 72%, 67%, 67% respectively compared to un-braced frame. It is observed that the lateral displacements are reduced to the largest extend for X-braced system.

4.2.1.5 Elastic Stiffness

The elastic stiffness results which are extracted in pushover curves are presented in Table 4.8.

Table 4.8: Elastic stiffness

Case	Un-braced	Diagonal-braced	Inverted V-braced	Zipper-braced	X-braced
stiffness (kN/m)	2377	3416	3552	3237	4433

The elastic stiffness of X-braced, Zipper-braced, Inverted V-braced and Diagonal-braced systems are increased by a ratio of 86%, 36%, 49%, 44% respectively compared to un-braced frame. It is observed that the elastic stiffness are increased to the largest extend for X-braced system

4.2.3 Pushover Results for the Nine Storey Frame

4.2.3.1 Capacity Curves

The pushover curves for all cases of the nine storey frames based on load control method are shown in Figure 4.5. It is observed that the influence of X-braced type is more than the other types of bracing. X-braced, Zipper-braced, Inverted V-braced and Diagonal-braced systems are affected the capacity curve from higher to less effect respectively.

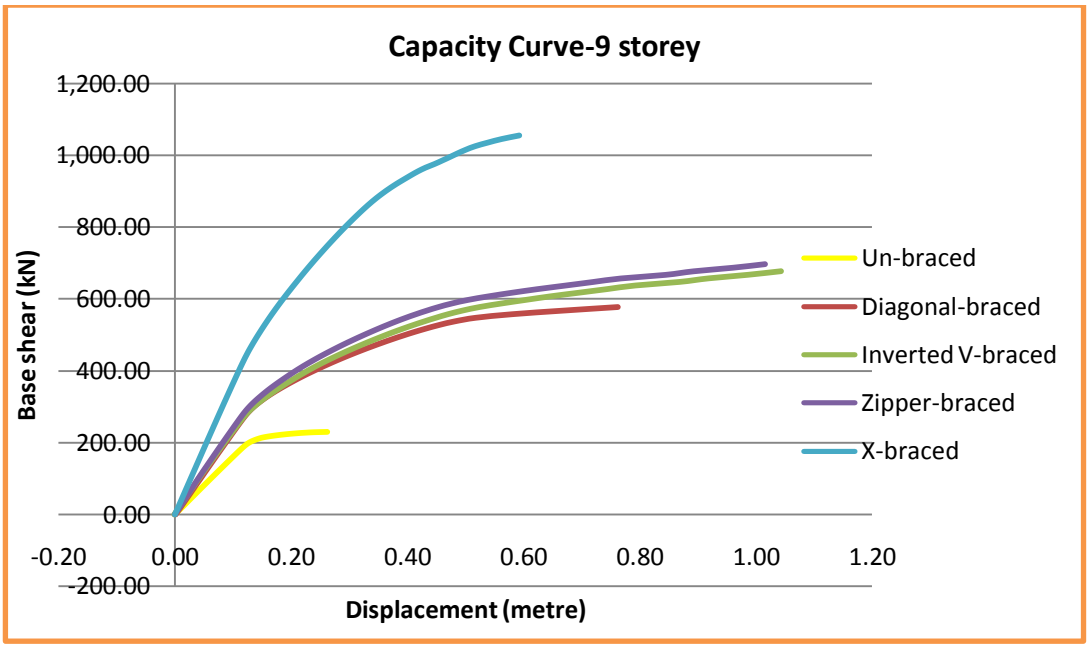

Figure 4.5: Capacity curve for the nine storey frames

4.2.3.2 Performance Criteria Checks for the Nine Storey Frame

Performance criteria checks are illustrated through the Table 4.9 and Figure 4.6. It affirms the difference of capacity curves between types of bracing.

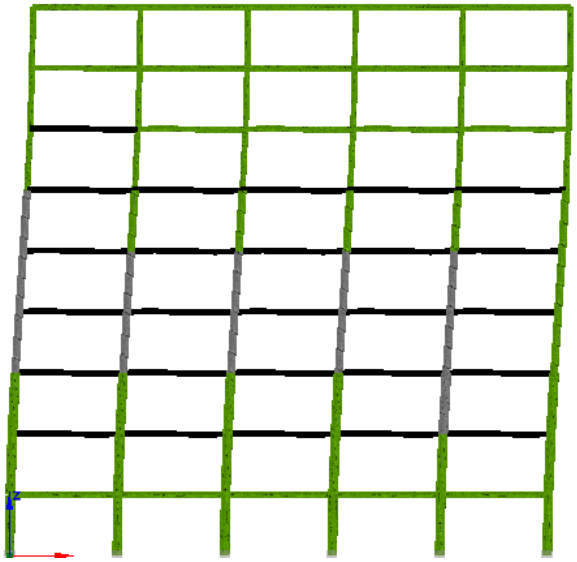

a- Performance criteria checks for the un-braced frame, 9 storey

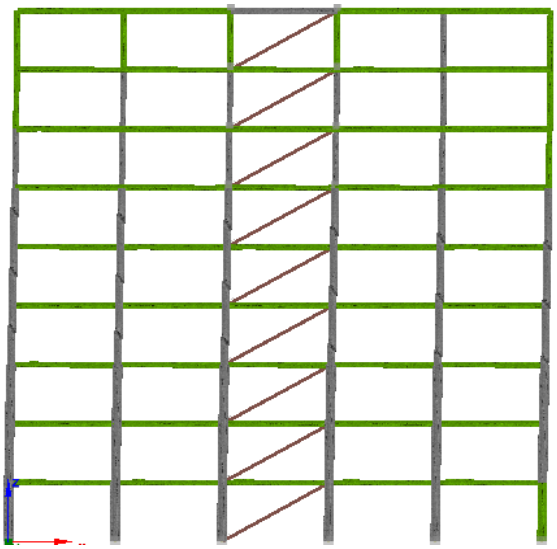

b- Performance criteria checks for the diag.-braced frame, 9 storey

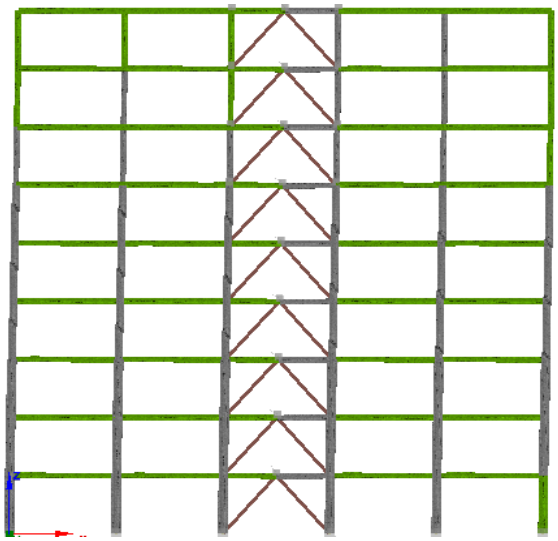

c- Performance criteria checks for the inverted-V frame, 9 storey

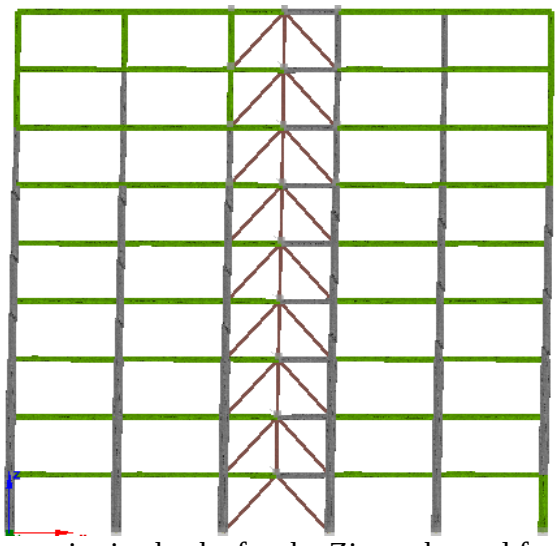

d- Performance criteria checks for the Zipper-braced frame, 9 storey

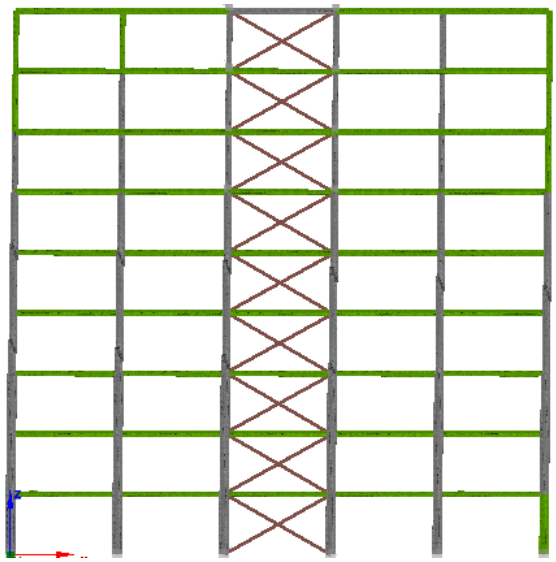

e- Performance criteria checks for the X-braced frame, 9 storey

Figure 4.6: The performance criteria checks for the nine storey frames, the concrete crack is identified by the green color, concrete cover crush by yellow, concrete core crush by red, steel yielding by black and steel fracture by blue color.

Table 4.9: Number of elements reached the criteria in the 9 storey frames

Type of criteria	**Un-braced**	**Diagonal-braced**	**Inverted V-braced**	**Zipper-braced**	**X-braced**
Concrete crack	87	53	53	53	51
Concrete cover crush	2	0	0	0	0
Concrete core crush	0	0	0	0	0
Steel yielding	26	0	0	0	0
Steel fracture	0	0	0	0	0

As shown in the Table 4.9 and Figure 4.6, the number of elements reached criteria is decreased in braced frames compared to un-braced frame. The compression has been taken for the lateral load when collapse occurs in un-braced frame.

4.2.3.3 Lateral Load Capacity

The lateral load capacity for different brace types is put in Table 4.10.

Table 4.10: Lateral load capacity

Case	Un-braced	Diagonal-braced	Inverted V-braced	Zipper-braced	X-braced
Lateral load (kN)	230	577	677	697	1055

As shown in the Table 4.10, compared to the brace type, for the nine storey frames, the lateral load of X-braced, Zipper-braced, Inverted V-braced and Diagonal-braced systems are increased by a factor of 4.6, 3.03, 2.94, and 2.51 respectively. This indicates that the lateral load capacity of RC frames can be greatly enhanced through the addition of steel braces especially with the X-braced systems.

4.2.3.4 Roof Lateral Displacement

The lateral displacement of un-braced frame is compared with that of braced frames in the same amount of lateral load which that collapse occurs in the un-braced frame (230 KN). Results presented in Table 4.11.

Table 4.11: Lateral roof displacements

Case	Un-braced	Diagonal-braced	Inverted V-braced	Zipper-braced	X-braced
Displacement (mm)	262	100	99	95	62

The lateral displacement of X-braced, Zipper-braced, Inverted V-braced and Diagonal-braced systems are decreased by a ratio of 76%, 64%, 62%, 62% respectively compared to un-braced frame. It is observed that the lateral displacements are reduced to the largest extend for X-braced system.

4.2.3.5 Elastic Stiffness

The elastic stiffness results which are extracted in pushover curves are presented in Table 4.12.

Table 4.12: Elastic stiffness

Case	Un-braced	Diagonal-braced	Inverted V-braced	Zipper-braced	X-braced
Stiffness (kN/m)	1572	2292	2380	2487	3653

The elastic stiffness of X-braced, Zipper-braced, inverted V-braced and Diag.-braced systems are increased by a ratio of 132%, 58%, 51%, 46% respectively compared to un-braced frame. It is observed that the elastic stiffness are increased to the largest extend for X-braced system

4.2.4 Pushover Results for the Twelve Storey Frame

4.2.4.1 Capacity Curves

The pushover curves for all cases of the twelve storey frames based on load control method are shown in Figure 4.7. It is observed that the influence of X-braced type is more than the other types of bracing. X-braced, Zipper-braced, Inverted V-braced and Diagonal-braced systems are affected the capacity curve from higher to less effect respectively.

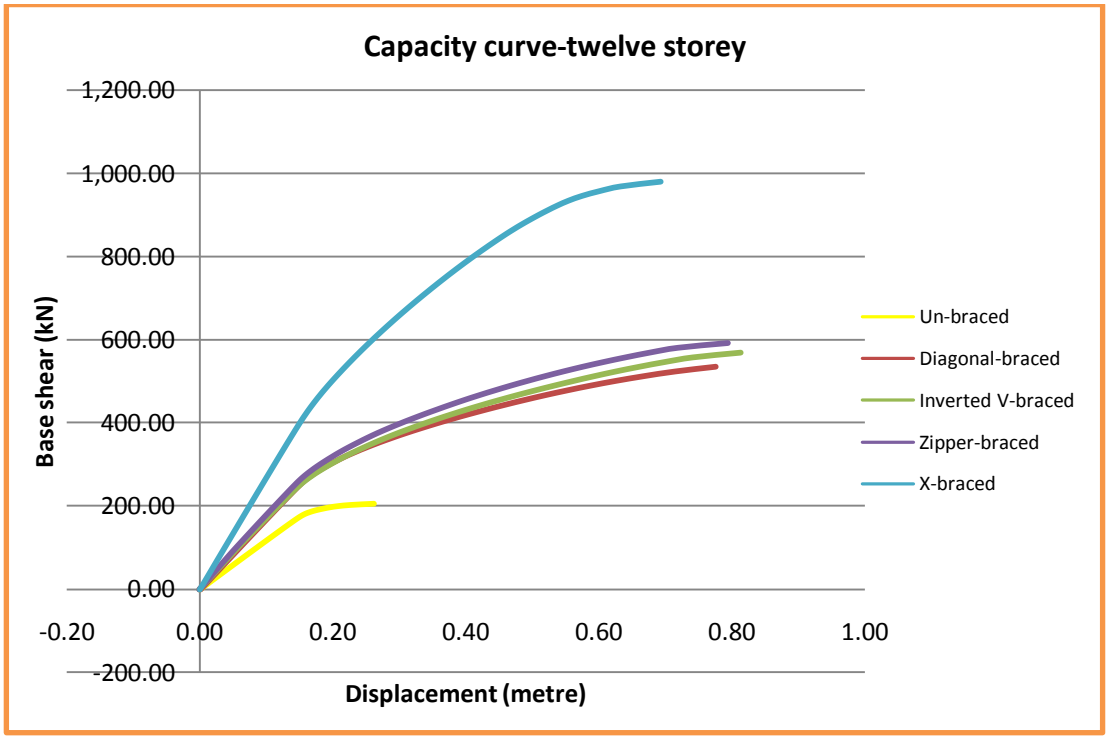

Figure 4.7: Capacity curve for the twelve storey frames

4.2.4.2 Performance Criteria Checks for the Twelve Storey Frame

Performance criteria checks are illustrated through the Table 4.13 and Figure 4.8. It affirms the difference of capacity curves between types of bracing.

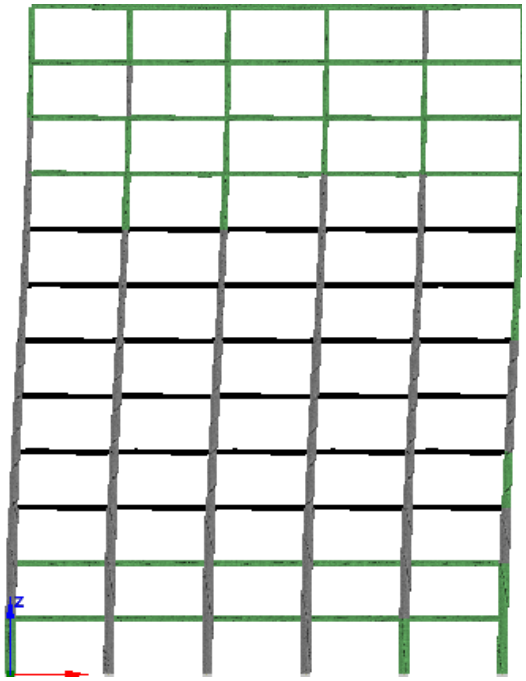

a- Performance criteria checks for the Un-braced frame, 12 storey

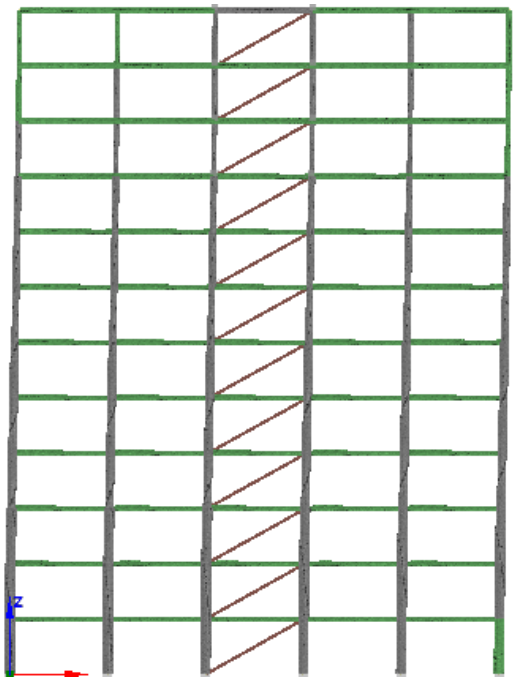

b- Performance criteria checks for the Diagonal-braced frame, 12 storey

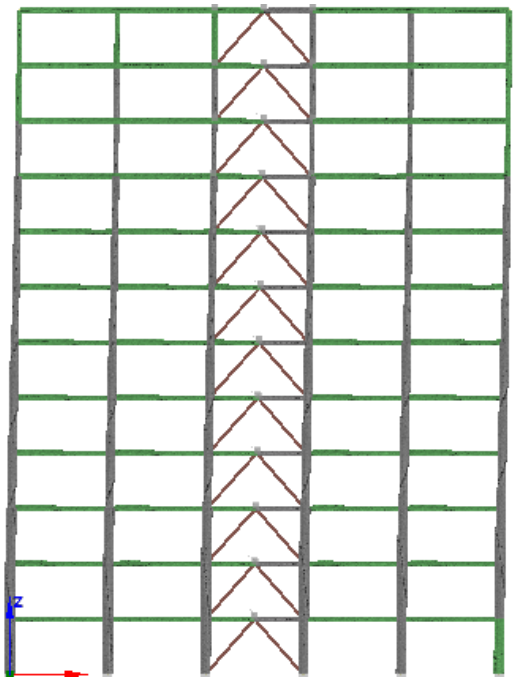

c- Performance criteria checks for the Inverted V-braced frame, 12 storey

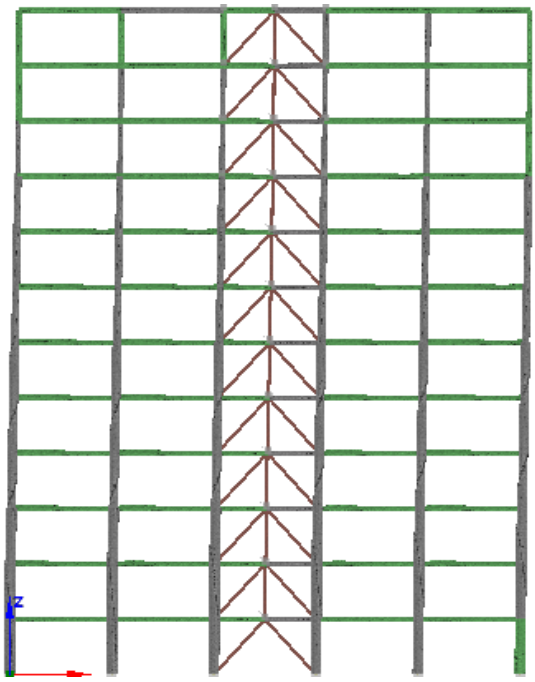

d- Performance criteria checks for the Zipper-braced frame, 12 storey

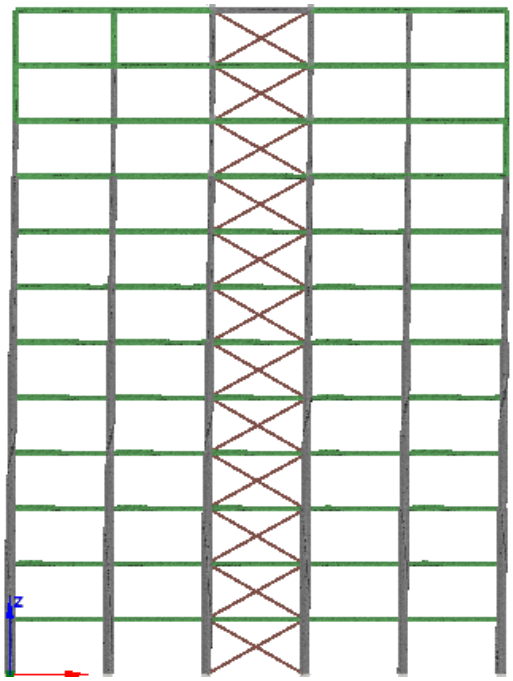

e- Performance criteria checks for the X-braced frame, 12 storey

Figure 4-8: The performance criteria checks for the twelve storey frames, the concrete crack is identified by the green color, concrete cover crush by yellow, concrete core crush by red, steel yielding by black and steel fracture by blue color.

Table 4.13: Number of elements reached the criteria in the 12 storey frames

Type of criteria	**Un-braced**	**Diagonal-braced**	**Inverted V-braced**	**Zipper-braced**	**X-braced**
Concrete crack	85	66	66	66	65
Concrete cover crush	2	0	0	0	0
Concrete core crush	0	0	0	0	0
Steel yielding	30	0	0	0	0
Steel fracture	0	0	0	0	0

As shown in the Table 4.13 and Figure 4.8, the number of elements reached criteria is decreased in braced frames compared to un-braced frame. The compression has been taken for the lateral load when collapse occurs in un-braced frame.

4.2.4.3 Lateral Load Capacity

The lateral load capacity for different brace types is putted in Table 4.14.

Table 4.14: Lateral load capacity

Case	Un-braced	Diagonal-braced	Inverted V-braced	Zipper-braced	X-braced
Lateral load (kN)	205	535	570	592	980

As shown in the Table 4.14, compared to the brace type, for the nine storey frames, the lateral load of X-braced, Zipper-braced, Inverted V-braced and Diagonal-braced systems are increased by a factor of 4.78, 2.89, 2.78, and 2.61 respectively. This indicates that the lateral load capacity of RC frames can be greatly enhanced through the addition of steel braces especially with the X-braced systems.

4.2.4.4 Roof Lateral Displacement

The lateral displacement of un-braced frame is compared with that of frames with that of braced frames in the same amount of lateral load which that collapse occurs in the un-braced frame (205 KN). Results presented in Table 4.15.

Table 4.15: Lateral roof displacements

Case	Un-braced	Diagonal-braced	Inverted V-braced	Zipper-braced	X-braced
Displacement (mm)	262	122	122	116	76

The lateral displacement of X-braced, Zipper-braced, Inverted V-braced and Diagonal-braced systems are decreased by a ratio of 71%, 56%, 53%, 53% respectively compared to un-braced frame. It is observed that the lateral displacements are reduced to the largest extend for X-braced system.

4.2.4.5 Elastic Stiffness

The elastic stiffness results which are extracted in pushover curves are presented in Table 4.16.

Table 4.16: Elastic stiffness

Case	Un-braced	Diag-braced	Inverted V-braced	Zipper-braced	X-braced
Stiffness (kN/m)	1159	1663	1737	1837	2687

The elastic stiffness of X-braced, Zipper-braced, inverted V-braced and Diag.-braced systems are increased by a ratio of 132%, 58%, 50%, 43% respectively compared to un-braced frame. It is observed that the elastic stiffness are increased to the largest extend for X-braced system

4.3 Incremental Dynamic Analysis

The IDA curve of the studied frames has been presented in terms of maximum drift ratio and maximum base shear. The scale factors are increased in multiple ratios until collapse occurs and analysis stops.

4.3.1 IDA Results for the Three Storey Frames

The IDA curve (dynamic pushover curve) for different ground motion records is shown in figures below:

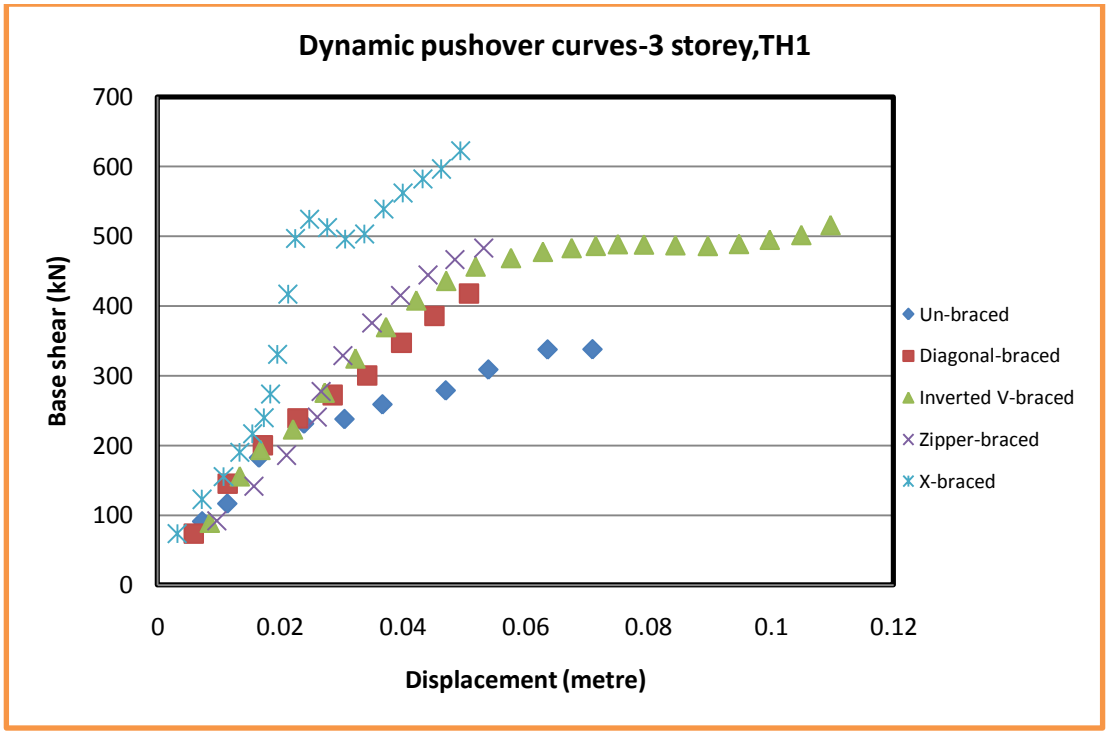

Figure 4.9: IDA curve for the three storey frames, TH1

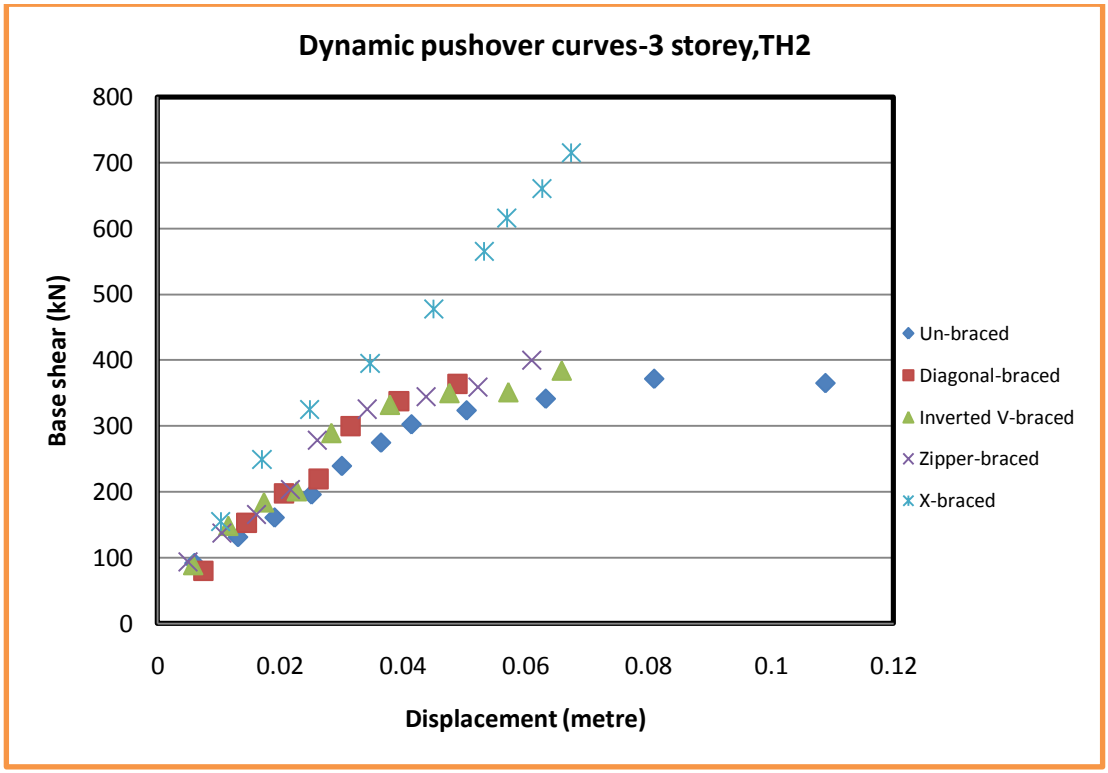

Figure 4.10: IDA curve for the three storey frames,TH2

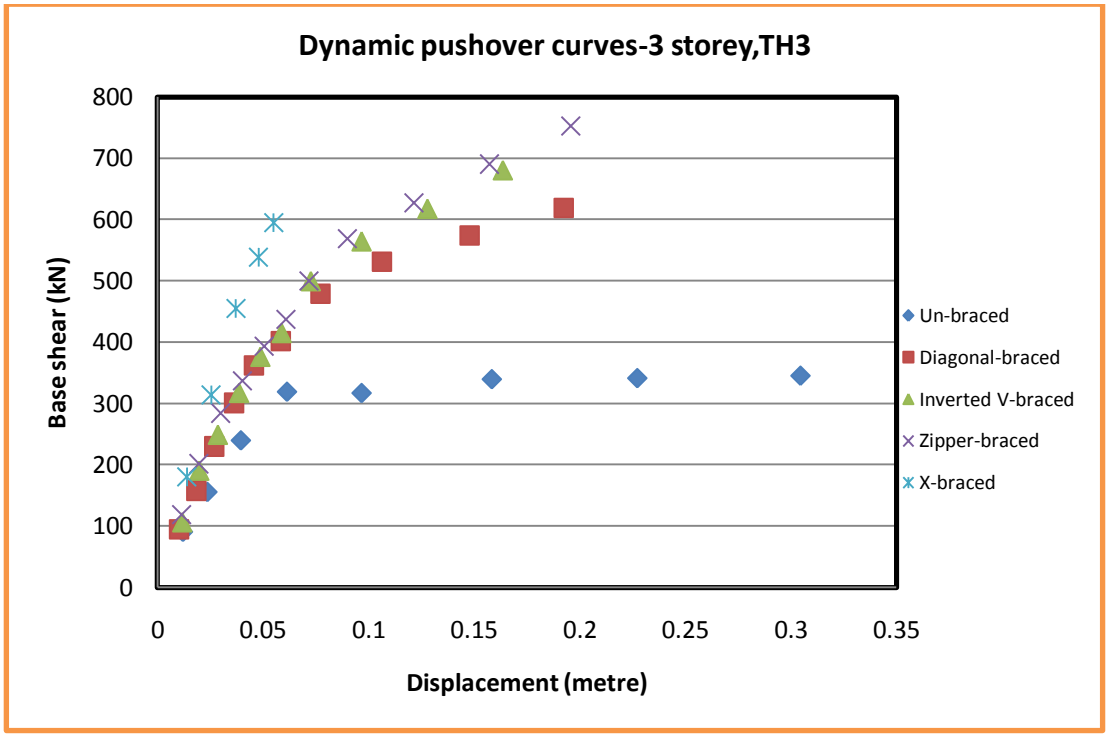

Figure 4.11: IDA curve for the three storey frames, TH3

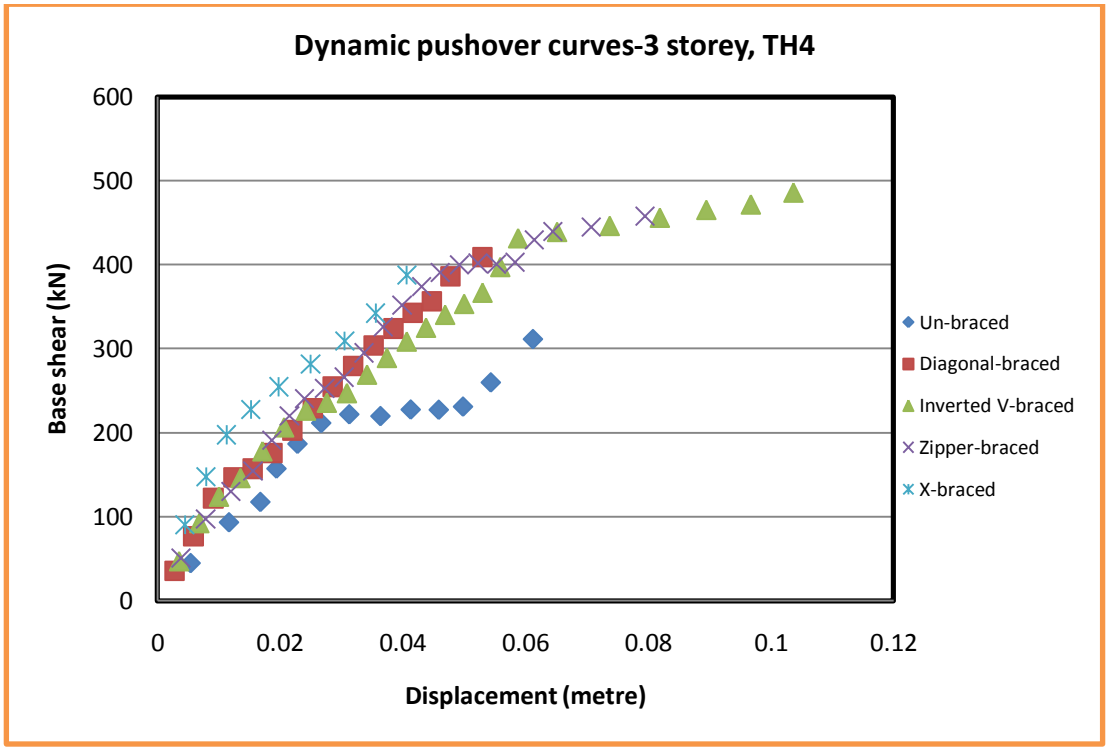

Figure 4.12: IDA curve for the three storey frames, TH4

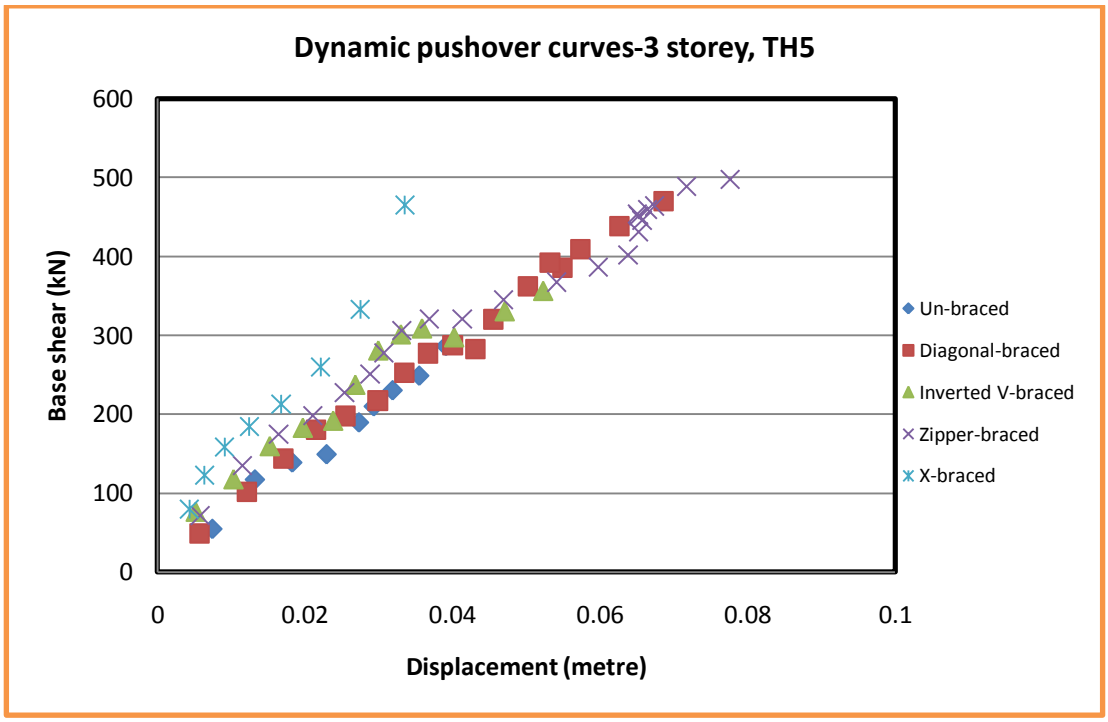

Figure 4.13: IDA curve for the three storey frames, TH5

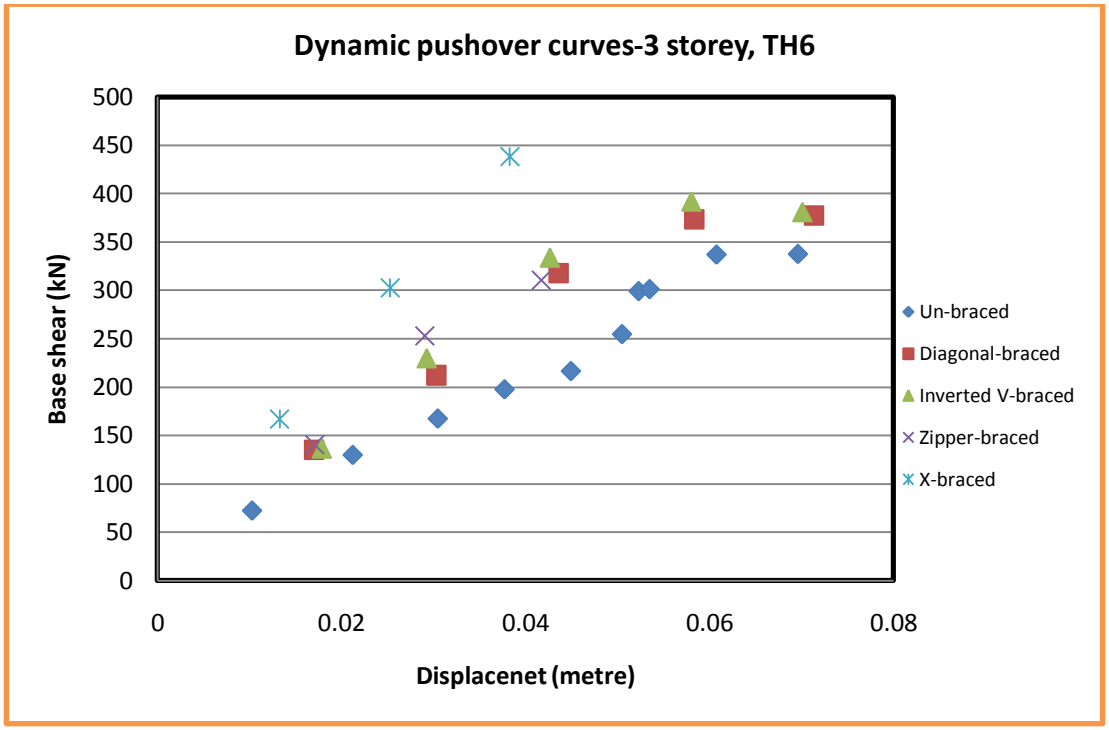

Figure 4.14: IDA curve for the three storey frames, TH6

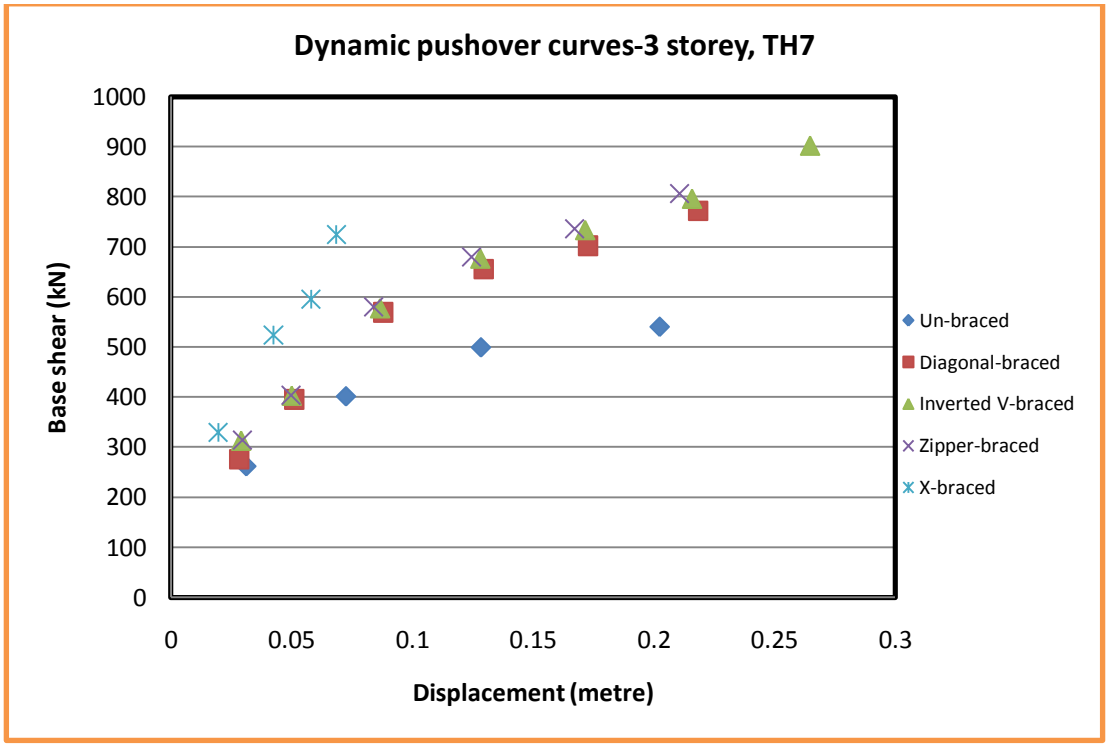

Figure 4.15: IDA curve for the three storey frames, TH7

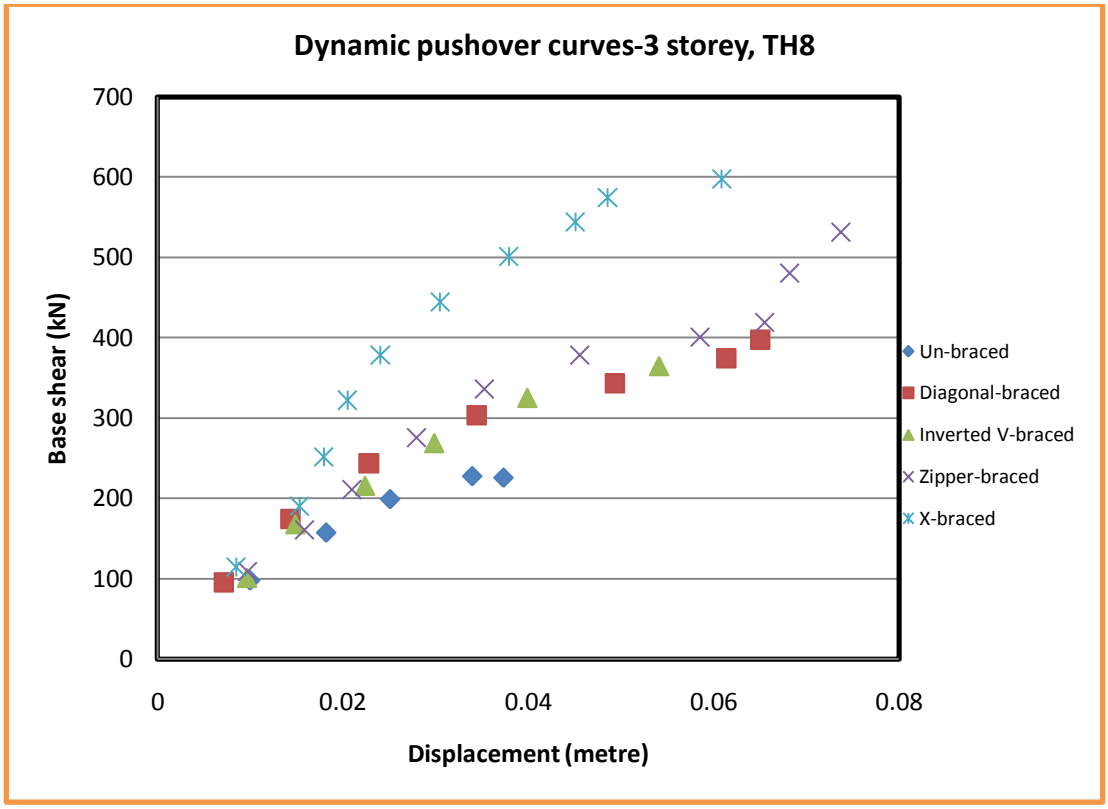

Figure 4.16: IDA curve for the three storey frames, TH8

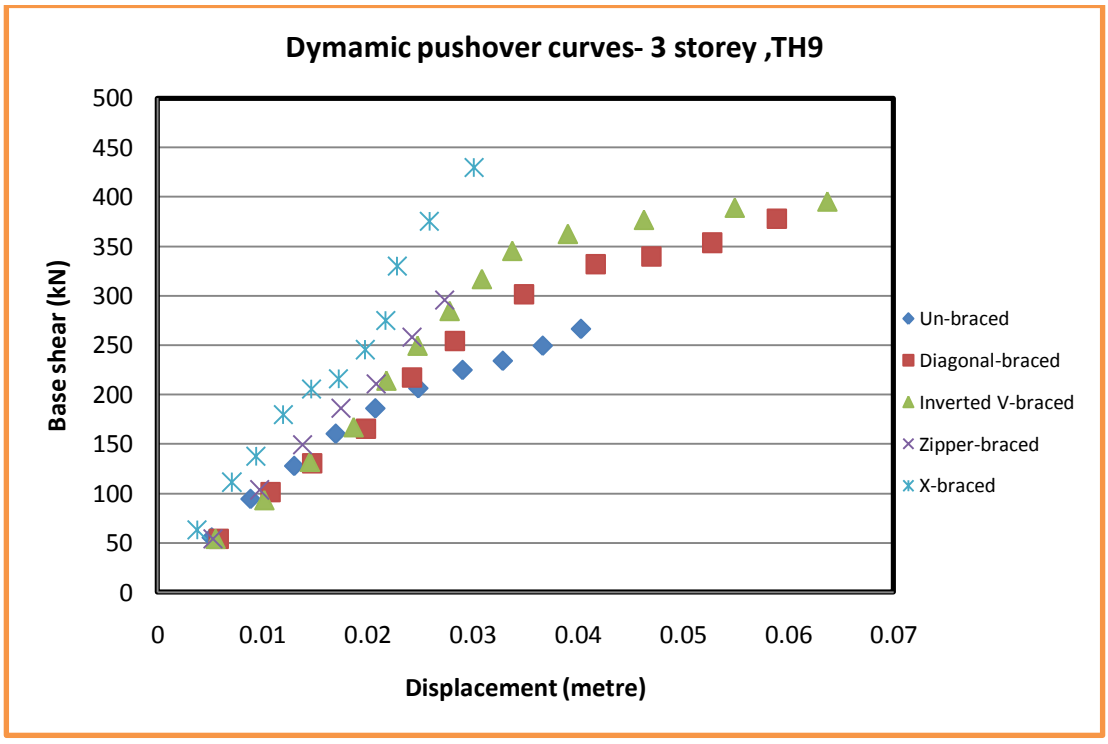

Figure 4.17: IDA curve for the three storey frames, TH9

4.3.2 IDA Results for the Six Storey Frames

IDA curve (dynamic pushover curve) for different ground motion records is shown out of figures below:

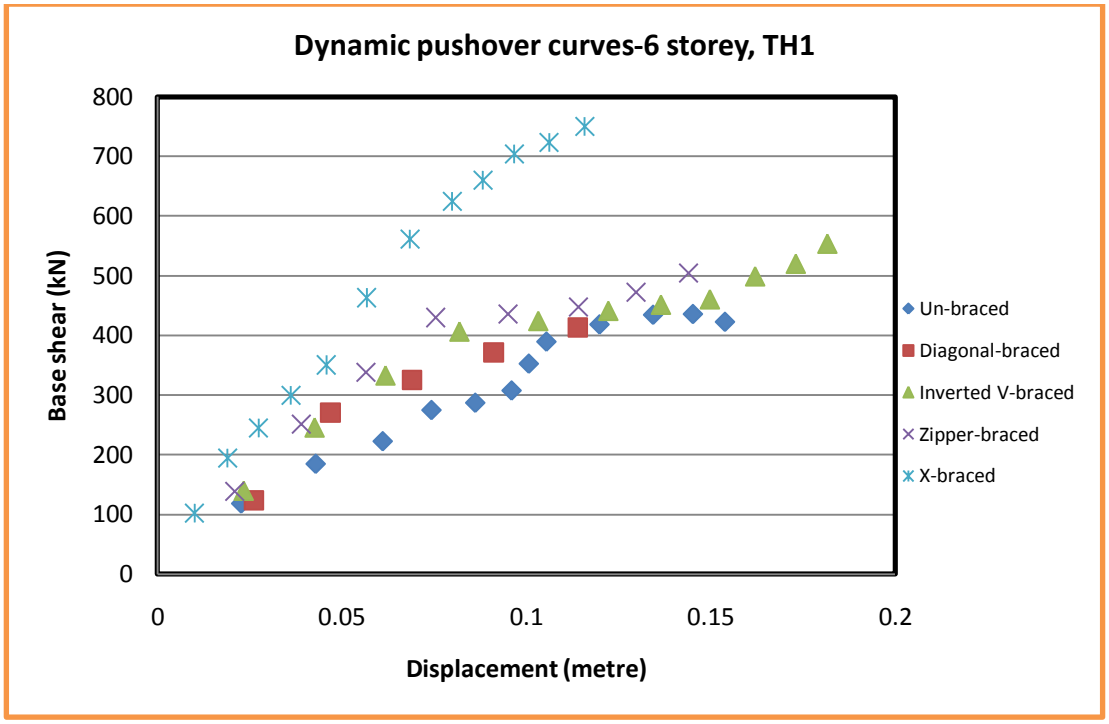

Figure 4.18: IDA curve for the six storey frames, TH1

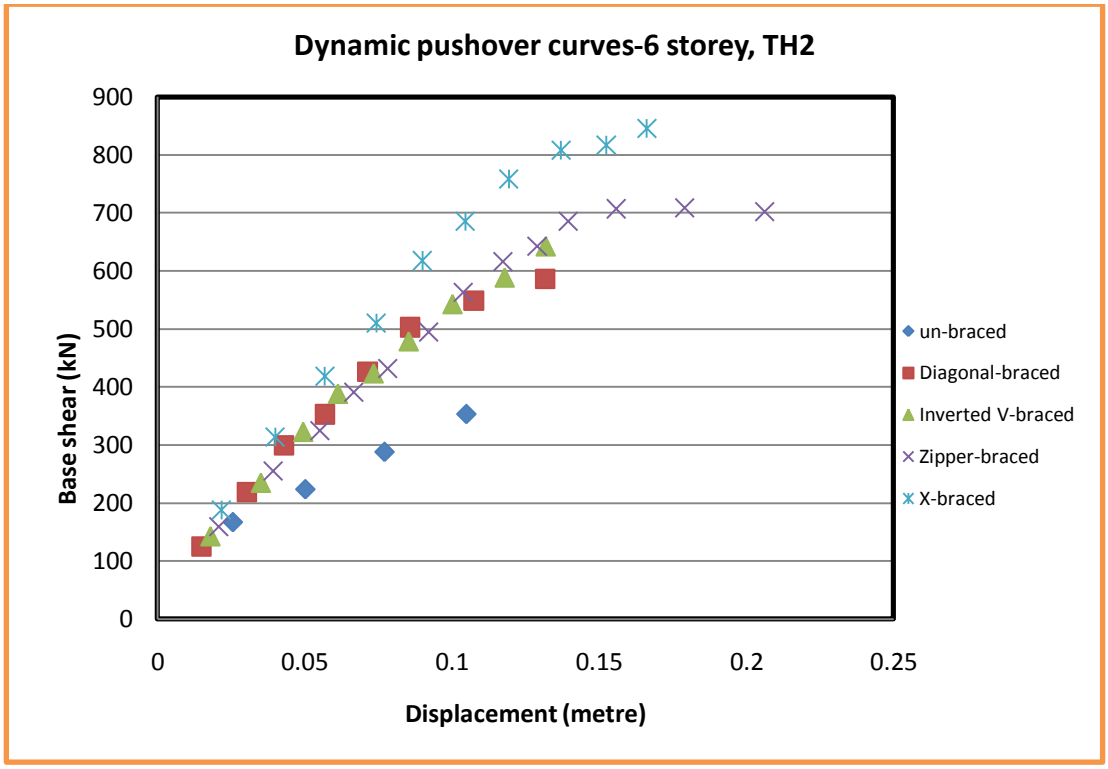

Figure 4.19: IDA curve for the six storey frames, TH2

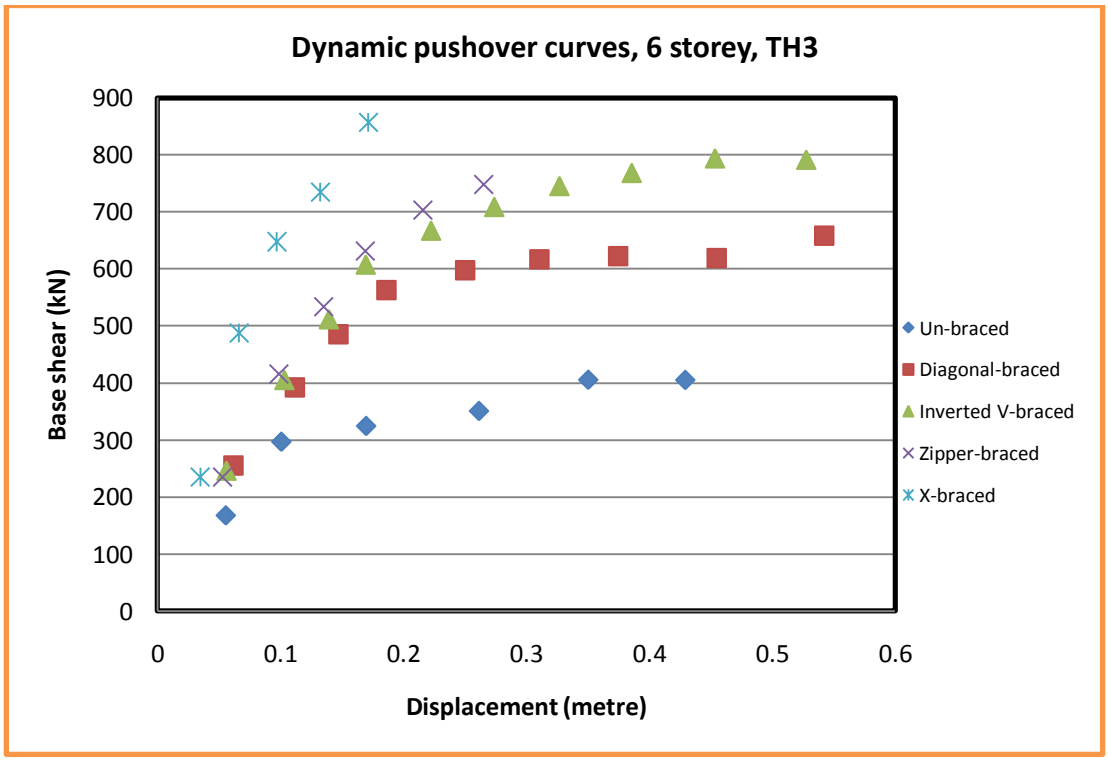

Figure 4.20: IDA curve for the six storey frames, TH3

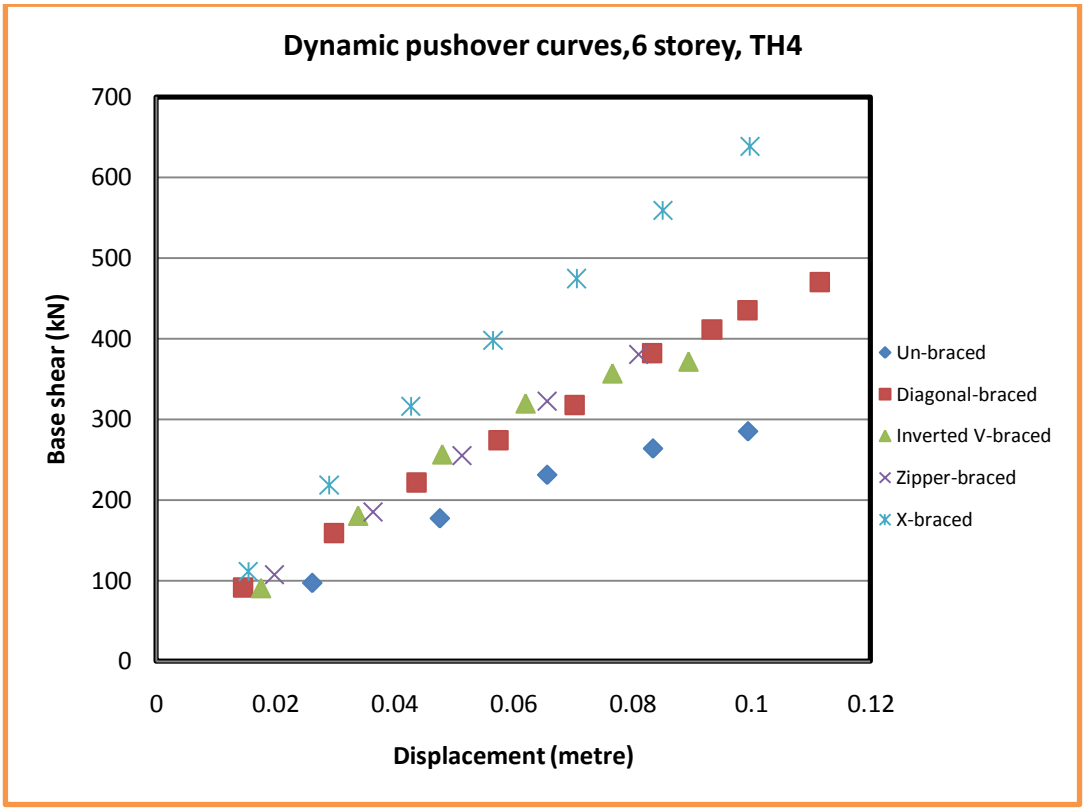

Figure 4.21: IDA curve for the six storey frames, TH4

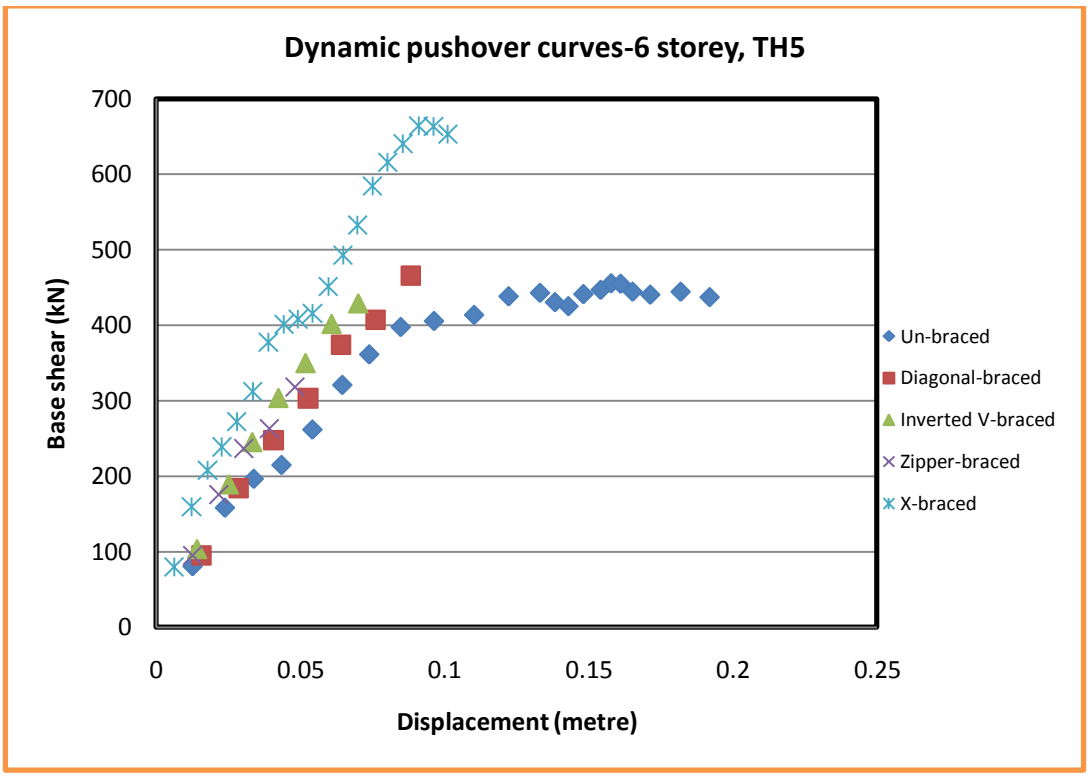

Figure 4.22: IDA curve for the six storey frames, TH5

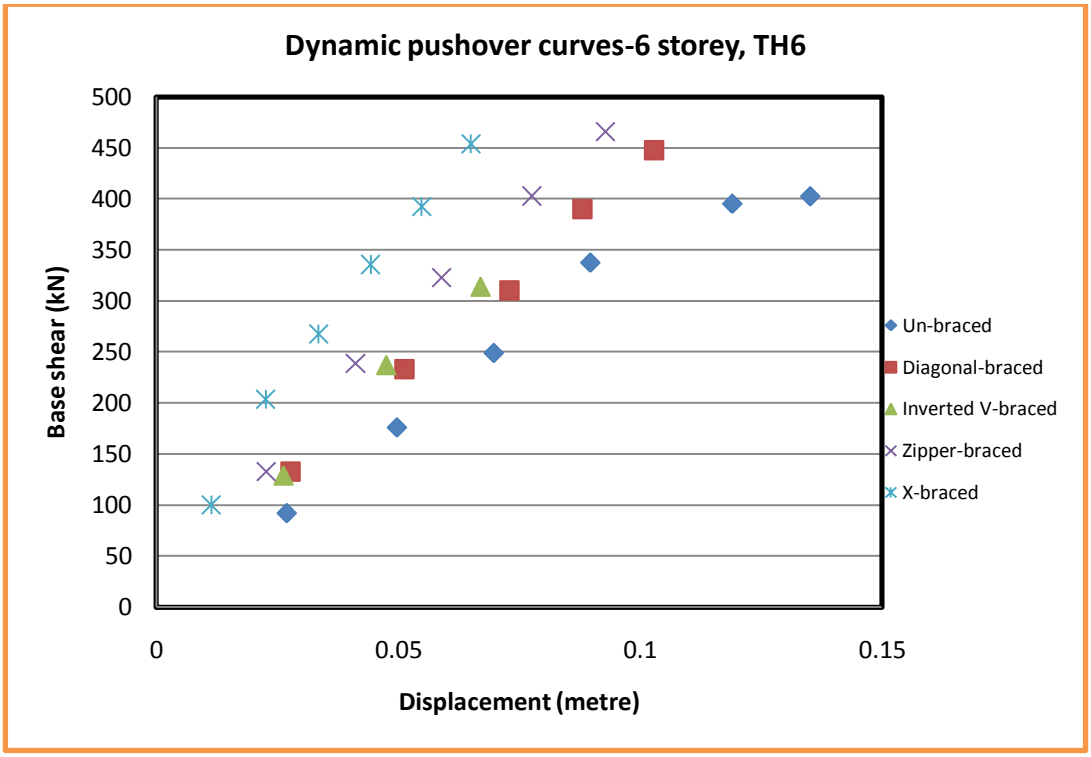

Figure 4.23: IDA curve for the six storey frames, TH6

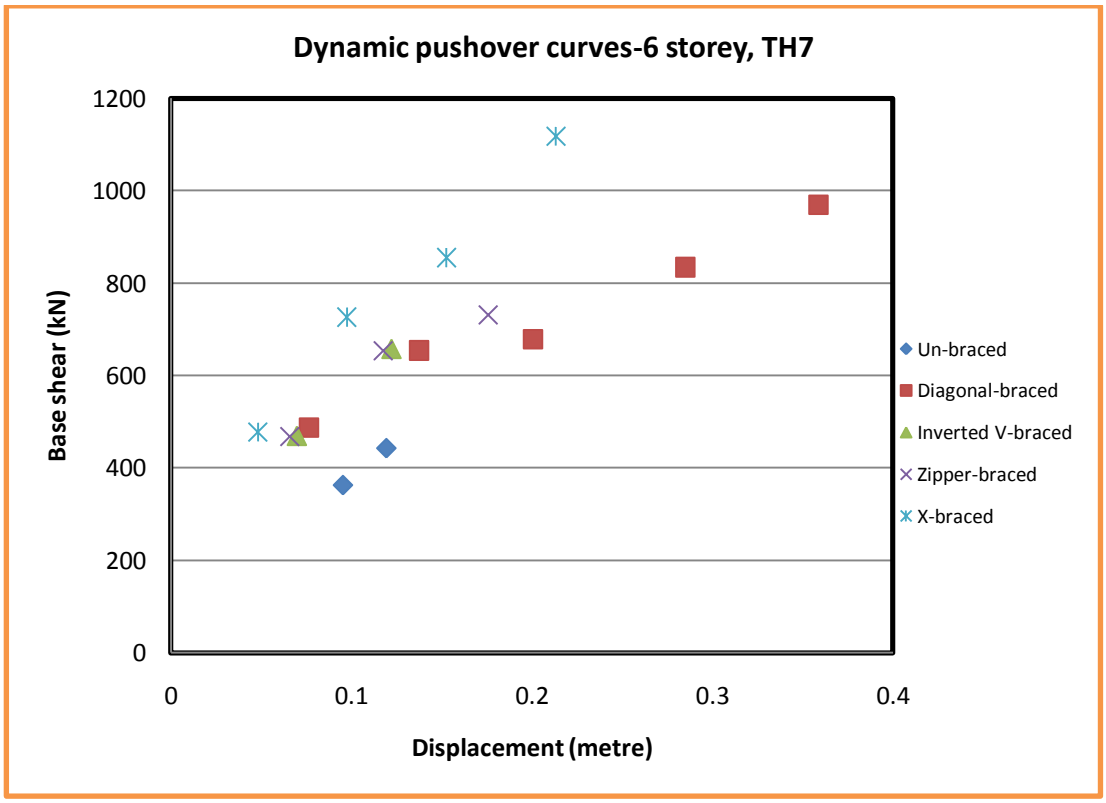

Figure 4.24: IDA curve for the six storey frames, TH7

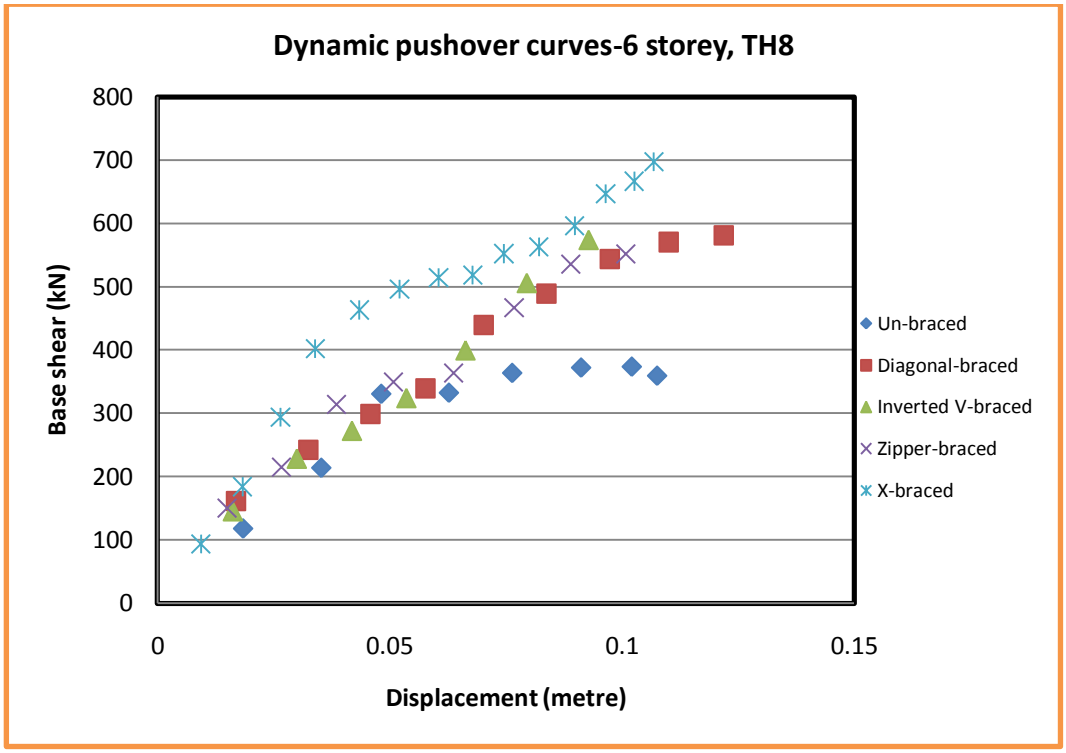

Figure 4.25: IDA curve for the six storey frames, TH8

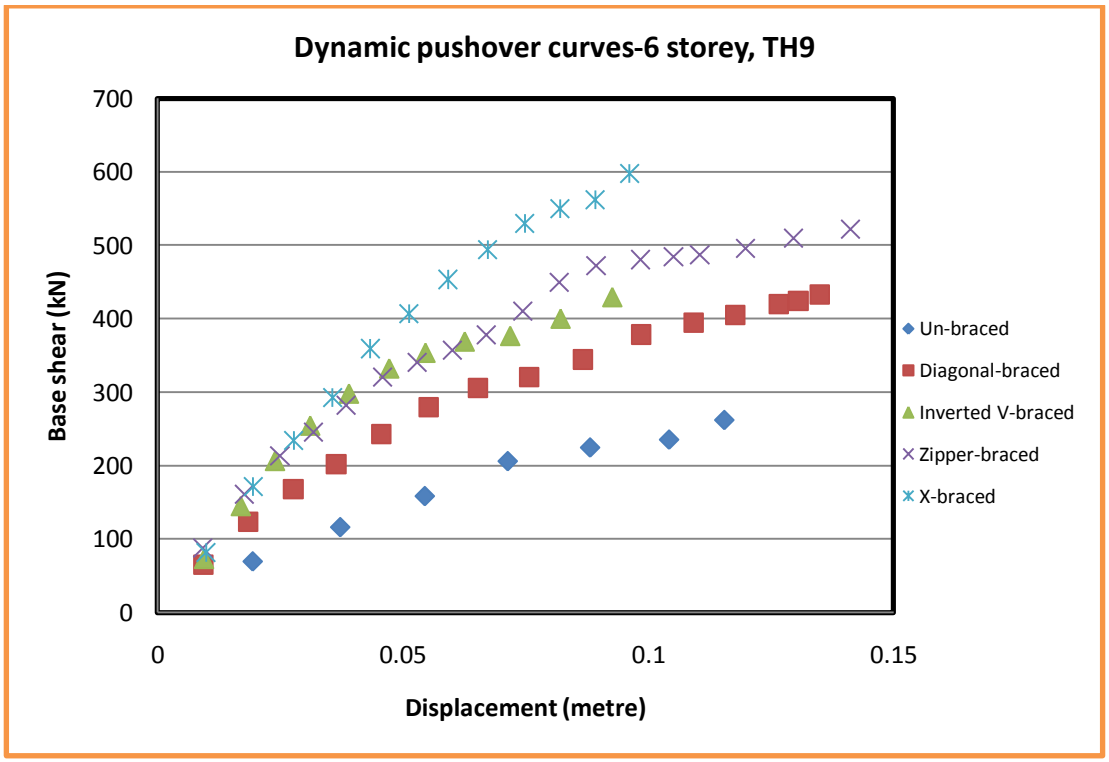

Figure 4.26: IDA curve for the six storey frames, TH9

4.3.2 IDA Results for the Nine Storey Frames

IDA curve (dynamic pushover curve) for different ground motion records is shown out of figures below:

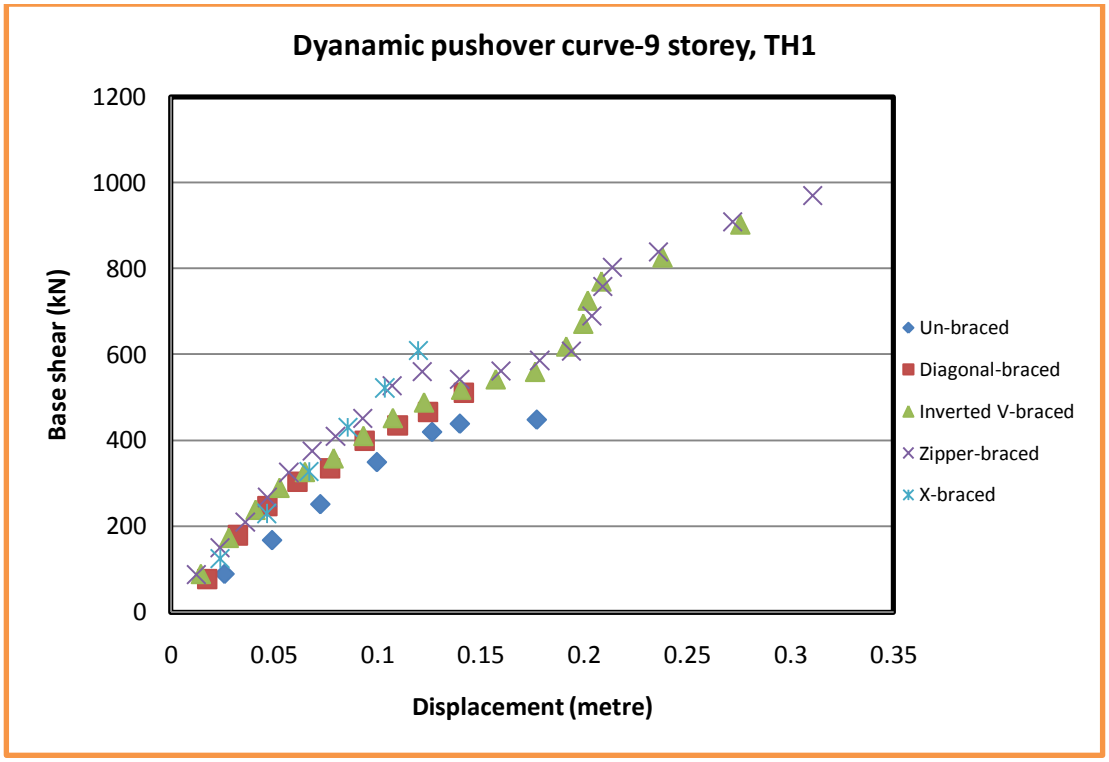

Figure 4.27: IDA curve for the nine storey frames, TH1

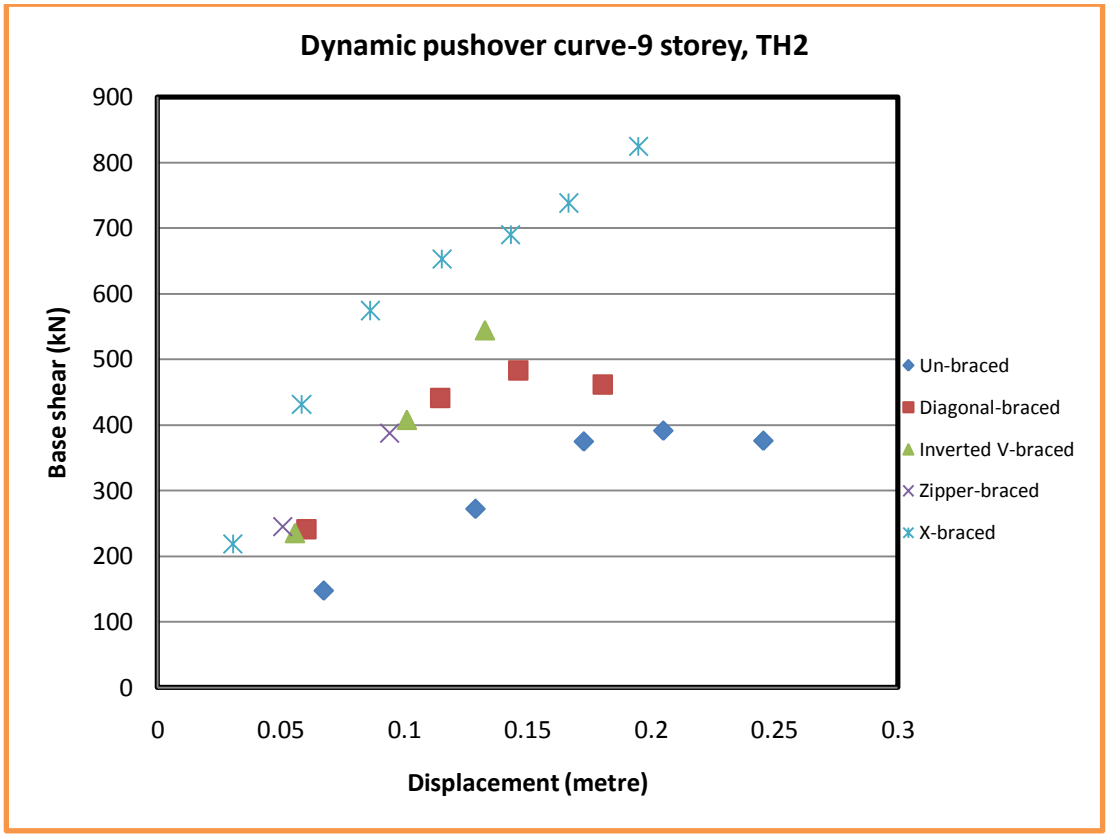

Figure 4.28: IDA curve for the nine storey frames, TH2

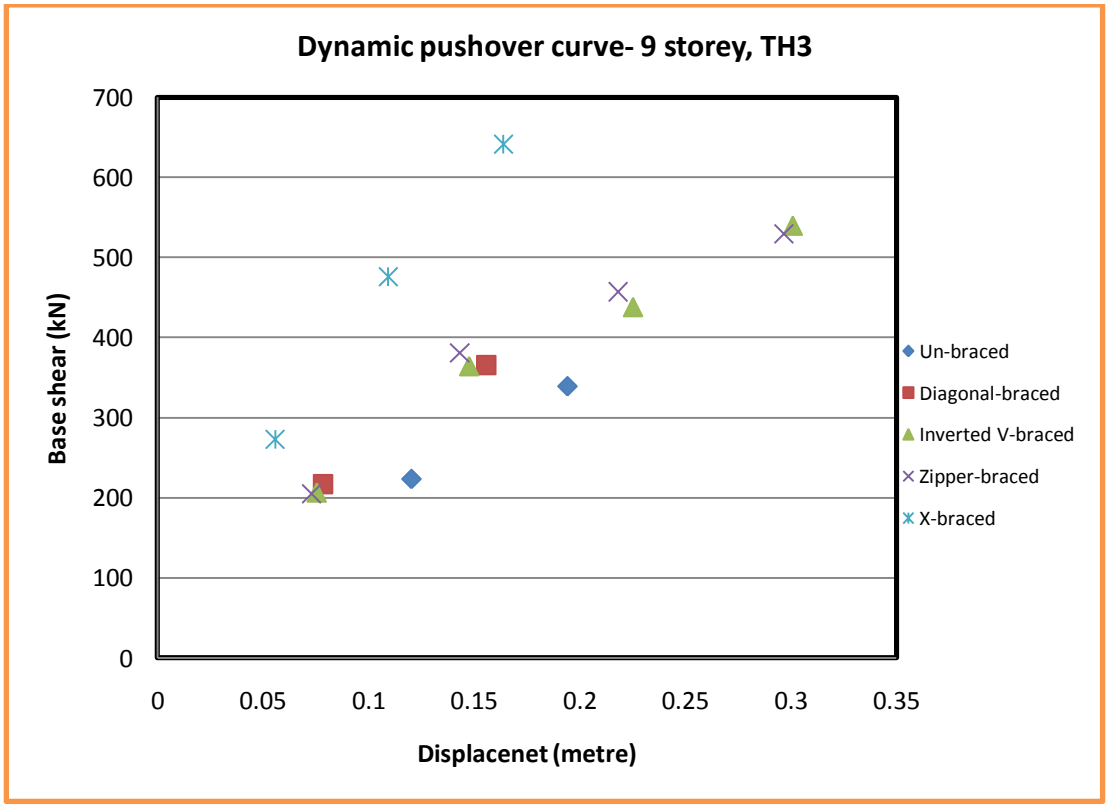

Figure 4.29: IDA curve for the nine storey frames, TH3

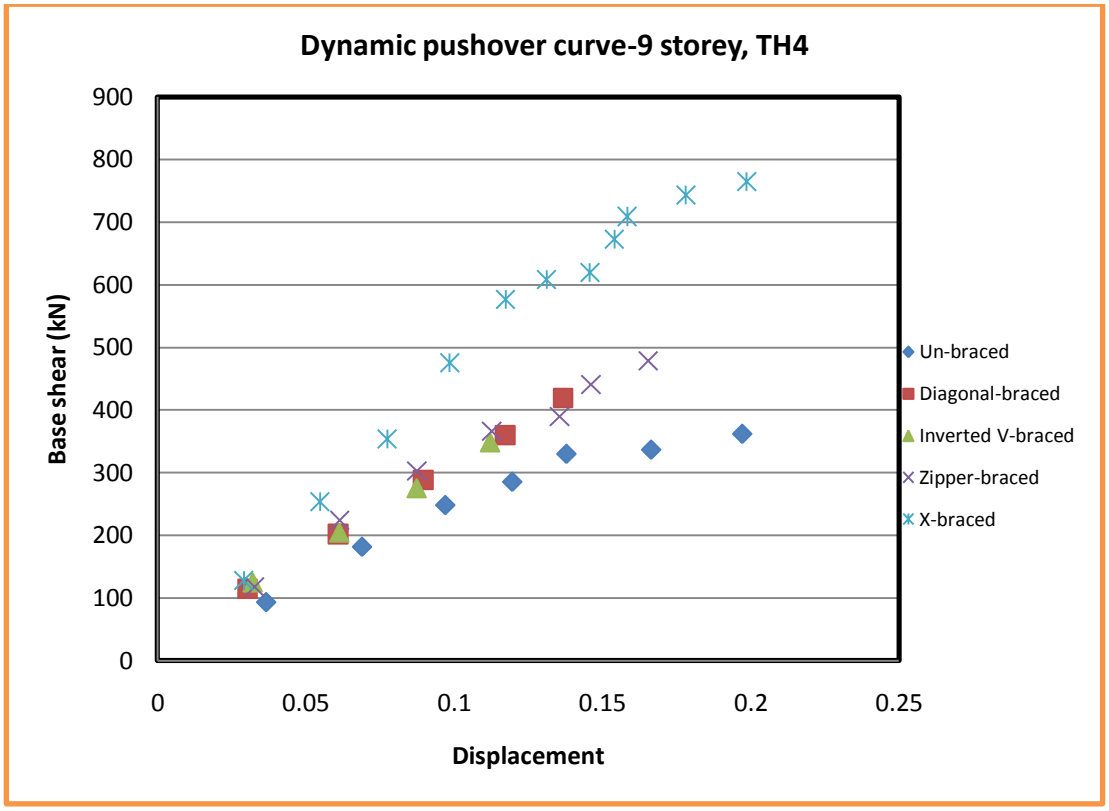

Figure 4.30: IDA curve for the nine storey frames, TH4

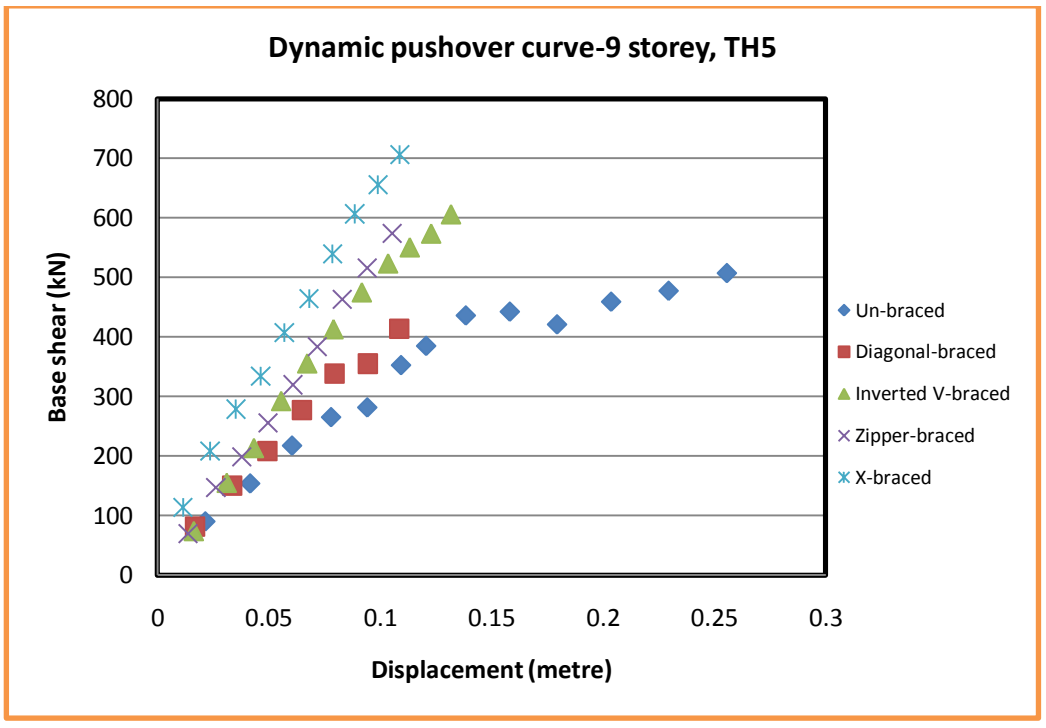

Figure 4.31: IDA curve for the nine storey frames, TH5

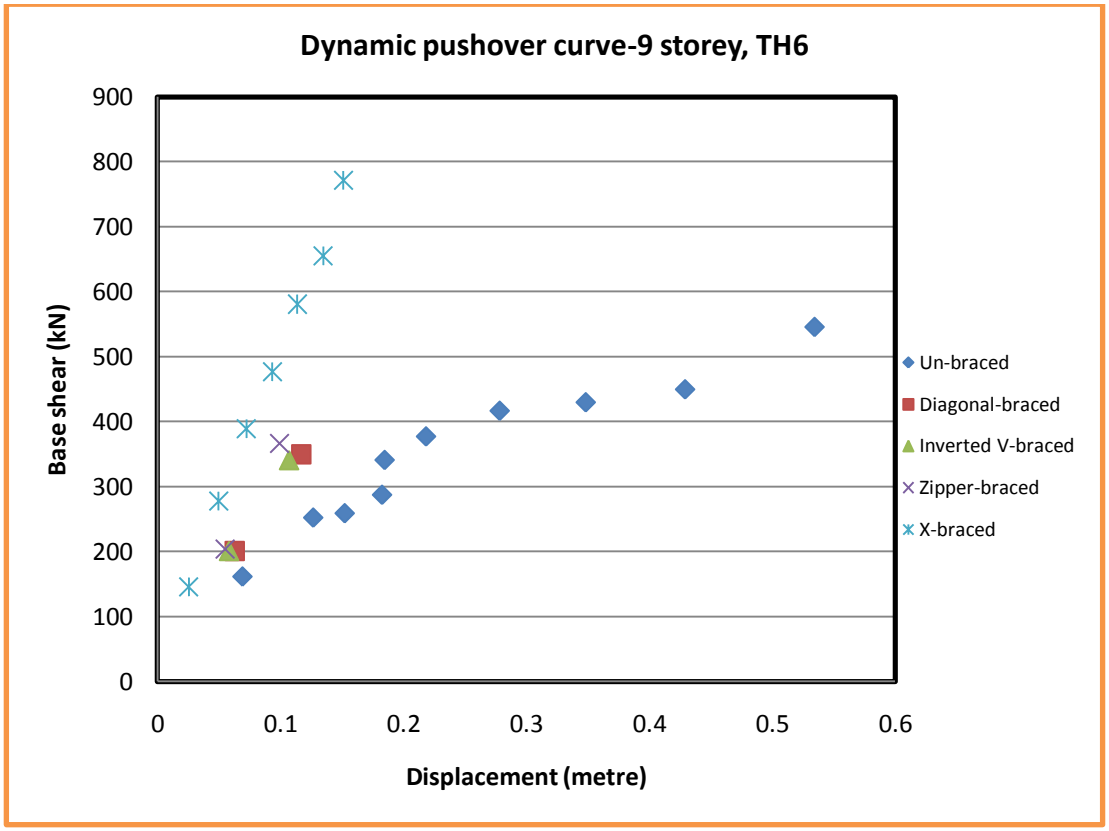

Figure 4.32: IDA curve for the nine storey frames, TH6

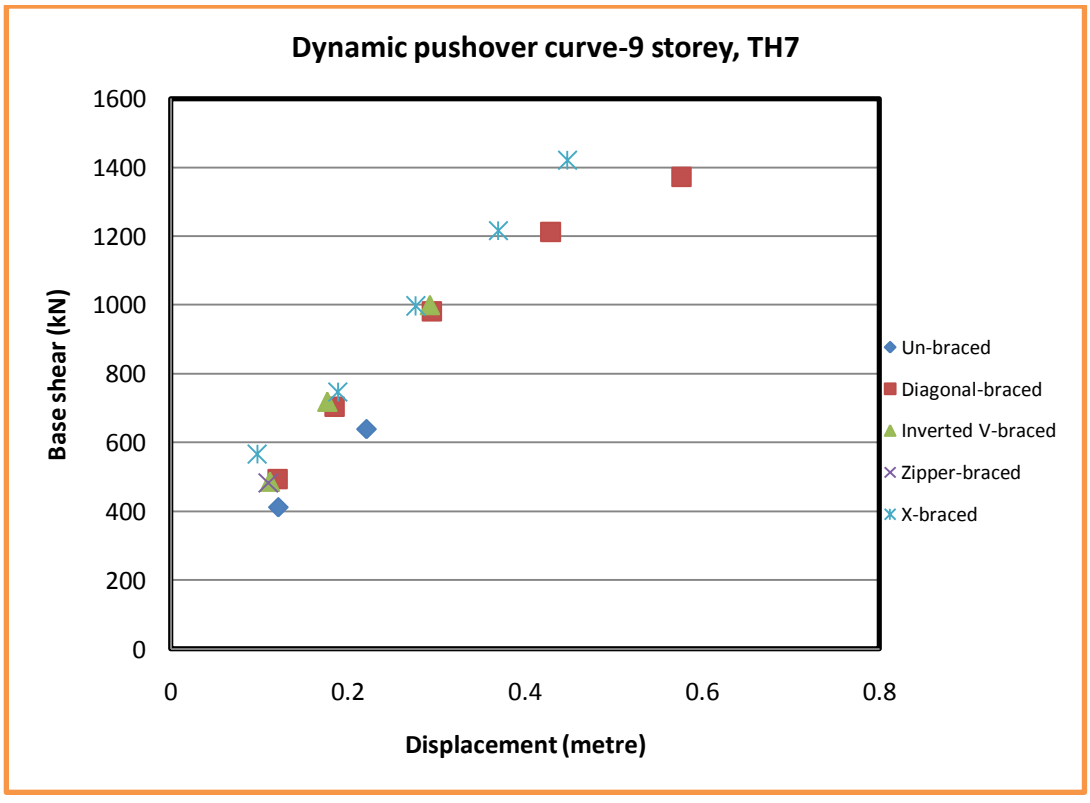

Figure 4.33: IDA curve for the nine storey frames, TH7

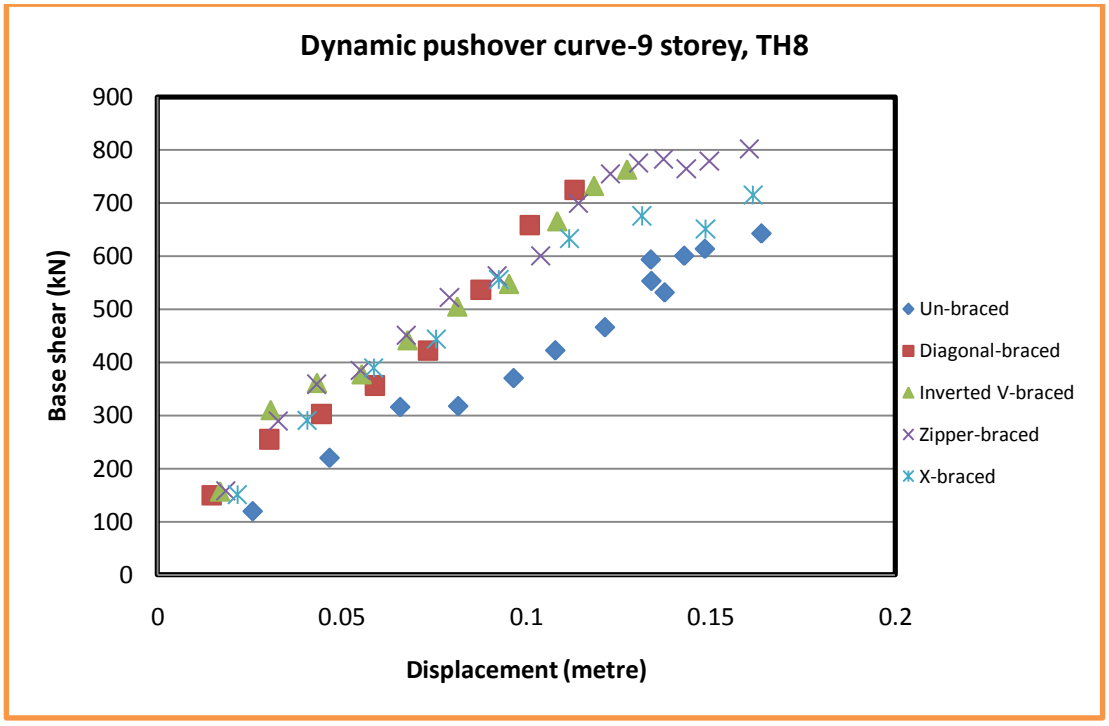

Figure 4.34: IDA curve for the nine storey frames, TH8

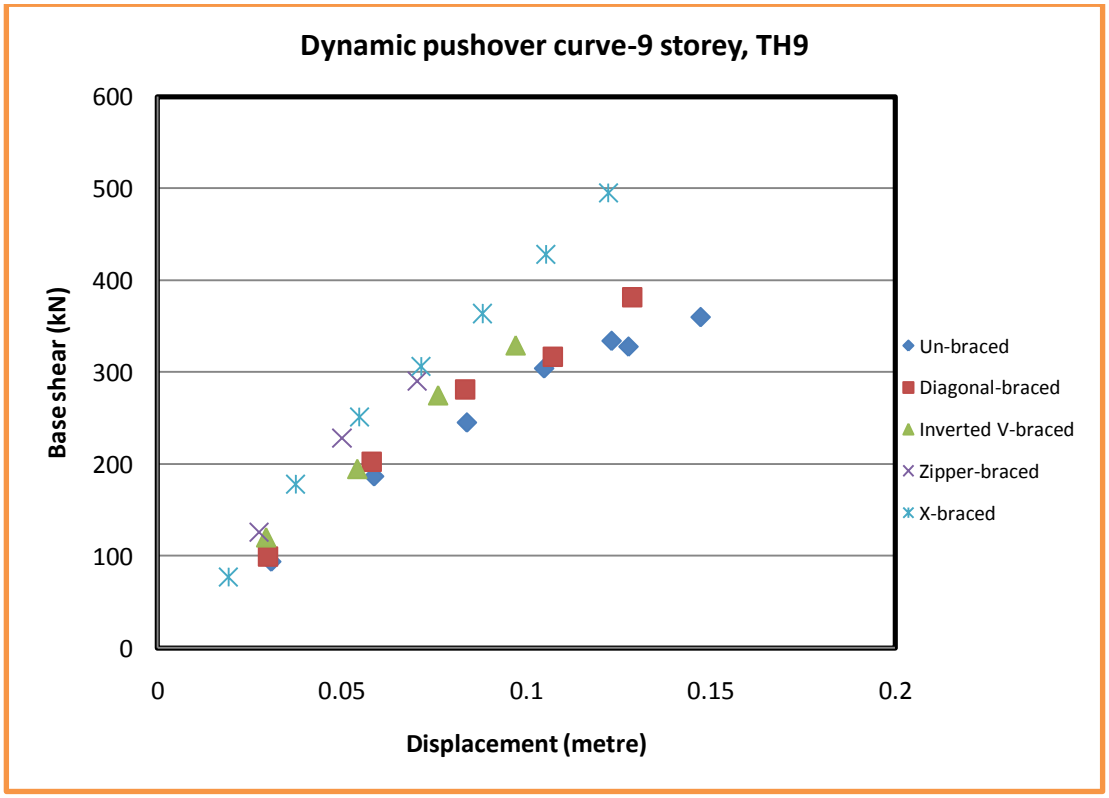

Figure 4.35: IDA curve for the nine storey frames, TH9

4.3.4 IDA Results for the Twelve Storey Frames

IDA curve (dynamic pushover curve) for different ground motion records is shown out of figures below:

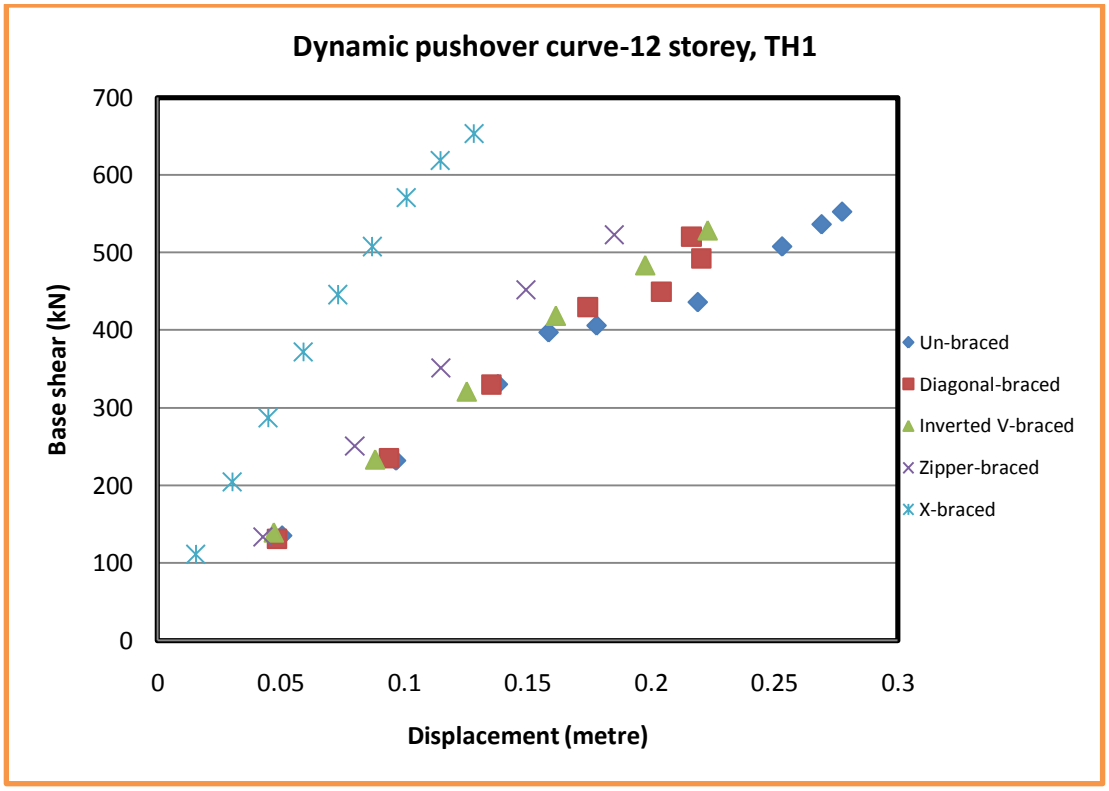

Figure 4.36: IDA curve for the twelve storey frames, TH1

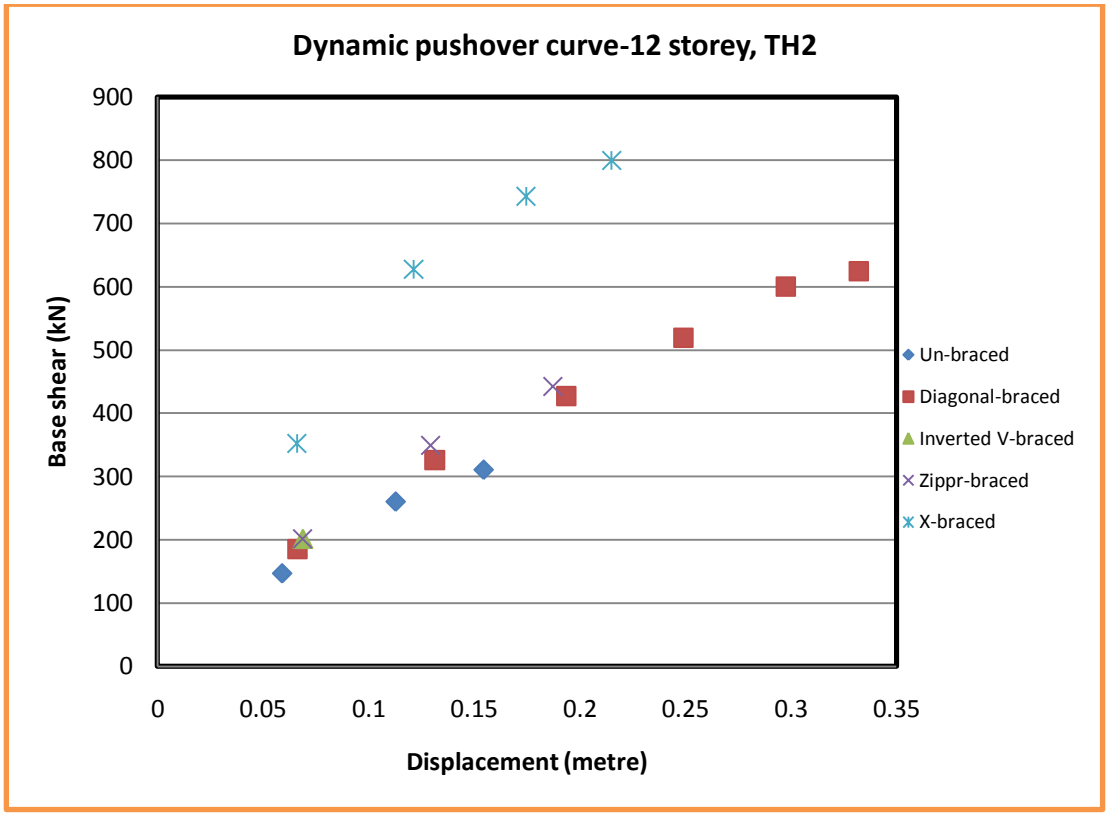

Figure 4.37: IDA curve for the twelve storey frames, TH2

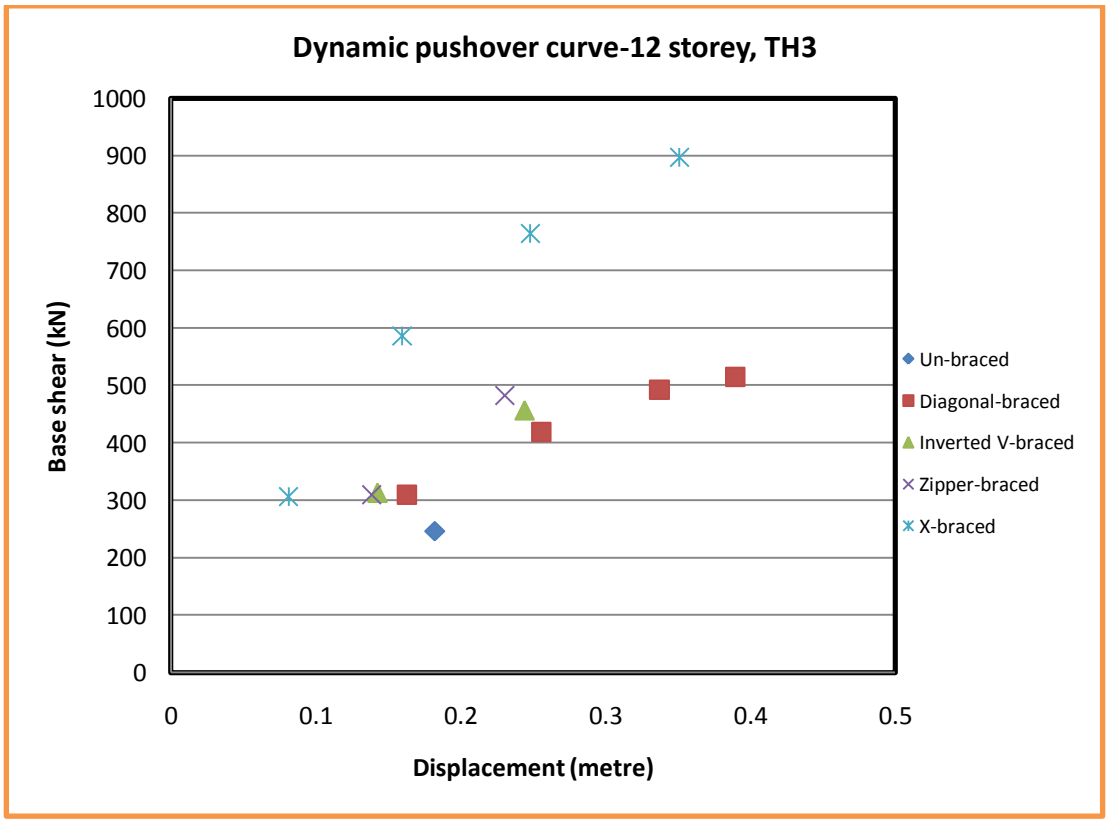

Figure 4.38: IDA curve for the twelve storey frames, TH3

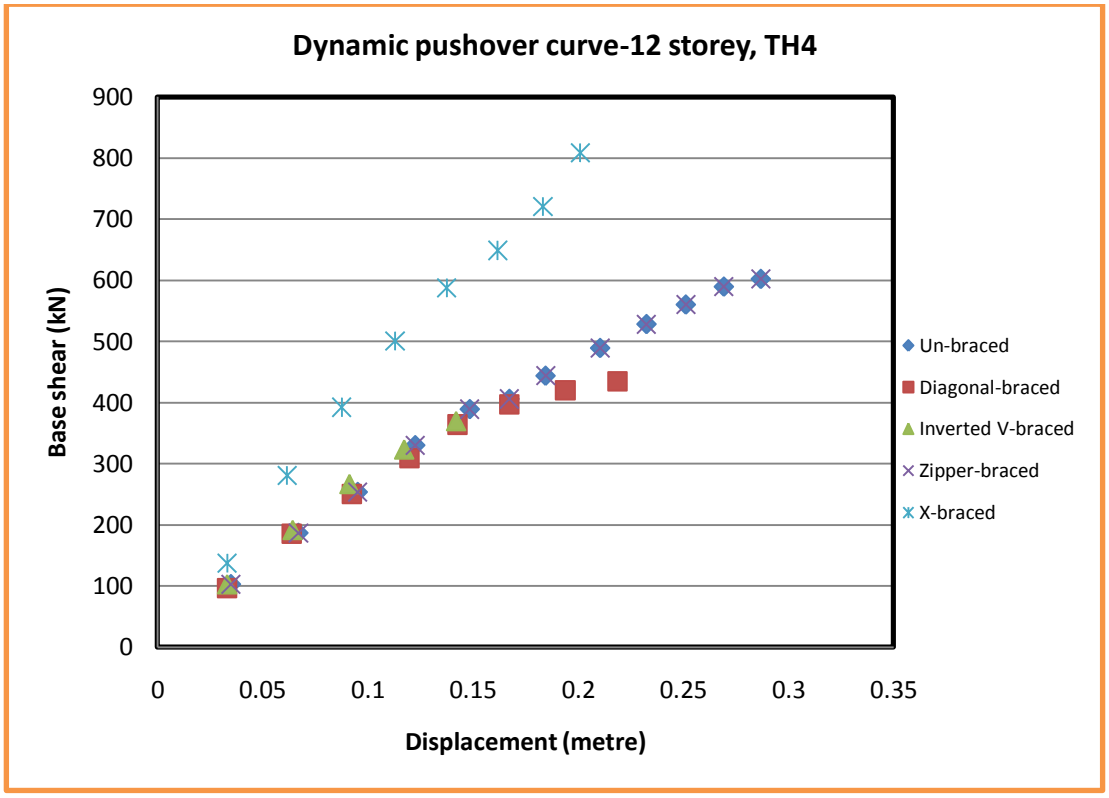

Figure 4.39: IDA curve for the twelve storey frames, TH4

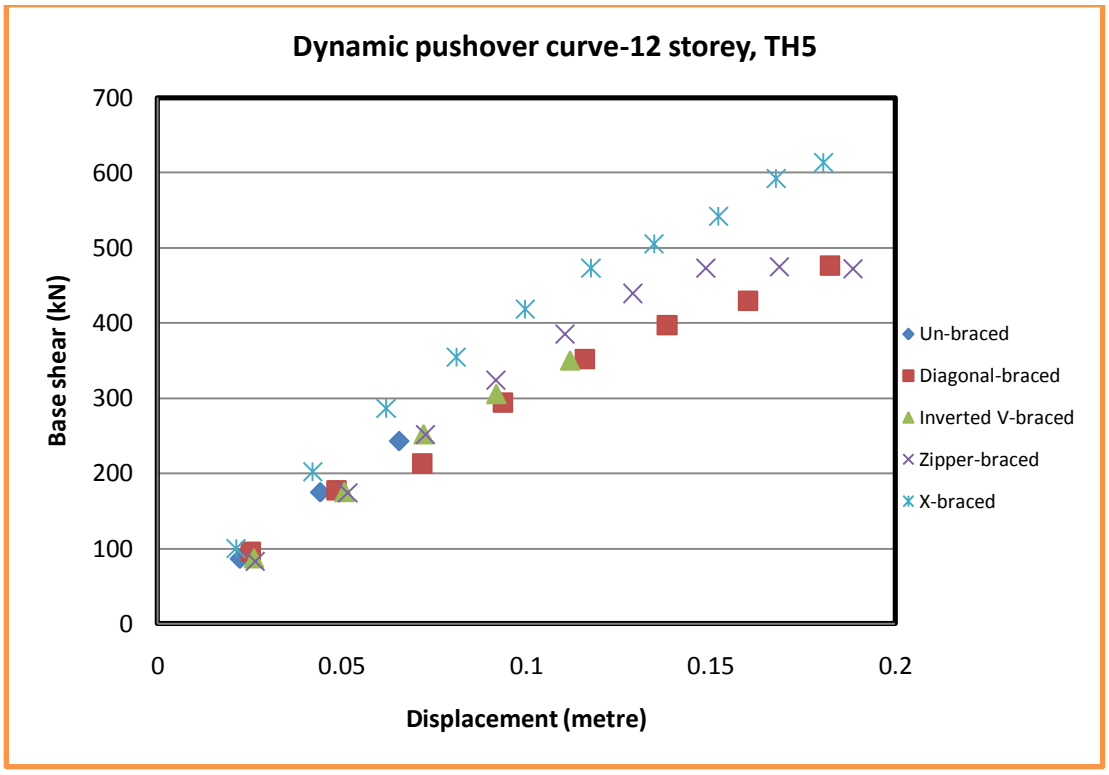

Figure 4.40: IDA curve for the twelve storey frames, TH5

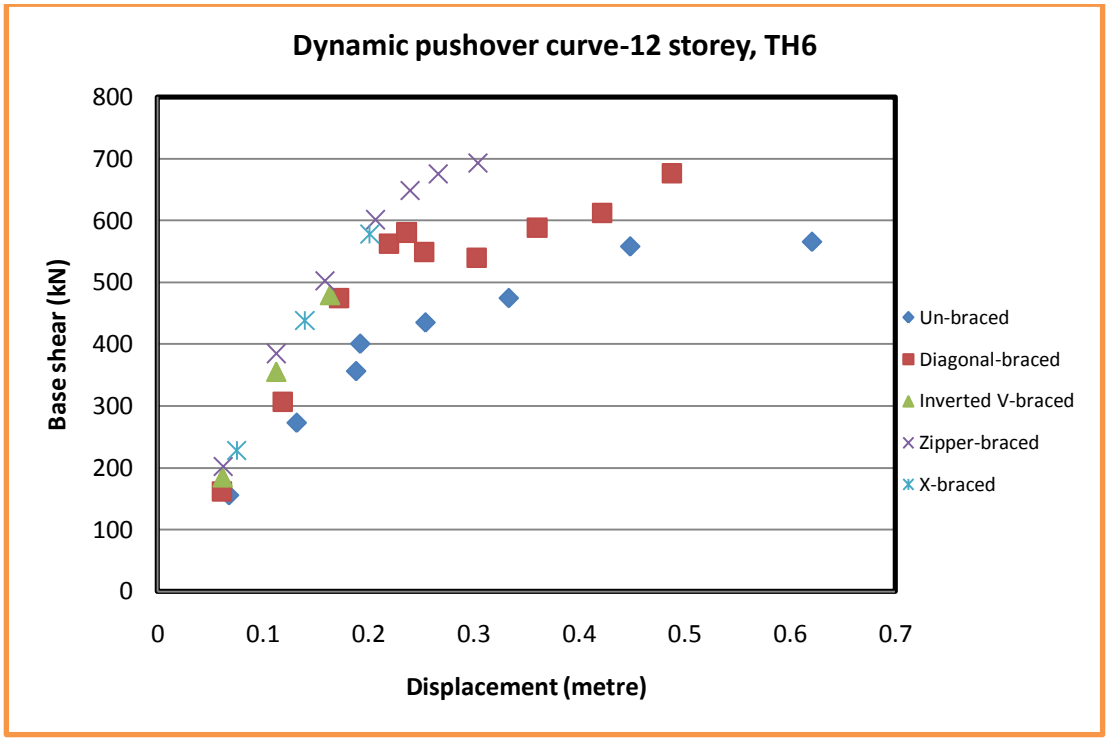

Figure 4.41: IDA curve for the twelve storey frames, TH6

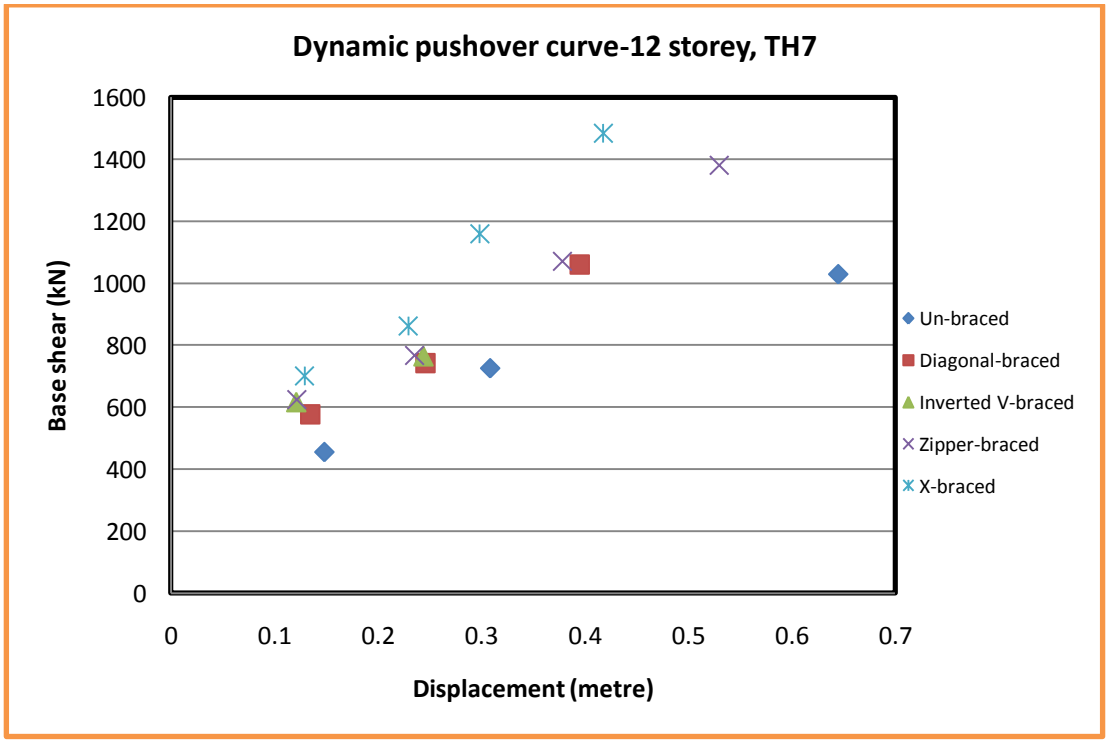

Figure 4.42: IDA curve for the twelve storey frames, TH7

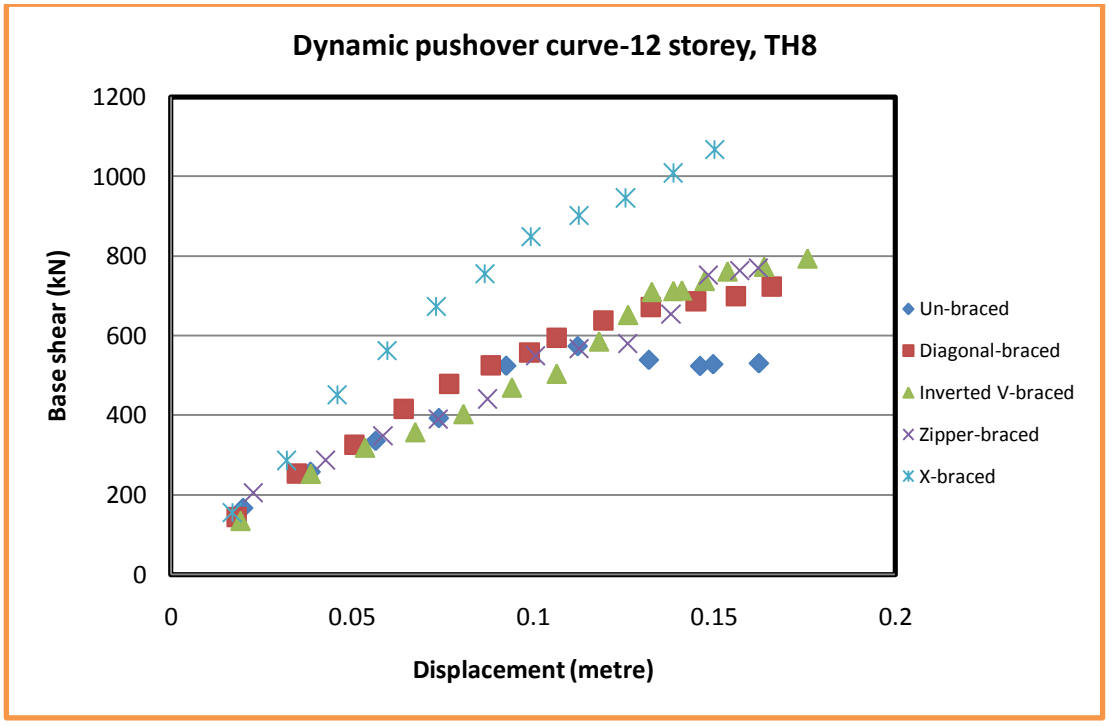

Figure 4.43: IDA curve for the twelve storey frames, TH8

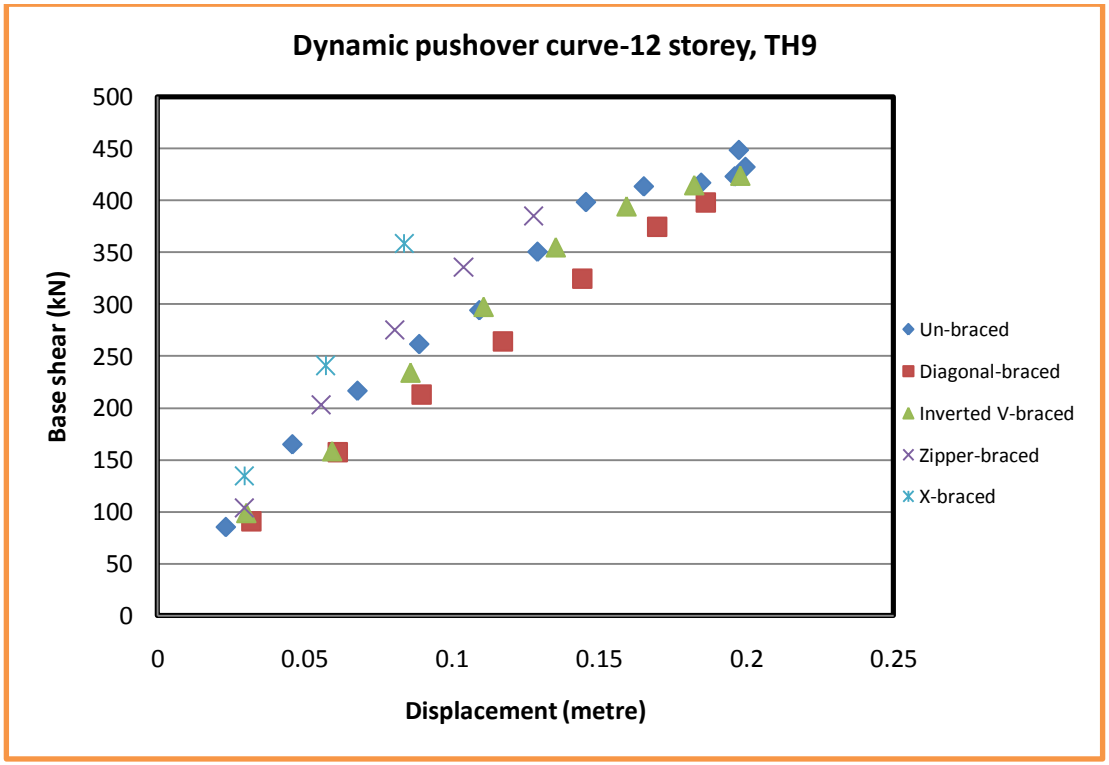

Figure 4.44: IDA curve for the twelve storey frames, TH9

4.3.5 General IDA Results and Discussion

Incremental dynamic analysis has been performed to make sure about the results obtained in the static pushover analysis. Figures 4.9 to 4.44 shows the distribution of maximum roof drift versus maximum base shear, which are the dynamic capacity curves.

The effect of the various types of braces in term of maximum base shear is presented in Tables 4.17 to 4.25.

Table 4.17: Maximum base shear (kN)-TH1

Frame	**Un-braced**	**Diagonal-braced**	**Inverted V-braced**	**Zipper-braced**	**X-braced**
3 storey	334	418	516	483	622
6 storey	423	414	554	504	750
9 storey	449	510	902	970	680
12 storey	553	520	528	523	653

Table 4.18: Maximum base shear (kN)-TH2

Frame	Un-braced	Diagonal-braced	Inverted V-braced	Zipper-braced	X-braced
3 storey	365	364	384	400	715
6 storey	354	586	642	702	845
9 storey	376	461	544	387	824
12 storey	310	624	201	422	799

Table 4.19: Maximum base shear (kN)-TH3

Frame	Un-braced	Diagonal-braced	Inverted V-braced	Zipper-braced	X-braced
3 storey	346	619	681	752	595
6 storey	405	659	791	748	857
9 storey	339	366	540	530	641
12 storey	246	515	456	482	897

Table 4.20: Maximum base shear (kN)-TH4

Frame	Un-braced	Diagonal-braced	Inverted V-braced	Zipper-braced	X-braced
3 storey	312	409	486	458	388
6 storey	285	470	372	381	638
9 storey	362	419	349	478	765
12 storey	602	435	370	602	809

Table 4.21: Maximum base shear (kN)-TH5

Frame	Un-braced	Diagonal-braced	Inverted V-braced	Zipper-braced	X-braced
3 storey	286	470	356	498	465
6 storey	437	465	429	318	653
9 storey	507	414	606	574	707
12 storey	243	476	351	472	614

Table 4.22: Maximum base shear (kN)-TH6

Frame	Un-braced	Diagonal-braced	Inverted V-braced	Zipper-braced	X-braced
3 storey	337	378	381	310	438
6 storey	403	448	314	466	454
9 storey	546	350	341	366	772
12 storey	566	677	479	693	578

Table 4.23: Maximum base shear (kN)-TH7

Frame	Un-braced	Diagonal-braced	Inverted V-braced	Zipper-braced	X-braced
3 storey	540	772	903	807	725
6 storey	443	969	658	731	1118
9 storey	640	1373	999	482	1420
12 storey	1029	1061	764	1381	1483

Table 4.24: Maximum base shear (kN)-TH8

Frame	Un-braced	Diagonal-braced	Inverted V-braced	Zipper-braced	X-braced
3 storey	225	398	365	531	597
6 storey	359	581	574	552	698
9 storey	642	724	763	802	715
12 storey	530	723	795	770	1068

Table 4.25: Maximum base shear (kN)-TH9

Frame	Un-braced	Diagonal-braced	Inverted V-braced	Zipper-braced	X-braced
3 storey	266	378	395	296	430
6 storey	262	433	429	522	598
9 storey	360	382	330	291	496
12 storey	449	398	424	384	359

The results represented here do not represent full IDA and has been carried out for comparison purpose and should be improved. In order to obtain more reliable and accurate results, different IM and DM parameters should be considered. Also, it is possible to achieve more reasonable results by applying smaller scale factor value, which leads to obtain more accurate results.

The results of the analysis show that the value of maximum base shear for 3 storey frames is not influenced much by change of ground motion frequency content. However, for the 6 storey frames, this variation is more significant. On the other hand, the maximum base shear for the 9 storey and 12 storey frames is influenced much by change of ground motion frequency content. It is shows that the effect of changing the frequency content increases with increase on the height of the frames.

It is observed that X-braced system is much better than the other systems and the influence of other types are very close to each other. Also from the figure it is evident that X -braced systems have much higher initial stiffness as compared to other systems.

Studying multiple Incremental Dynamic Analysis curves shows that their extension up to the same levels is not reliable for all records, because of the records' natural differences. Thus, in IDA more than one ground motion must be applied to get more reliable results.

Chapter 5

CONCLUSION AND RECOMMENDATION

5.1 Pushover Analysis Summary

Throughout this study, various types of steel bracing systems have been investigated as effective methods to retrofit and strengthen existing reinforced concrete frames. The bracing types are X-braced, Zipper-braced, Inverted V-braced and Diagonal-braced. The models that have been studied are 3-storey, 6-storey, 9-storey and 12 storey buildings which are designed by Etabs.

The analysis has been carried out by using Seismostruct program, static capacity curves constructed by applying pushover analysis. The pushover analysis is carried out to check performance criteria and to estimate lateral load capacity, roof displacement and stiffness.

The frames have been designed only to resist gravity loads without any seismic consideration. Thus, results obtained show that the buildings are not safe and all un-braced frames failed to resist these lateral loads which are calculated by Turkish Earthquake Code 2007, and they reach to collapse state before applying entire calculated base shear.

5.2 Pushover Analysis Conclusion

Major conclusions obtained from the present study are as follows:

- The existing RC buildings, which are designed without seismic consideration cannot resist and prevent collapse at moderate earthquakes.
- Steel bracing systems are a good alternative to retrofit existing RC buildings because braces are less in weight, economically and easy to installation.
- Adding steel braces enhance greatly the strength capacity of the buildings.
- Adding steel braces decrease the building element strains. Therefore, the probability of collapse will decrease.
- X-braced type is more effective among other types of bracing.
- Diagonal-braced, Inverted V-braced and Zipper-braced systems have acceptable results also and their effects are close to each other. Therefore, most economic and workable one which should be used which is diagonal bracing type.
- While number of story increases, capacity and stiffness decreases in the existing RC frames.
- As the number of storey increases, the effective rate of bracings on existing buildings is generally stable and difference is slight.

5.3 Incremental Dynamic Analysis Summary

The Incremental Dynamic Analysis has been carried out by using Seismostruct program, dynamic capacity curves were constructed in terms of maximum base shear versus maximum drift. IDA has been carried out to validate the pushover analysis results.

In order to perform IDA, nine different ground motions downloaded from PEER based on design spectrum. They are scaled for different PGAs to obtain dynamic capacity curves. Many limitations are used to choose suitable ground motions to the

seismic zone and local site conditions. Each ground motion applied starting from low intensity and increasing gradually until collapse occurs.

5.4 Incremental Dynamic Analysis Conclusion

Major conclusions obtained of the IDA are as follows:

- IDA is another choice to create capacity curves.
- It is reasonable to say that the maximum base shear value is affected by the frequency content of the earthquake records.
- Because of records' natural differences, multiple ground motion records are preferred.
- The influence of various frequency contents on frames increases with increasing of height of frames.
- The maximum base shear for braced frames is more than un-braced frame, and X-braced frame has the greatest effect.
- X-braced system has greater initial stiffness than other bracing systems.
- The IDA results represented in this study do not represent full IDA and has been carried out for comparison purpose and should be improved.

5.4 Recommendations for future studies

In this study the capacity of concentric bracing systems assessed for the 2-dimensional frames. The same study is recommended for 3-dimensional frames and also for eccentric bracing systems and knee braced systems.

Same study considering other types of site and local conditions, earthquake magnitude and different seismic zone are also recommended.

REFERENCES

[1] Ghoborah, A. and H.A. Elfath(2001). “Rehabilitation of a Reinforced Concrete Frame Using Eccentric Steel racing” Engineering Structures 23(7): 745-755.

[2] Safarizki, H. A., et al. (2013). "Evaluation of the Use of Steel Bracing to Improve Seismic Performance of Reinforced Concrete Building." Procedia Engineering 54: 447-456.

[3] Massumi, A. and A.A. Tasnimi. (2008). “Strengthening Of Low Ductile Reinforced Concrete Frames Using X-Bracings With Different Details” Beijing, china: The 14th World Conference on Earthquake Engineering

[4] Dubina, D.,et al. (2011). “Experimental And Numerical Investigation Of Non-Seismic Reinforced Concrete Frames Strengthened With Concentric Steel Braces” Corfu, Greece.

[5] Kevadkar, M.D. and P.B. Kodag. (2013). “Lateral Load aAnalysis of R.C.C. Building” International journal of modern engineering research, Vol.3, Issue.3: pp-1428-1434

[6] Mohammad, E.K. (2012). “Seismic Propensity of Knee Braced Frame (KBF) As Weighted Against Concentric Braced Frame (CBF) Utilizing ETABS and OPEENSEES” International journey of engineering and advanced technology, Volume-5

[7] Mehmet, A. (2008). “Strengthening Of Reinforced Concrete Frames By Using Steel Bracings” Master’s Thesis: The Middle East technical university, Istanbul, Turkey.

[8] Amini, M. and M. Alirezaei. (2013). “Response Evaluation of Braced Frames With Suspended Zipper Struts and Chevron Braced Frames in Near-Fault Earthquake Ground Motions” American Journal of Sustainable Cities and Society: Issue 2, Vol.1.

[9] Kadid, A. and D. Yahiaoui. (2011). “Seismic Assessment of Braced RC Frames” Procedia Engineering 14: 2899-2905.

[10] Fedral Emergency Management Agency (FEMA). (2000). “Prestandard And Commentary For The Rehabilitation Of Buildings” FEMA-356, Washington DC.

[11] Applied Technology Consul, ATC-40 (1996).”Seismic Evaluation and Retrofit of Concrete Buildings” Vol 1-2, Redwood City, California

[12] Paddala, P. (2013). “Pushover Analysis Of Steel Frames” Master’s thesis, National Institute Of Technology: Rourkela, Orissa.

[13] Krawinkler, H. and G.D.P.K. Seneviratna. (1998). “Prose and cones of a pushover analysis of seismic performance evaluation” Engineer Structures Vol.20: pp.452-464.

[14] Kunnath, S.K. and E. Kalkan. (2011). “IDA Capacity Curves: The Need for Alternative Intensity Factors” University of California Davis, One Shields Avenue, Engineering III.

[15] Vamvatsikos, D. and C.A. Cornell. (2002). “Incremental Dynamic Analysis” Earthquake Engng Struct. Dyn. 31: 491-514.

[16] Alnashai, A.S. and L.D. Sarno (2008). “Fundamenatls of earthquake engineering” A John Wiley and Sons, Ltd, Publications, West Sussex, United Kingdom.

[17] Caponi, C. (2008). “Design Verification Of A Displacement-Based Designed Three Dimensional Wall-Steel Frame Building” Master’s Thesis: European School For Advanced Studies In Reduction Of Seismic Risk, Rose school, Italy.

[18] Central Public Works Department And Indian Building Congress. (2007). “Handbook On Seismic Retrofit Of Buildings” Manu Santhanam, India

[19] Seismosoft Ltd. (2013)“Seismostruct user manual” www.seismosoft.com, Pavia, Italy.

[20] Turkish Earthquake Code (2007). “Specification For Structures To Be Built In Disaster Areas” Ministry of public works and settlement, Ankara, Turkey.

[21] Yardimci, Y. (2009). “Seismic Performance Assessment and Strengthening of Gazimagusa Namik Kemal Licesi” Master’ Thesis: Eastern Mediterranean University, Gazimagusa, Cyprus.

[22] Khajehhesameddin, P. (2010). “Probabilistic Seismic Demand of 2-D Steel Moment Resisting Frames in Estimation of Collapse Under Earthquake Ground Motions” Eastern Mediterranean University, Gazimagusa, Cyprus.

[23] http://peer.berkeley.edu/peer ground motion database/site.

[24] American Concrete Institute (2002) “ACI 318: Building Code Requirements for Reinforced Concrete” Washington, D.C.

.